C. Richter, G. Acton, C. Endris, and M. Radsted
ODP Technical Note 34

Handbook for Shipboard Paleomagnetists[1, 2]

Carl Richter,[3] Gary Acton,[4] Charles Endris,[5] Mads Radsted[6]

ABOUT THIS TECHNICAL NOTE

The shipboard paleomagnetic laboratory, the Ocean Drilling Program (ODP) database structure, and the hardware and software environment on the *JOIDES Resolution* have changed almost entirely since the first publication of *Technical Note* 18 in 1993 (Stokking et al., 1993). Although in constant flux, the shipboard paleomagnetic laboratory environment, equipped in the past few years with new magnetometers, a new demagnetizer, a new database structure (a relational Oracle database), and new software, has come to a point where it is stable enough to redefine the paleomagnetic data acquisition and archiving procedures and requirements. In contrast, the role of the shipboard paleomagnetist has changed little since 1993, so part of this technical note builds upon the information that was provided in Stokking et al. (1993). In addition, we have benefitted from the input of many paleomagnetists and shipboard paleomagnetism technicians who have sailed on the *JOIDES Resolution* over the past decade.

Draft versions of this technical note were available during the last 2 years of ODP. The completed version of this technical note will become a legacy document for ODP and a starting point for the Integrated Ocean Drilling Program (IODP).

The objectives of this note are to

1. Introduce the novice laboratory user to procedures and equipment,
2. Provide expert users with a reference of measurement principles and data specifications,
3. Document the laboratory practices that were typical of the final 6 years of ODP, and

[1]Richter, C., Acton, G., Endris, C., and Radsted, M., 2007. Handbook for shipboard paleomagnetists. *ODP Tech. Note,* 34 [Online]. Available from World Wide Web: <http://www-odp.tamu.edu/publications/tnotes/tn34/INDEX.HTM>. [Cited YYYY-MM-DD]
[2]See **Disclaimer,** p. 60.
[3]Department of Geology, University of Louisiana at Lafayette, PO Box 44530, Lafayette LA 70504-0002, USA.
[4]Department of Geology, University of California, One Shields Avenue, Davis CA 95616, USA.
acton@geology.ucdavis.edu
[5]1275 Country Club Drive, Ben Lomond CA 95005, USA.
[6]Lasbygade 67-69, 6000 Kolding, Denmark.

4. Create a foundation for effective management and further development of the shipboard paleomagnetism laboratory for the current program and for future programs focused on ocean drilling.

This handbook is divided into eight sections and four appendixes. **"Introduction,"** p. 3, discusses research objectives of paleomagnetic measurements and gives an overview of the shipboard laboratory, paleomagnetic sampling strategies commonly used, and the new ODP database. **"Remanent Magnetization,"** p. 12, and **"Magnetic Susceptibility,"** p. 21, are dedicated to magnetic remanence and magnetic susceptibility measurements that are routinely obtained on the ship. These sections give a brief introduction to paleomagnetism principles, shipboard environmental factors that influence data quality, and some common uses of the paleomagnetic data. They also describe the equipment, the physical property being measured, measurement principles and procedures, and equipment calibration and performance. Each section covering a measurement system also presents the exact data model implemented in the new ODP database, the Web-based data queries available to the user for data retrieval, and algorithms used in the queries.

Each section covering a measurement system presents calibration and measurement procedures in only a generic way, focusing on issues essential for maintaining the best data quality possible. Step-by-step tutorials for operating the data acquisition programs and instruments are not included here. The programs controlling the instrumentation evolve rapidly as new computer hardware and software become available, and user interfaces are improved almost continuously. In most cases, these upgrades do not affect the principles and data models presented here, but do slightly modify the hands-on procedures. ODP typically staffs a shipboard technician who has experience running equipment in the paleomagnetism laboratory and is available to assist with details of instrument use. In addition, the "Explanatory Notes" chapters from previous cruises, the technical reports written at the end of each cruise by the paleomagnetism-laboratory technician, and other laboratory manuals or "cook books," which are available for most of the instruments and software, provide valuable resources for the shipboard paleomagnetists.

"Alternating Field and Thermal Demagnetization," p. 27, and **"Laboratory-Induced Magnetization,"** p. 31, introduce the equipment available for the demagnetization (thermal and AF) and magnetization (isothermal and anhysteretic) of discrete samples. The magnetic orientation of hydraulic piston cores is discussed in **"Core Orientation,"** p. 33. **"Measurement Guidelines and Strategies,"** p. 35, provides a practical guide to what can be measured during a cruise. The drilling magnetic overprint and other common problems in ODP cores are examined in **"Problems with Magnetic Measurements in the Shipboard Environment,"** p. 36. This section also summarizes problems encountered on past cruises, the identification of coring-induced overprints and deformation, and experiments that have been done to narrow down the sources of the drilling overprint.

The appendixes contain a list of magnetic units (**"Appendix A,"** p. 50), example data files with information on file formats (**"Appendix B,"** p. 51), operation and calibration procedures for the Kappabridge (**"Appendix C,"** p. 57), and a table to convert voltage to magnetic fields for the IM-10 impulse magnetizer (**"Appendix D,"** p. 59). The first version of *Technical Note* 18 by Stokking et al. (1993) is available online (**www-odp.tamu.edu/publications/tnotes/tn18/f_pal.htm**).

INTRODUCTION

Objectives of Paleomagnetic Measurements

The Ocean Drilling Program (ODP) is an international partnership of scientists and governments who have joined together to explore the structure and history of the earth beneath the ocean basins. On a typical ODP cruise, some form of coring is conducted. As a result, there are commonly several tens of meters to several kilometers of core available for scientific analysis, which begins with a variety of shipboard analyses and extends to postcruise shore-based studies.

Shipboard paleomagnetists provide the initial paleomagnetic and rock magnetic analysis of sediments and rocks recovered during an ODP cruise. This information is summarized in the *Proceedings of the Ocean Drilling Program Initial Reports* volumes and is often used by shipboard and shore-based scientists as the basis for subsequent sampling and investigations and as a primary data source for interpreting the geologic history of the drilling site. The shipboard paleomagnetists are responsible to the scientific community for collecting the appropriate data for characterizing the paleomagnetism and rock magnetism of sites drilled and for ensuring the data are accurate, reliable, and archived. Hence, the paleomagnetism laboratory on board the *JOIDES Resolution* contains state-of-the-art equipment to perform detailed paleomagnetic and rock magnetic measurements.

Paleomagnetic objectives for ODP are identified in "Paleomagnetic Objectives for the Ocean Drilling Program," a report from a 1986 JOI/USSAC workshop held at the University of California, Davis (Verosub et al., 1986). A copy of this report can be obtained from Joint Oceanographic Institutions, Inc. (JOI) (**www.joiscience.org**). Summarizing from this report, paleomagnetic objectives can be divided into four general areas:

1. Magnetostratigraphy: high-resolution correlation techniques and the magnetic polarity timescale (with emphasis on the Jurassic marine magnetic anomalies M38–M25, Early Cretaceous marine magnetic anomalies M10–M5, and middle and late Miocene polarity sequences). Since the writing of the report, a large emphasis has also been placed on using high-resolution correlation techniques to date Pleistocene-to-recent sediments more precisely, mainly through correlating relative paleointensity records with global paleointensity stacks or correlating rock magnetic records (e.g., susceptibility) with oxygen isotope stacks (e.g., SPECMAP).
2. Behavior of the geomagnetic field: time-averaged behavior of the field, short polarity intervals, polarity transitions, geomagnetic excursions, and secular variation.
3. Tectonics: plate motion, origin of oceanic plateaus, and polar wander paths.
4. Oceanic crust: origin of marine magnetic anomalies, ridge processes, old ocean crust, and seamounts.

Duties of the Shipboard Paleomagnetists

Shipboard scientists collect, analyze, and compile data in accordance with ODP standards and formats. They assist in the production of shipboard scientific reports, which includes helping to write the site chap-

ters for the *Proceedings of the Ocean Drilling Program Initial Reports* volumes. After the leg, they are responsible for analyzing their samples and reporting the results in manuscripts in the *Proceedings of the Ocean Drilling Program Scientific Results* volumes or in any recognized international journal that publishes in English, as outlined in the Publications Policy on the ODP Web site (**www-odp.tamu.edu/publications/policy.html**). All shipboard scientists are encouraged to assist the Co-Chief Scientists in preparing a press release for general distribution to news media immediately after the cruise.

Quick Guide to Getting Started as a Shipboard Paleomagnetist

This section is intended for paleomagnetists who have never participated in an ODP leg or who have not been on a leg for more than 2–3 years. First and foremost, you should prepare before getting to the ship. If you have preferred sampling tools, plastic sample boxes, data analysis software, and reference material, then start packing these in advance. If you do not have a strong preference, the ship has plenty of sampling tools and plastic boxes as described in **"Discrete Samples,"** p. 8, in "Coordinate Systems and Sampling Conventions." The shipboard library has many standard paleomagnetism textbooks, some of which we keep in the paleomagnetism laboratory for quick reference. The reference material overall is sparse. Plan to bring papers related to the specific science of the cruise in which you will be participating. If you have questions about equipment on the ship or you want to bring some of your own equipment or a computer, contact the staff scientist for your cruise as early as possible.

One of the main steps in being prepared is to understand what is done on the ship. Prior to sailing it is a very good idea to read the "Explanatory Notes" chapters from the *Initial Reports* volumes of several recent cruises, particularly those with coring objectives most similar to the leg on which you plan to participate. Focus on the paleomagnetism section and at least skim the other sections to understand core flow from the time the core is pulled up to the rig floor, as it passes through the laboratories, and until it is stored for shipping to one of the repositories. *Initial Reports* volumes are available on the Web (**www-odp.-tamu.edu/publications/IR.HTML**).

Each cruise has a scientific prospectus that gives background information about the cruise and outlines the cruise objectives, operations plan, logging plan, and sampling strategy. The prospectuses are available on the Web (**www-odp.tamu.edu/publications/SCIPROSP.HTML**). In addition, oncoming paleomagnetists should read as much of this technical note and the papers cited in it as possible.

All oncoming paleomagnetists would also benefit from communicating with the offgoing paleomagnetists and the offgoing paleomagnetism laboratory technician in port. If this is not possible, much can be learned from reading the draft version of the "Explanatory Notes" chapter of the previous leg, which is kept in black three-ring binders in the shipboard library. The paleomagnetism section of the site chapters and the technician's report for the previous leg and other past legs also provide valuable information. Look over the Long Core Labview manual. Ask the oncoming paleomagnetism laboratory technician for an overview of the laboratory. If possible, have him or her teach you how to operate the cryogenic magnetometer (also referred to as the superconducting rock magnetometer or long-core magnetometer), and then

practice, learn about the noise level, and test the calibration of the instrument while in port. Remember that all the technicians are busy with port call activities, so they may not be available until after the ship is under way. Feel free to look around the laboratory to familiarize yourself with the equipment that is available, but use caution and discretion before using instruments or software unless you are very familiar with them or have been trained by the technician.

Overview of the Shipboard Laboratory

The shipboard paleomagnetism laboratory is shown in Figure F1, and a virtual tour of the Bridge Deck, which includes the paleomagnetism laboratory, is available from the ODP Web site at www-odp.tamu.edu/drillship/index_6.html. Detailed descriptions of the equipment available in the shipboard paleomagnetism laboratory are provided in "Remanent Magnetization," p. 12, "Magnetic Susceptibility," p. 21, "Alternating Field and Thermal Demagnetization," p. 27, "Laboratory-Induced Magnetization," p. 31, and "Core Orientation," p. 33. Two basic magnetic measurements are conducted on whole- and split-core sections and discrete samples: (1) magnetic remanence and (2) magnetic susceptibility.

F1. Schematic of ship and shipboard paleomagnetism laboratory, p. 61.

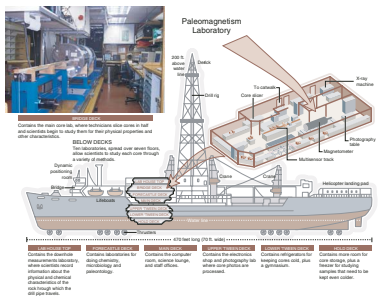

Measurements of magnetic remanence include natural remanent magnetization (NRM), NRM after thermal or alternating field (AF) demagnetization, and remanence resulting from magnetizations induced in the laboratory, such as isothermal remanent magnetization (IRM), anhysteretic remanent magnetization (ARM), and partial anhysteretic remanent magnetization (pARM).

Magnetic susceptibility is measured routinely at a high resolution (2–10 cm) on whole-round core sections. Equipment to monitor the susceptibility of standard-sized discrete samples and to measure the anisotropy of magnetic susceptibility (AMS) is available for special rock magnetic projects.

The majority of the paleomagnetic equipment is housed on the starboard side of the core laboratory between the photo table and the core description area (Fig. F1). The whole-core susceptibility meter is installed on the multisensor track (MST) in the physical properties area. Whole-core susceptibility data are collected by the physical properties scientists (see Blum, 1997) and shared with paleomagnetism and other shipboard scientists (e.g., the stratigraphic correlator for hole-to-hole correlation) (e.g., Hagelberg et al., 1992).

Superconducting Rock Magnetometer

The work-horse of the paleomagnetic shipboard laboratory is the 2G Enterprises superconducting rock magnetometer (SRM). It is used primarily for continuous remanence measurements on archive halves of cores. AF coils arranged on-axis with the magnetometer and set within the magnetometer's mu-metal shielding allow uniform demagnetization of the cores, so that both NRM and demagnetized remanences can be measured. The cryogenic magnetometer can also be used to measure and demagnetize discrete samples.

Spinner Magnetometer

The Molspin Minispin spinner magnetometer is a basic field unit interfaced with a personal computer (PC) for control and data acquisi-

tion. After the upgrade of the SRM in 1996, the usage of the Molspin magnetometer is minimal.

Magnetic Susceptibility Meter

The Bartington magnetic susceptibility meter has two sensors: one for discrete samples, and a loop for whole-core pass-through measurements. The 80-mm susceptibility loop is part of the MST (see Blum, 1997). The second susceptibility meter with a loop for discrete samples is available in the paleomagnetic laboratory.

Kappabridge KLY-2 Magnetic Susceptibility System

The Kappabridge KLY-2 magnetic susceptibility system measures magnetic susceptibility (MS) and AMS of discrete samples. Because the shipboard environment is magnetically noisy, the sensitivity is less than in shielded rooms in shore-based laboratories but is sufficient for most shipboard purposes, especially when measuring igneous rocks. The instrument is a semiautomatic inductivity bridge, operated in conjunction with a Pentium PC.

Alternating Field Demagnetizer

A DTECH alternating field demagnetizer (model D-2000) is available for demagnetization of discrete samples of rock or sediment. The unit can demagnetize multiple samples (e.g., 5 of the 10 cm^3 samples) at the same time at peak AFs of up to 200 mT. The D-2000 can also be used to impart an ARM, in which a direct current (DC) magnetic field is produced continuously across the AF demagnetizer coil, or a pARM, in which the user selects the demagnetization interval over which the field is applied.

Thermal Demagnetizer

A Schonstedt thermal demagnetizer (model TSD-1) is used for thermal demagnetization of dry samples over a temperature range of 0°–800°C. The instrument contains magnetically shielded heating and cooling chambers.

Impulse Magnetizer

An ASC impulse magnetizer (model IM-10) is available for studies of the acquisition of IRM, the anisotropy of IRM, and the coercivity of remanence. The unit provides short-term fields of up to 1.3 T.

Fluxgate Magnetometer

The Schonstedt Portable Three-Axis fluxgate magnetometer can measure small ambient fields, with a range of ±200 µT and a sensitivity of 1 nT. The sensor fits into small spaces such as the sample access tube of the cryogenic magnetometer.

Hall-effect Magnetometer

A Hall-effect magnetometer (model MG-5DP), capable of measuring DC and alternating-current (AC) fields over three orders of magnitude

(±0.01, ±0.1, and ±1T), is available for calibration of demagnetization coils and measurement of strong DC fields.

Tensor Tool

The Tensor tool measures the orientation of cores recovered by the advanced hydraulic piston corer (APC) with respect to the downhole ambient magnetic field. The instrument contains a three-axis magnetometer and two perpendicular gravity sensors that record the orientation of the core liner with respect to magnetic north and vertical.

Coordinate Systems and Sampling Conventions

Coordinate System

After cores arrive on deck, they are cut into 1.5-m-long sections and stored in racks for temperature equilibration. The first measurement station is the MST in the core receiving area, where MS, compressional wave (*P*-wave) velocity, gamma ray density, and natural gamma radiation are measured on whole-core sections (see Blum, 1997).

After cores are split either with a wire line or a saw, the half cores are designated as archive-half cores and working-half cores. A single line on the outside of the core liner indicates the archive half, and a double line indicates the working half (a mnemonic aid is that "A," as in "archive," has one pointed end = single line, whereas "W," as in "working," has two pointed ends = double line). Figure F2 shows the relative core orientation conventions (+x is vertical upward from the split-core surface of archive halves, +y is left along split-core surface when looking upcore, and +z is downcore) established to place core measurements in a relative reference frame. The same coordinate system is used for physical properties and structural measurements. Placement of this relative coordinate system in a geographical reference frame can be achieved in some instances with the Tensor tool, a downhole orientation device (see "Core Orientation," p. 33), or the ChRM. It may also be possible to reorient core pieces by matching images of the core exterior with downhole logging images of the borehole wall, such as those obtained with the Formation MicroScanner or Ultrasonic Borehole Imager logging tools. On the ship, nondestructive measurements are made on the archive-half cores, whereas the working-half cores are available for measurements that physically disturb parts of the cores and for the removal of samples for shipboard and shore-based studies.

F2. Orientation system, p. 62.

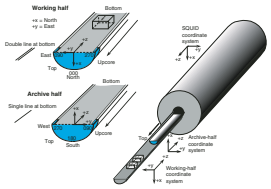

The archive-half core is used for visual core description, paleomagnetic measurements using the cryogenic magnetometer, color reflectance measurements, and photography. After core photographs have been taken, the archive-half cores are stored in plastic tubes and refrigerated.

The working-half core is used for physical property measurements that require inserting probes into the sediment (*P*-wave velocity, vane shear strength, and thermal conductivity). Afterward, it is sampled by the paleomagnetic and physical properties scientists before sampling for general shore-based projects on the sampling table for immediate shipboard measurements.

Figure F2 illustrates the coordinate system of the SRM in comparison to the archive- and working-half coordinate systems for reference. The magnetometer software handles the conversion into the core coordinate system, but the raw superconducting quantum interference device

(SQUID) voltages are provided in the magnetometer coordinate system (see "Magnetic Susceptibility," p. 21).

Discrete Samples

Hard rocks are sampled with a nonmagnetic drill (standard 2.45 cm diameter or other smaller diameter bits that are available on the ship) on a drill press in the sample preparation area. Alternatively, cubes may be cut in a variety of sizes, with the standard being 2 cm × 2 cm × 2 cm, although smaller sizes may be preferred for strongly magnetized rocks or when core material is rare.

There are currently three different nonmagnetic plastic sampling boxes in use for soft sediment sampling (Fig. F3):

1. The "old" ODP standard box with 2.5 cm × 2.5 cm × 1.87 cm external dimensions (internal volume = 6.8–7.1 cm^3). This box is currently being phased out.
2. The "new" ODP standard box ("French cubes") with 2.2 cm × 2.2 cm × 2.3 cm external dimensions (internal volume = ~6.9–7.2 cm^3).
3. The "Japanese cubes" with 2.2 cm × 2.2 cm × 2.3 cm external dimensions and cut corners (internal volume = ~6.8–7.1 cm^3).

F3. U-channel and boxes, p. 63.

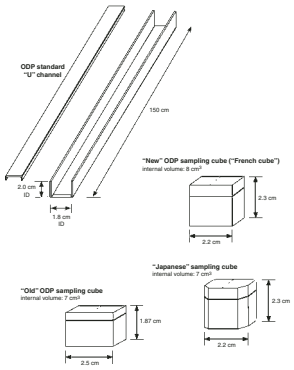

Internal volumes were estimated by filling the cubes with water and then measuring the volume of water in a graduated cylinder. Calculation of volumes from caliper measurements of the interval dimensions are slightly larger than the values given above. For all practical purposes, the sample volumes are 7 cm^3 for any of the plastic sample boxes when they are filled.

Samples are typically collected in the boxes in two ways. The box can be pushed into the sediment and removed with a U-shaped wire mounted on a handle (Fig. F4). Alternatively, an extruder can be pushed into the sediment to remove the sample, which is then extruded into a plastic box with the aid of a piston (Fig. F4). Extruders that are longer than the sample box is deep work better because they allow the bottom portion of the sediment (that closest to the core liner) to be removed, leaving a flat and less deformed surface for inserting into the sample box. It is also possible to retain just enough sample in the extruder to always fill the sample box by marking the appropriate distance on the piston. Extruders with sharp cutting edges work especially well in more indurated sediments, where pushing sample boxes or drilling or cutting samples may not be practical. The azimuthal orientation of the extruded samples is 180° opposite (equivalent to the orientation of the archive-half) to the orientation of the pushed samples. *Caution:* The extrusion process introduces one additional step during sampling, which can lead to orientation errors if not done carefully.

F4. Sampling techniques, p. 64.

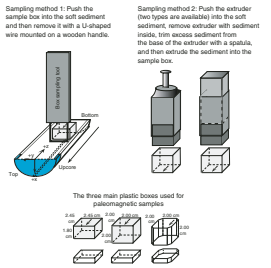

U-Channel Samples

U-channel samples (Tauxe et al., 1983; Nagy and Valet, 1993; Weeks et al., 1993) have become increasingly popular because of the large amount of paleomagnetic and rock magnetic data that can be obtained rapidly and at a high resolution when the samples are measured in a the narrow-access long-core SRM (often referred to as a U-channel magnetometer). The revised sampling policy from July 1998 (last updated June 1999) allows the sampling of the "temporary" archive

halves, which brought the opportunity to sample spliced core sections of considerable length. More than 3300 U-channels have been taken since Leg 138, with >2300 of them taken just within the last 3 years. They are usually sampled postcruise in the repository; however, a few U-channels are usually stocked on the ship for shipboard sampling. U-channels are collected by pushing rigid U-shaped plastic liners (2 cm × 2 cm cross-section; up to 1.5 m in length) into the split core sections (Fig. F5). Each sample is taken out of the core by guiding a fishing line under the U-channel. A plastic cap is then placed on the U-channel, and the ends are sealed with tape to minimize dehydration of the sediment. To further prevent dehydration, the U-channels can be stored similarly to the split-core sections, which are put in D-tubes with wet sponges in the plastic end caps. Typically four or five U-channels fit within a D-tube.

F5. U-channel sample being collected in soft sediment, p. 65.

Shipboard Data Management Environment

Data Acquisition Interfaces and Controls

Data acquisition programs on the ship have been written in a variety of programming languages. In some cases, the acquisition programs are provided by the instrument vendor, and in other cases, they have been written by ODP staff to provide interfaces more applicable to the unique shipboard environment. Over the past several years, Labview has been used as the programming language for many of the acquisition programs. Data acquired by the acquisition programs for most instruments are uploaded into the ODP database.

The SRM control program Long Core (version 3, at the time this was written) is written in Labview (PC) for 2G Enterprises by Bill Mills and customized for ODP. The Minispin program PMagic (version 1.2) is written in Visual Basic by Jakub Rehacek, and the DTECH-2000 control program has been supplied by the vendor. The control program for the Kappabridge is a Fortran program supplied by the vendor, Geofyzika Brno. Neither the Minispin nor the Kappabridge are interfaced with the database. Instead, it is the role of the shipboard paleomagnetists to ensure that data collected with these instruments are archived in the *Initial Reports* volume.

Data Upload Utilities

Once data are acquired with the SRM and located on a local drive, they must be uploaded to the Oracle database. Although this procedure could be fully automated and become part of the data acquisition program, it was decided that an interactive user quality control should separate the two functions. Invalid or erroneous data are frequently acquired, particularly on highly automated systems such as the SRM. The user has the option to delete such data from the local directory before triggering upload to the database, which avoids excessive editing within the database, a process that involves significantly more risk and effort. The data upload is handled through a separate upload utility (CRYOEDIT; **www-odp.tamu.edu/isg/appsdev/docs/cryoedit.pdf**) and is the responsibility of the ODP technical support representative, but scientists may learn the procedure and operate it themselves.

Database and Data Models

The ODP Oracle database is designed specifically for ODP's unique shipboard environment and user needs. The system includes >250 data tables in a complex relational scheme, capturing data from the initiation of a leg through core recovery and curation, operational aspects, physical and chemical analyses, core description, and sampling. The paleomagnetic data model is relatively simple. Data for the SRM are contained in four tables (Fig. F6) with related tables for sample identification and depth data shared with other laboratories. MS as part of the physical properties area database model contains five tables (see Blum, 1997). The Tensor tool data tables are presented in Figure F7. Updated data models can be viewed on the Web (**www-odp.tamu.edu/database/janusmodel.htm**) and are included in *Technical Note* 37 (ODP Information Technology and Data Services, 2007). Details of the file formats and example data files are given in **"Appendix A,"** p. 50.

Discrete MS data, AMS data, and magnetic data acquired with the spinner magnetometer are not routinely collected and are not stored in the database. AMS data are usually few and are reported in the *Initial Reports* volume. Spreadsheets containing these data are stored at ODP and can be obtained from the ODP Data Librarian. As noted above, the shipboard paleomagnetists should also ensure that data collected with these instruments are archived in the *Initial Reports* volume.

Data Access and Standard Queries

Access to the database is provided by standard Web queries either through the shipboard network or on shore through the Internet (Fig. F8) (**www-odp.tamu.edu/database**). Standard queries allow the download of discrete and long-core data, MS values, and Tensor tool core orientation data in a format that can be used for data analysis and representation with commercial plotting software.

Sample Identifiers and Depth Calculation

Sample Identifiers

In the relational ODP database, redundancy of information is minimized for efficient data management. For example, site, hole, core, and section information is entered in specific tables linked in a logical way, and all measurement locations in a particular section are linked to the <Section> table. Similarly, if a core specimen is extracted for shipboard or shore-based analysis, the basic curatorial information is accessed through the <Sample> table, which is linked to the <Section> table, and so on. In the paleomagnetic database models presented in the following sections, the field <section_id> alone or with the fields <interval_top> and <interval_bottom> are the links to the more specific information in the appropriate tables. The <Sample> and <Section> tables are listed in Figure F9.

Depth Types

Measurement locations or sampling locations are identified by leg, site, hole, core, core type, section, and interval (measured in centimeters with 0 cm starting at the top of each section). For example, an SRM measurement made at 40 cm from the top of the third section from the second core collected with the APC in Hole E at Site 1062 during Leg

F6. Database data model for paleomagnetism data, p. 66.

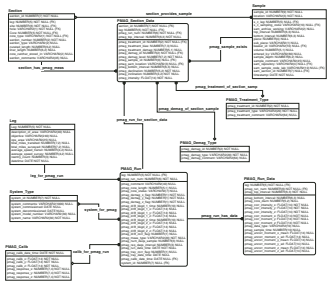

F7. Database data model for core orientation data, p. 67.

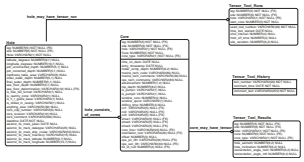

F8. Web page for database queries, p. 68.

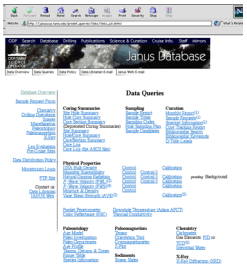

F9. Database data model for core log information, p. 69.

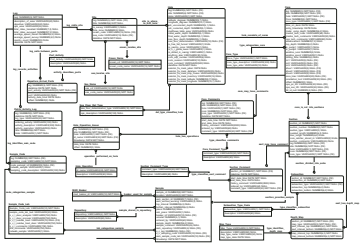

172 would be identified as Sample 172-1062E-2H-3, 40 cm. Similarly, a plastic box sample taken from the same section, but from the interval that is 50 to 52 cm below the top of the section, would be referred to as sample 172-1062E-2H-3, 50–52 cm.

The actual depth of the sample in the borehole can be calculated in a number of ways. The standard method is to place the top of the core at the top of the cored interval, where the cored interval is determined by drill pipe measurements and is given in units of meters below seafloor (mbsf). Each cored interval is generally 9.5 or 9.6 m long, which is the length of a core barrel, although the length may be shorter than this.

Of course, mbsf depth is only an estimate of the true depth below seafloor and may differ from the true depth for several reason. Ship motion, tides, heave, and deviation of the drill hole from vertical can all cause errors in drill pipe measurements. Depth errors may also result from biases in core recovery estimates, which commonly exceed 100% for APC cores. These artificially high recovery percentages probably result from decompression of sediments (Farrell and Janecek, 1991; Hagelberg et al., 1995; MacKillop et al., 1995; Moran, 1997), entrance of excess sediment into the core barrel as some of the sediment displaced by the walls of the coring shoe is forced inward (pp. 93–96 of Hvorslev, 1949), and to curation practices, in which soupy core material commonly occurring at the top of many cores are curated as part of the core (Acton et al., 2001). In reality, much of the soupy material results from sediment falling into hole or from sediment being stirred at the bottom of the hole. This happens as the roller cone bit, which is part of the bottom-hole assembly (BHA), advances from the top of the core previously recovered to the top of the core that is next to be recovered. If the ship heaves upward as the piston strokes into the sediment, then the debris in the hole can be recovered. Additional expansion of the upper part of each core can occur because the top of the core is exposed to circulating water, particularly as the water jets from the BHA are cleaning out the hole.

Incomplete recovery also results in potential depth errors because ODP curation convention assumes the top of the core corresponds to the top of the cored interval. For example, in the case where there is only 1 m recovered from a 9.6-m-long cored interval, the top of the core may have come from as much as 8.6 m deeper than that estimated by the mbsf convention.

Duplicate recovery within a hole, in which the piston corer repenetrates the same sediment sequence either by piercing the side wall of the borehole or by the BHA shifting laterally in very water saturated and unconsolidated sediment, can also cause depth errors (e.g., Robinson, 1990). Depth errors also result from core deformation, such as "suck-in" that occurs when sediment is sucked up into the core liner. Smaller depth errors result from minor core distortion that occurs to some degree in most APC cores, such as bowed or sheared sediment near the core liner caused by friction as the sediment passes through the coring shoe and into the core liner (pp. 93–100 of Hvorslev, 1949; Acton et al., 2002).

If a complete stratigraphic section is to be constructed, multiple holes are drilled at the same site and a composite section is developed using the meters composite depth (mcd) scale. Examples of composite depth scales and background information on their construction is available (e.g., Prell, Gardner, et al., 1982; Ruddiman et al., 1987; Ruddiman, Kidd, Thomas, et al., 1987; Ruddiman, Sarnthein, Bauldauf, et al., 1988; Alexandrovich and Hays, 1989; Robinson, 1990; Farrell and Janecek,

1991; Hagelberg et al., 1992, 1995; Curry, Shackleton, Richter, et al., 1995; Acton et al., 2001; Barker, 2001). The mcd scale is constructed with its own rigorous conventions and should not be confused with a true depth scale. Most mcd scales are expanded by 2%–20%. Contraction of the mcd scale to one closer to a true depth scale can be done by correlating the complete stratigraphic section constructed from the mcd scale with downhole logging data, where depths are determined by a wireline measurement.

Additional corrections can be applied to derive a more accurate approximation to depth below seafloor. These and other depth issues are explained in detail in a workshop report (Blum et al., 1995). The redefined concepts are integrated in the new database, which features a depth map that allows the rapid calculation of any depth type provided that pertinent data have been acquired and entered.

REMANENT MAGNETIZATION

Principle

Physical Background

The permanent magnetism present in a rock before any treatment is termed the NRM. Often the magnetization remaining after various demagnetization treatments, but not after imparting artificial magnetization, is also referred to as the NRM. Because many artificial magnetization components are commonly demagnetized and analyzed by paleomagnetists today (e.g., ARM and IRM), the usage for NRM has become somewhat complicated. To be specific that the remanence being measured is that before any laboratory treatment, terms like "original NRM" or "NRM prior to demagnetization" are commonly used, although some paleomagnetists would still simply use the term "NRM." Similarly, common usages for the remanent magnetization following some level of demagnetization are, for example, "NRM following AF demagnetization at 20 mT," "NRM after 20 mT demagnetization," or "NRM after thermal demagnetization at 250°C." Simply stating "remanent magnetization after 20 mT demagnetization" is ambiguous because the remanence could have been imparted by a variety of means. The use of "natural" in front of remanence magnetization as in "NRM after 20 mT demagnetization" clarifies that the investigator is not looking at an artificially imparted magnetization that has been subsequently demagnetized.

The NRM is usually the vector resultant of the primary magnetization acquired when the rock was formed and the secondary magnetization (which may include several components) acquired during subsequent geological time, or during coring and sampling. The major part of all paleomagnetic investigations involves the recognition and separation of these magnetic components. Magnetic components are commonly isolated by means of partial demagnetization of the natural remanence (thermally or in an AF), as the primary component will normally have a different stability to demagnetization procedures than the secondary components. The ways in which most natural materials acquire their primary remanence is by no means simple and, ideally, each sample needs to be examined in detail to determine the nature and origin of its remanence prior to any interpretation. Because it is often difficult to conclude a magnetization is primary without uncer-

tainty, many paleomagnetists prefer use the term characteristic remanent magnetization (ChRM), which avoids genetic connotations. The different types of remanence acquisition and the magnetization of natural materials are discussed in every standard paleomagnetic textbook (e.g., Stacey and Banerjee, 1974; Piper, 1987; Butler, 1992; Opdyke and Channell, 1996; McElhinny and McFadden, 2000).

Environmental Effects

The NRM can be affected by the coring process, core splitting, sampling, and the magnetic shipboard environment. Although these overprints are generally soft and can be successfully removed by demagnetization techniques, cases where a removal of the coring-induced overprint was not possible have been described (e.g., Curry, Shackleton, Richter, et al., 1995; Fuller et al., 1998; Acton et al., 2002). In addition, the NRM may be ephemeral because alteration of magnetic minerals can be rapid in some sediments when they are exposed to oxygen after being buried in reducing conditions (e.g., Richter et al., 1999; Yamazaki et al., 2000). A detailed discussion of the overprint and other problems is provided in **"Problems with Magnetic Measurements in the Shipboard Environment,"** p. 36.

Use of Remanent Magnetization Data

The ChRM of sediment cores is primarily used for initial *magnetostratigraphic* interpretation in consultation with biostratigraphy to establish an age model. If it is possible to find a proper normalizer to account for variations in the concentration of magnetite and to fulfill a set of established reliability criteria (Tauxe, 1993), magnetic intensity can be used to determine variations in the relative geomagnetic *paleointensity*. Magnetic remanence is also an essential tool in *tectonics and geodynamics* because magnetic inclination is directly related to the latitude at which the magnetization was acquired and changes in the magnetic declination record small- or large-scale block rotations. Declination may also be an important tool for azimuthal core orientation.

Superconducting Rock Magnetometer

Principle

Superconductivity and Josephson Junctions

The most sensitive device for magnetic field detection is the Superconducting Quantum Interference Device (SQUID). The device has been developed for traditional low-temperature superconductors requiring cooling with liquid helium to 4 K (–269°C) and is commercially available from several suppliers.

The key device is a Josephson junction, which is made by sandwiching a thin layer of a nonsuperconducting material between two layers of superconducting material. The devices are named after Brian Josephson, who predicted in 1962 that pairs of superconducting electrons could "tunnel" right through the nonsuperconducting barrier from one superconductor to another.

To understand the unique and important features of Josephson junctions, it is first necessary to understand the basic concepts and features of superconductivity. Many metals and alloys exhibit a phase transition at very low temperatures (within 20° or less of absolute zero). At this

critical temperature (T_c), the metal goes from what is known as the normal state, where it has electrical resistance, to the superconducting state, where there is essentially no resistance to the flow of direct electrical current. What occurs is that the electrons in the metal become paired. Above T_c, the net interaction between two electrons is repulsive. Below T_c, though, the overall interaction between two electrons becomes very slightly attractive as a result of the electrons' interaction with the ionic lattice of the metal.

This very slight attraction allows them to drop into a lower energy state, opening up an energy "gap." Because of the energy gap and the lower energy state, electrons can move (and therefore current can flow) without being scattered by the ions of the lattice. When the ions scatter electrons, it causes electrical resistance in metals. There is no electrical resistance in a superconductor and therefore no energy loss. There is, however, a maximum supercurrent that can flow, called the critical current. Above this critical current the material is normal. There is one other very important property for our purposes: when a metal goes into the superconducting state, it becomes perfectly diamagnetic and expels all magnetic fields, as long as the magnetic fields are not too large.

Until a critical current is reached, a supercurrent can flow across the nonsuperconducting barrier that separates the two superconductors; electron pairs can tunnel across the barrier without any resistance. But when the critical current is exceeded, another voltage will develop across the junction. That voltage will depend on time; that is, it is an AC voltage. This in turn causes a lowering of the junction's critical current, causing even more normal current to flow and a larger AC voltage.

The frequency of this AC voltage is nearly 500 gigahertz (GHz) per millivolt across the junction. So, as long as the current through the junction is less than the critical current, the voltage is zero. As soon as the current exceeds the critical current, the voltage is not zero but oscillates in time. Detecting and measuring the change from one state to the other is at the heart of the many applications for Josephson junctions.

Josephson junctions can be fashioned into circuits called SQUIDs (an acronym for Superconducting Quantum Interference Device). These devices are extremely sensitive and very useful in constructing extremely sensitive magnetometers and voltmeters.

A SQUID consists of a ring with two Josephson junctions interrupting the loop. A SQUID is extremely sensitive to the total amount of magnetic field that penetrates the area of the loop—the voltage that you measure across the device is strongly correlated to the total magnetic field around the loop. In a cryogenic magnetometer, a current is induced into the superconducting ring when a magnetized specimen is placed within it. The magnitude of the generated flux can then be measured and processed by a computer to determine the direction and intensity of magnetization of the specimen. For a complete account of the theory see Goree and Fuller (1976).

Superconducting Rock Magnetometers

In the early 1970s, SRMs, also known as cryogenic magnetometers ("cryo"), were developed that can measure weakly magnetized samples more quickly than spinner magnetometers. Superconducting magnetometers contain magnetic sensors that are composed of pick-up coils with SQUID detectors, which are superconducting at liquid helium temperatures (4 K). The magnetic sensors are surrounded by an insulated evacuated space cooled by helium. Pick-up coils connected to SQUID detectors are employed to measure the NRM along one axis or

simultaneously along two or three mutually perpendicular axes. Mu-metal shields are employed to blanket external field variations, and automated systems have been developed to complete AF demagnetizations within this field-free environment. The deployment of superconducting cryogenic technology and the development of long-core magnetometers have important implications for the shipboard paleomagnetic investigations:

1. Remanence can be measured with a single insertion into the sense coils.
2. The increase in sensitivity by one to three orders of magnitude and the rapidity of the measurements permit measurement of a wide range of rock types.
3. Whole cores and split cores can be measured at a high resolution (~5 cm) allowing the real-time acquisition of magnetostratigraphic profiles. The main advantage of the cryogenic magnetometer over all others is not the greater sensitivity but the fact that each measurement only takes a few seconds. This means that numerous repeat measurements are practicable, even on very weakly magnetized specimens, thereby allowing improved resolution of the remanence.

2G Enterprises 750R Superconducting Rock Magnetometer

Equipment

The paleomagnetism laboratory aboard the *JOIDES Resolution* is equipped with the world's only seagoing cryogenic magnetometer (Figs. F1, F10). The system, provided by 2G Enterprises of Mountain View, California, consists of a 2G 750R SRM as the principal instrument.

The first cryogenic magnetometer was installed in the shipboard laboratory in April 1985 during the Leg 103 port call. The built-in AF demagnetization capacity of the long-core magnetometer was 9 mT prior to Leg 123 and was limited to 30 mT until the addition of the new magnetometer at the Leg 168 port call (June 1996).

To extend the time needed between liquid helium fills, the new SRM magnetometer is fitted with a CTI Cryogenics refrigeration unit capable of cooling the magnetometer's inner (vapor-cooled) thermal shield to 18 K, just a few degrees above the liquid helium temperature of 4.2 K. The refrigerator consists of a cold head, mounted on the magnetometer, which is basically a heat pump fed compressed helium by the compressor unit and the compressor itself, which is in turn cooled by the ship's chill water supply. External electronics include the three SQUID consoles and their power supply console, controls and power supply for the Compumotor sample-handling system (Fig. F11), the Compumotor itself, and a power supply and relays for the in-line demagnetization coils.

The cryogenic magnetometer lies inside three concentric mu-metal cylinders. Its AF coil assembly is also contained within these shields. The AF field is limited to 80 mT. A superconducting lead shield surrounds the sensing region and maintains an absolutely stable field within that region (Fig. F12).

The paleomagnetism Marine Specialist monitors the vital signs of the instrument on a regular basis to ensure that temperatures remain constant within the instrument and to check helium boil-off. The cryocooler adsorber is changed annually.

F10. Shipboard cryogenic magnetometer, p. 70.

F11. Electronic boxes for the cryogenic magnetometer, p. 71.

F12. Magnetic field profile, p. 72.

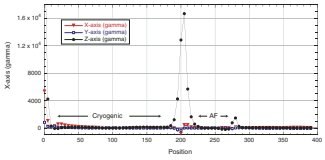

The magnetometer system, including the sample track movement, the energizing of the demagnetization coils, and the measurement of moment, is controlled through a dedicated Pentium PC. The controlling program is called 2G Long Core and is written in Labview. A detailed user guide to the Labview software is available in the laboratory. The main Long Core control panel screen is shown in Figure F13. Sample holders for whole/split cores and for discrete samples are available and can be exchanged easily.

F13. Long Core application screen, p. 73.

Data Acquisition and Algorithms

The 2G 750R SRM is a three-axis instrument configured for split- and whole-core pass-through measurements. The three SQUIDS and their sensors operate simultaneously and continuously, providing the user with a constant voltage output on the digital panel meters of the axis consoles.

The magnetic moments are obtained from the SQUID measurements (see Goree and Fuller, 1976). The SQUID output (S_x, S_y, and S_z) is given as a voltage, which is estimated from the number of flux counts (i.e., flux quanta) plus a proportion of a single flux count that occurred when the sample was in the sensor region. This proportion of a single flux count has been called the analog signal (f_a). For the new magnetometer, f_a is a fairly small part of the total signal (i.e., the number of flux counts will generally be >>1). The voltage (V) is directly related to the analog flux; thus, the SQUID output can be considered to be in units of flux quanta or voltage. SQUID voltage is converted to a magnetic moment in units of emu by multiplying by a calibration constant (supplied by 2G Enterprises) for each coil (C_x, C_y, and C_z). Calibration constants used with the system configuration as of October 1996 are $C_x = 8.21 \times 10^{-5}$ emu, $C_y = 8.34 \times 10^{-5}$ emu, and $C_z = 4.32 \times 10^{-5}$ emu.

Thus, to obtain the magnetic moments in emu units (M_x, M_y, and M_z) the SQUID output needs to be multiplied by the calibration constants

$$M_x = S_x C_x,$$

$$M_y = S_y C_y, \text{ and}$$

$$M_z = S_z C_z.$$

Discrete Sample Intensity

The magnetization per unit volume J is obtained by normalizing the magnetic moments by the volume of the discrete sample (V):

$$J_x = M_x/V$$

$$J_y = M_y/V$$

$$J_z = M_z/V$$

Whole and Split Core Intensity

The volume normalization for whole and split cores is more difficult because the volume of core measured by each coil varies because each coil senses a slightly different length of core. In addition, the z-axis of the sample is long relative to the other sample axes, and the z-axis sensor senses a longer interval than the other sensors. This length is re-

ferred to as the effective sensor length. To determine the effective sensor length for each coil, a small sample (effectively a dipole point source) is moved through the sensor region at 1-cm intervals. The variation in the moment as a function of position along the three axes is obtained (Fig. **F14**). The curves are normalized and the area under each curve is estimated. If the curves have negative side lobes (x- and y-axes), the area under the side lobes is subtracted from the total area. The area under the normalized curves gives the effective sensor length (L_x, L_y, and L_z). The effective sensor lengths for the x-, y-, and z-axes, respectively, as estimated during Leg 168 are:

F14. SQUID voltage, p. 74.

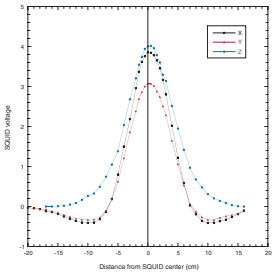

L_x = 6.071 cm
L_y = 6.208 cm
L_z = 9.923 cm

The effective volume (V_e) and intensities for each sensor are determined as follows:

$$V_{ex} = L_x A$$

$$V_{ey} = L_y A$$

$$V_{ez} = L_z A$$

where A is the cross-sectional area of a long sample and r the radius:

$$A = 0.5\ \pi r^2$$

for split cores and

$$A = \pi r^2$$

for whole cores. ODP core liners have an internal radius of 3.3 cm.

The magnetization per unit volume J is obtained by normalizing the magnetic moments by the effective volume:

$$J_x = M_x / V_{ex}$$

$$J_y = M_y / V_{ey}$$

$$J_z = M_z / V_{ez}$$

Magnetic inclination and declination are then calculated from J_x, J_y, and J_z using standard procedures as outlined in any paleomagnetic reference book and the Long Core User's guide that is available in the shipboard laboratory.

Performance: Calibration and Noise

A cube standard purchased from Geofyzika, which has a volume of 8 cm^3 and an intensity of 7.62 A/m (moment of 6.096×10^{-5} Am^2), is available on the ship for testing the calibration of the magnetometers. Tests conducted on Leg 200 confirmed that all three axes of the SRM agree to >1% with this standard. In addition, the automated tray positioning was checked by putting the standard at known positions and

measuring the tray. The position indicated by the software was found to be good to within 1 cm, which is reasonable given the stretch in the pulley system used to move the sample boat (Shipboard Scientific Party, 2003).

Based on tests conducted during Leg 186 and 200, the background noise level of the magnetometer in the shipboard environment is about 2×10^{-9} Am^2 (Shipboard Scientific Party, 2000, 2003). When the discrete sample tray is placed in the sample boat, the noise level increases, being slightly greater than $\pm 2 \times 10^{-9}$ Am^2 before cleaning (where cleaning consists of using window cleaner and AF demagnetization) and slightly less after. The clean discrete sample tray measurement with the addition of empty plastic cubes in the tray results in noise that can exceed $\pm 3 \times 10^{-9}$ Am^2. From repeated tests made with sample boats and trays before and after cleaning, it can be concluded that dirt on the sample boat or tray dominates the background signal. Even with diligence, it is difficult to keep the trays clean given the amount of core material measured on a typical leg. Furthermore, the split-core sections are in a plastic core liner that generally has been stored in dusty conditions prior to coring and that resides in a metal core barrel just prior to core collection. The noise associated with the core liners will therefore likely be several times greater than the noise associated with the sample boat.

Under favorable clean conditions, the noise level will be thus be about $\pm 2 \times 10^{-9}$ Am^2 or higher. For a split core, given the large volume of core material within the sensing region of the magnetometer, which is ~100 cm^3, the minimum measurable remanent intensities will be greater than $\sim 2 \times 10^{-5}$ A/m. For discrete samples, which typically have volumes of 6–10 cm^3, the minimum measurable remanent intensities will be greater than $\sim 4 \times 10^{-4}$ A/m. Results from measurements from several cruises indicate that accurate measurements are likely to be obtained when both split-core and discrete samples have intensities approximately two to five times higher than the background noise level or when they have intensities greater than $\sim 10^{-4}$ A/m and 10^{-3} A/m, respectively.

Additional directional uncertainty occurs because the tray rotates a few degrees one way or the other as it is pulled through the magnetometer. This affects the accuracy of the moments for the x- and y-axes and, hence, the declination. On Leg 209, Jeff Gee and Miguel Garces noted that the rotation of the tray was systematic. Using calibration standards from Scripps, they determined that a rotation of 7° about the z-axis was necessary to remove the bias when measuring discrete samples. How systematic the rotation is with time and different types of samples is unknown.

Standard Queries

Standard queries through a Web browser (Fig. **F15**) allow discrete and long-core data to be downloaded in a format that can be used for data analysis and representation with commercial plotting software.

The Web queries allow the user to

1. Retrieve long-core NRM and susceptibility data. Depth is expressed either as standard mbsf or mcd if multiple holes were cored and a composite depth model has been established.
2. Cull data at section and core breaks at the desired distance from the break (e.g., half the response curve of the sensor).

F15. Web browser interface for downloading paleomagnetic data, p. 75.

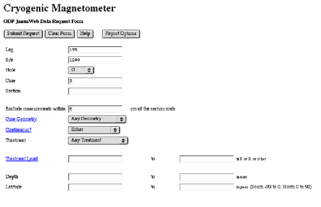

3. Obtain demagnetization data of discrete samples for analysis and representation with ZPlot, a program to analyze and plot paleomagnetic data written and provided by Steve Hurst.

ZPlot files have the following format:

File Name: 0000000
Ancestor File:
Date: 04-01-2001 01:50:54
User Name:
Project Name:
Study Type:
Sample Depth(mbsf)DemagValueDeclinationInclinationIntensityTreatment
1951200A006R01(0)41.400.00292.1629.491.283300E–02standard
1951200A006R01(0)41.405.00290.56–3.056.817800E–03standard
1951200A006R01(0)41.4010.00283.91–16.184.270200E–03standard
1951200A006R01(0)41.4015.00263.71–16.652.439500E–03standard
1951200A006R01(0)41.4020.00240.77–17.032.098700E–03standard
1951200A006R01(0)41.4025.00233.95–14.511.676700E–03standard
1951200A006R01(0)41.4030.00230.79–15.021.400700E–03standard
1951200A006R01(0)41.4035.00227.36–4.671.085300E–03standard
1951200A006R01(0)41.4040.00212.82–11.281.116500E–03standard
1951200A006R01(0)41.4050.00196.40–17.942.955000E–04standard
1951200A006R01(0)41.4060.00154.613.283.831800E–04standard

Documentation and User Manual

A detailed manual for the Long Core software and user manuals for the Zplot program are available in the paleomagnetism laboratory. The Zplot manual is also available on the Web (**www-odp.tamu.edu/isg/appsdev/docs/zplot.pdf**).

Spinner Magnetometer

Principle

The principle of spinner instruments is the generation of an alternating voltage by the continuous rotation of a magnetized sample within or near a coil or fluxgate system. For a given sensor configuration, the amplitude of the output voltage is proportional to the component of magnetic moment perpendicular to the rotation axis, and the phase of the voltage is utilized to relate the direction of the measured component to a reference direction in the sample. The total vector is determined by spinning the sample about a second orthogonal axis, although in practice the sample is rotated successively about three axes to obtain average values of the NRM components and reduce the effect of inhomogeneity.

Molspin Minispin Magnetometer

The Molspin Minispin spinner magnetometer (Fig. **F16**) is a basic, portable field unit interfaced with a computer (currently a laptop) for control and data acquisition. The software (PMagic) driving the Minispin executes spin sequences and calculates declination, inclination, and intensity corrected for the volume of the sample. PMagic also contains procedures for statistical analysis and plotting. A series of mea-

F16. Molspin Minispin spinner magnetometer, p. 76.

surements is made on each sample as it is run through a demagnetization sequence. Ordinarily, six separate spin orientations are required to produce an accurate measurement. In general, the processing rate will vary with the NRM intensity and in response to demagnetization of the samples from a particular lithologic unit.

The Minispin can measure both rock and sediment samples up to 2.54 cm (1 in) cubed in size. According to the manual, the noise level varies from 0.2 mA/m (short spin) to 0.1 mA/m (long spin) for a 12.87-cm^3 sized sample. The minimum measurable intensity is on the order of 0.1 mA/m and the maximum is on the order of 2500 mA/m. Parameters that can be specified in the PMagic software include short (6 s for 24 spins) vs. long (25 s for 120 spins) integration time and sensitivity range and four or six spin positions per sample. In general four spins are sufficient. Six spins are used when the operator is trying to get the maximum accuracy for a weak rock.

Calibration and Measurement

The absolute calibration of the Minispin is carried out with a standard calibration specimen provided by the manufacturer of the instrument. Turn the power supply and the Minispin on, and the motor will spin for ~1 s and the liquid crystal display (LCD) will display "32," indicating that the instrument is functioning correctly. Allow 5 min equilibration time before calibrating.

Start the PMagic software and select the "Spin" menu option to start the spinner session. Select calibration and mount the calibration standard with the V-nick toward the operator and the arrow on the standard pointing away. Select position 1 on the attenuator and select short spin. Rotate the white ring around the sample access clockwise or counterclockwise to adjust the declination to ±2° of 0°. Be careful to adjust only the white ring, not the entire shield cylinder. If the declination value is significantly off (i.e., ~180°), do not try to move the ring all the way around. Something is wrong; likely the standard is backward or the sample holder is not rotating smoothly.

The intensity of the standard needs to be entered next. The value of the current standard in use is 761 mA/m. The Minispin will remeasure the standard and calibrate itself. If the intensity value is not close enough, the calibration procedure can be repeated until the values are satisfactory. Molspin recommends calibrating the Minispin every hour of operation.

After finishing the calibration procedure the Minispin is ready for the measurement of rock specimens.

Note that spinner data are rarely collected and that the ODP relational database model does not include Minispin data. Thus, an interface between the Minispin and the ODP relational database does not exist.

Documentation and User Manual

A detailed manual for the PMagic software and user manuals for the Minispin are available in the paleomagnetism laboratory.

Portable Magnetometer and Probes

Hall Effect Magnetometer

A Hall effect gaussmeter (model MG-5DP), capable of measuring DC and AC fields over three ranges of ±100.0 Gauss (±0.01 T), ±1.000

kGauss (±0.1 T), and ±10.00 kGauss (±1 T) (with 100% over-range capacity in each range) is available in the laboratory for calibration of demagnetization coils and measurement of strong DC fields.

This portable gaussmeter operates according to the Hall effect principle. When a current-carrying conductor is subjected to a magnetic field that is perpendicular to the current flow, a drift current is produced that is perpendicular to both the control current and the magnetic field. If the conductor is a semiconductor, a substantial voltage is produced in the direction of the Hall drift current. The Hall voltage produced is directly proportional to the product of the control current and the strength of the magnetic field.

Precalibrated transverse and axial probes are supplied with the instrument for measuring fields perpendicular and parallel to the axis of the probe, respectively. The instrument is equipped with a peak-reading mode that, when selected, provides peak readings of either positive or negative magnetic field levels. The MG-5DP model will operate either from AC or from sealed lead acid batteries.

Three-Axis Fluxgate Magnetometer

The portable APS520 fluxgate magnetometer in the shipboard laboratory enables measurement of small ambient magnetic fields over the range of 10^{-7} Oe up to 1000 mOe and a sensitivity of 10^{-6} Oe (0.1 gamma). The field is measured simultaneously along three orthogonal directions and is displayed on three front panel digit LCDs.

The fluxgate system consists of a magnetic field measuring probe connected by a 3-m interconnect cable to a power supply and electronic readout console. The small probe size permits measurements to be made in restricted spaces, such as the sample access tube of the cryogenic magnetometer. Other applications for the fluxgate system include measurement of magnetic fields inside steel and mu-metal enclosures, measurement (and zeroing) of the magnetic field trapped in superconducting shields, study of the geomagnetic field, and measurement of magnetic properties of materials.

MAGNETIC SUSCEPTIBILITY

Principle

Physical Background

Magnetic susceptibility is the degree to which a material can be magnetized in an external magnetic field. If the ratio between the induced magnetization and the inducing field is expressed per unit volume, volume susceptibility (k) is defined as

$$k = M/H,$$

where M is the volume magnetization induced in a material of susceptibility k by the applied external field H. Volume susceptibility is a dimensionless quantity. The value depends on the measurement system used:

$$k(\mathrm{SI}) = 4\pi\, k(\mathrm{cgs}) = 4\pi\ \mathrm{G\ Oe^{-1}},$$

where G and Oe are abbreviations for Gauss and Orstedt, respectively. The SI system should be used.

Mass, or specific, susceptibility is defined as

$$\chi = k/r,$$

where r is the density of the material. The dimensions of mass susceptibility are therefore cubic meters per kilogram.

The commonly used MS is measured at very low fields, usually not exceeding 0.5 mT, which have no influence on the NRM. It is therefore referred to as low-field susceptibility (k_{lf}). For comparison, fields of ~50 mT are required to change orientation in magnetite domains. High-field susceptibilities are measured in fields of a few hundred millilteslas and require equipment that is not available in the shipboard laboratory.

In practice, volume susceptibility is generally measured with core logging devices, for which calibration factors must be established to account for the specific geometry and effects of core conveyors and core liners. In the case of discrete specimen measurements, the mass of the specimen can be determined more accurately than volume and specific susceptibility is directly obtained. If average grain density and moisture content of the specimen are known, the specimen measurements can be compared with core logging measurements. Susceptibility values can then be normalized to mass and volume corrected for porosity. This can make susceptibility data more useful for quantitative estimates in conjunction with other mineral phases, such as carbonate, which are always normalized to dry mass.

Anisotropy of Magnetic Susceptibility

MS is a symmetrical second rank tensor that relates the induced magnetization M to the inducing field H:

$$M_i = k_{ij} \times H_j.$$

Six independent components must be determined to define the susceptibility ellipsoid. AMS measures the shape, preferred crystallographic orientation, preferred particle orientation, or preferred distribution of ferr(i)omagnetic and paramagnetic grains. Analysis and interpretation of AMS data requires a detailed characterization of the sources of MS. Studies of AMS are occasionally carried out on hard-rock legs using the Kappabridge. The AMS of sediments is generally too weak to be measured in the magnetically noisy shipboard environment, and the higher rate of core recovery usually limits the work in the laboratory to routine measurements. Although the equipment for AMS measurements is available onboard, the software and analysis programs are very basic and not linked to the Janus database.

Environmental Effects

Cores should be equilibrated to room temperature because MS of most materials is a temperature-dependent property. The temperature dependence of paramagnetic minerals such as clays is described by the Curie-Weiss law, $k = c/T$, where c is the Curie constant and T is the temperature in Kelvin. Assuming a room temperature of 20°C the MS of pure paramagnetic material that is 5°C (10°C; 20°C) below room temperature will be 1.7% (3.5%; 7.1%) higher than the room temperature

susceptibility. The temperature dependence of other materials in the temperature range between 0°C and 20°C is less significant.

Use of Magnetic Susceptibility

MS is used primarily as a relative proxy indicator for changes in composition that can be linked to paleoclimate-controlled depositional processes. The high precision and sensitivity of susceptibility loggers makes this measurement extremely useful for core-to-core and core-downhole log correlation. The physical link of MS to particular sediment components, ocean or wind current strength and direction, or provenance usually requires more detailed magnetic properties studies in a specialized shore-based laboratory.

Magnetic susceptibility is monitored on discrete samples during thermal demagnetization experiments to recognize changes in the magnetic mineralogy caused by phase transitions or oxidation that may occur during heating.

AMS measures the preferred orientation, distribution, or shape of ferromagnetic, paramagnetic, or ferromagnetic and paramagnetic minerals, which can be linked in many cases to bottom currents, compaction, or deformation (Tarling and Hrouda, 1993). The interpretation of AMS measurements usually requires a detailed characterization of the magnetic properties in order to determine the sources of MS.

Bartington MS2C Logger for Whole Cores

Equipment

A Bartington Instruments MS2C system is integrated in the MST for whole-core logging. The main unit is the widely used, versatile MS2 susceptometer for rapid measurements with a number of sensors. The unit has a measuring range of 1×10^{-5} to 9999×10^{-5} (SI, volume specific) or 1×10^{-8} to 9999×10^{-8} (SI, mass specific). It has five front panel controls: on-off switch, sensitivity range switch, SI or cgs unit switch, zero button, measure button, and continuous measurement switch. None of these controls needs to be operated because the instrument is controlled by the MST program. The unit switch should always be on SI. The range switch is typically on the lower sensitivity (1.0), which allows rapid 1-s measurements. The MST program allows the collection of multiple 1-s measurements, which are immediately averaged. This is useful if the sampling period is set, for example, at 3 s for the GRA measurement and there is time to take three susceptometer readings simultaneously. The MS2C loop sensor has an internal diameter of 80 mm, which corresponds to a coil diameter of 88 mm. It operates at a frequency of 0.565 kHz and an AF intensity of 80 A/m (= 0.1 mT). Temperature drift is $<10^{-5}$ SI/hr. The resolution of the loop is 2×10^{-6} SI on the 0.1 range (9 s measuring time).

Dual-Frequency Measurements

Fine-grained magnetic material (single domain; diameter = ~0.003 µm) exhibits frequency-dependent susceptibility. The coefficient of frequency dependence can be determined from measurements in dual-frequency mode. The high frequency used is 5.65 kHz. This mode of measurement is rarely used in general and is therefore not implemented for routine measurements in the MST program.

Drift Correction

The Bartington instrument is automatically zeroed at the beginning of each run, before the core enters the loop. Instrument drift may occur during the period of a core section scan. To correct for the drift, a zero-background measurement (MS_{bkgd}) is taken at the end of a core section log. The drift is corrected under the assumption that it is linear over the time of interest (~10 min). The time elapsed between the zeroing of the instrument at the beginning of the run and the background measurement, t_{bkgd}, is measured. For each measurement within the core (MS_{meas}) the elapsed time (t) is also measured, and the background-corrected susceptibility, Ms_{corr}, is calculated as

$$MS_{corr} = MS_{meas} + MS_{bkgd}/t_{bkgd} \times t.$$

Absolute Susceptibility Values

The Bartington instrument output values are relative, volume-specific susceptibilities ($k_{relative}$), which must be corrected before they can be reported in SI units. Currently, no correction is implemented for standard queries from the database. Two ways of correcting the susceptibilities are described here (see also Blum, 1997).

1. Bartington correction factors. Theoretically, the instrument output is in volume-specific SI units for cores with diameters (d) passing exactly through the coil diameter (D) (i.e., if $d/D = 1$). Bartington provides a table relating values of d/D to correction factors that must be applied to the relative susceptibility readings from the meter. For $d = 66$ mm and $D = 88$ mm, $d/D = 0.75$ and the corresponding correction factor is 1.48. Then,

   $$k = k_{relative}/1.48 \times 10^{-5} = 0.68 \times 10^{-5}\ k_{relative}.$$

   This correction does not take into account other effects such as those from core liner and core conveyer boat, and so on.
2. Calibration with laboratory measurements. Absolute susceptibility is easily measured on sample cubes in shore-based or shipboard laboratories (Kappabridge). These measurements can be compared with corresponding readings from the Bartington instrument. Empirical correlation from Leg 154 and Leg 162 data gave correction factors of 7.7×10^{-6} and 8.0×10^{-6}, respectively. On Leg 154, volumes of specimens were not exactly determined and may have been slightly smaller than assumed, which would underestimate the factor.

Performance

Precision is 2×10^{-6} (SI). Susceptibility values in natural marine sediment samples over an interval of only a few meters (Milankovitch or millennial-scale cyclicity) can range from a few tens to several thousands of 10^{-6} SI units. Typically, variations are two to three orders of magnitude greater than the precision. This makes MS one of the most precise proxies for stratigraphic changes and extremely useful for core-to-core correlation. Accuracy is 5% (according to Bartington).

Spatial Resolution

Blum (1997) determined the full-width-half-maximum (FWHM) response from measurements of four thin discs with varying amounts of iron dust and determined that the widths associated with half-maxima ranged from 4.0 to 4.4 cm. The width along the core axis corresponding to >99% response is ~15 cm. It is recommended that the first and last measurement in each core section be taken 3–4 cm away from the edge to avoid any deconvolution of edge effects.

Bartington Sensor for Discrete Samples

Equipment

The paleomagnetism laboratory is equipped with a Bartington Instruments magnetic susceptibility meter (model MS2), a power supply, and a dual-frequency sensor unit (MS1.B 10 cm^3 single sample well) for performing discrete measurements of MS (Fig. F17).

F17. Bartington Instruments magnetic susceptibility meter, p. 77.

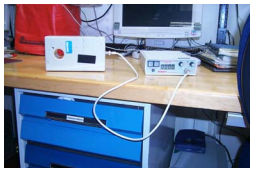

The MS1 sensor contains an inductor, which, together with a capacitor and a current-controlled oscillator, creates a low-frequency alternating magnetic field at a frequency of 0.565 KHz and an AF intensity of 80 A/m (= 0.1 mT). Any magnetic material brought within the influence of this field will effect a change in frequency of oscillation. This change is transmitted to the MS2 meter via a coaxial interconnection cable.

The MS2 meter converts the pulse information from the sensor into an initial susceptibility value. Power for the instrument may be supplied from either a 12-V DC adaptor or from internal rechargeable NiCd batteries.

Dual-Frequency Measurements

Fine-grained magnetic material (single domain; diameter = ~0.003 µm) exhibits frequency-dependent susceptibility. The coefficient of frequency dependence can be determined from measurements in dual-frequency mode. The high frequency used is 5.65 kHz.

Absolute Susceptibility Values

The instrument is preset to display the susceptibility value directly in one of the dimensional systems, thus producing a basic mass or volume specific unit of:

	Mass	Volume
Symbol	X	k
S.I. (used by ODP)	10^{-8} (kg/m^3)	10^{-5}
cgs	10^{-6} (g/cm^3)	10^{-6}

Susceptibility values assume a sample volume of 10 cm^3. Displayed susceptibility values ($k_{display}$) have to be corrected for their volume (V in cm^3) by

$$k = k_{display} \times 10/V \times 10^{-5}$$

for volume specific susceptibility in the SI system.

Performance

Two sensitivity positions are provided with the instrument: range 1 or 0.1. Accuracy on the order of 1.0×10^{-5} SI can be obtained with a 1-s measurement cycle (1 range) and an accuracy of 0.1×10^{-5} SI with the 10-s cycle (0.1 range). The Zero (Z) and Measure (M) functions are selected on a three-position toggle switch. Measurements are displayed on a four-digit LCD panel.

Kappabridge KLY-2

The Kappabridge KLY-2 magnetic susceptibility system (Fig. F18) measures MS and AMS of hard rock or sediment samples at sensitivities of 0.05×10^{-6} SI to $200{,}000 \times 10^{-6}$ SI within a series of 11 ranges. The instrument's operation is based on measurements of inductivity changes in a coil due to a rock specimen. The semiautomatic inductivity bridge is operated in conjunction with a Pentium PC and manufacturer-supplied software. The software package includes tensor calculation and statistics, graphic data display and printout, and data storage.

For magnetic anisotopy determinations, susceptibilities are measured in 15 directions (Fig. F19); the susceptibility tensor is determined using the least-squares method, and the accuracy of the anisotropy is determined according to the methods of Hext (1963) and Jelinek (1978). The standard sample size is 10 cm^3, although fragments may be measured in a 40-cm^3 container. The front panel contains the power and start/reset switches, a range selector, a status display, a zero setting, and a digital data display. Details of instrument operation and data analysis are provided in a manual supplied by the manufacturer. Other accessories include a computer interface manual, a step-by-step operation manual, and reports from users on previous legs. Also, various specimen holders and a calibration standard can be found in a black briefcase stored in the laboratory.

Note: The instrument's high accuracy, fast measuring rate, and outstanding sensitivity makes it possible to measure specimens with very weak magnetic properties. But as a shipboard instrument onboard the *JOIDES Resolution,* the Kappabridge receives relatively little use because of its very high sensitivity amidst magnetically noisy surroundings. Thus, the location of the sensor is an important factor when using the system. Avoiding placement of the sensor near computer terminals, other instruments, and metal fixtures will certainly improve its performance. Overall, the best results come from measuring samples that have fairly strong magnetic properties (Range 5 and higher).

Zeroing and Calibration

After turning the Kappabridge on, the instrument needs to be zeroed with the Im (on the meter) and Re (on the sensor) knobs until the needles in the two displays on the left side of the meter point to zero. Detailed instructions are provided in the manual and in "Appendix B," p. 51. A calibration standard is provided in the black briefcase together with other accessories. The instrument is very stable and calibration should not be necessary, but it is good practice to measure the standard occasionally to make sure the instrument is properly calibrated ("Appendix B," p. 51).

F18. Kappabridge KLY-2 magnetic susceptibility system, p. 78.

F19. Determining magnetic anisotropy, p. 79.

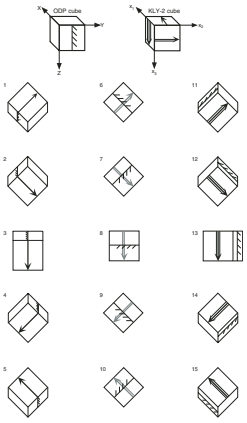

Maintenance

Turn the susceptibility bridge off when not in use. Keep the bridge and sensor covered when not in use.

ALTERNATING FIELD AND THERMAL DEMAGNETIZATION

Principle

Recognition and removal of secondary NRM is the major goal of paleomagnetic laboratory work. Thus, paleomagnetists stress the importance of isolating the characteristic component of NRM by selective removal of secondary NRM. Partial demagnetization experiments, using either AF or thermal demagnetization, are routinely performed in the laboratory using various instruments to isolate ChRM.

Alternating Field Demagnetization

Demagnetization consists of applying a decaying alternating magnetic field to a sample. In the absence of external direct magnetic fields and significant distortion in the applied AF, the sample will be "cleaned" of any remanent magnetization of coercivity less than the peak intensity of the applied AF. This cleaning is the result of randomizing the mobile magnetic domains along the axis of the applied field.

Because it is decaying, the amplitude of each half-cycle of the applied AF is smaller than its predecessor. With each half-cycle, the domains whose coercivities are less than the applied field align themselves with the field. During each half-cycle of the AF, a small percentage of these mobile domains will have coercivity greater than the following half-cycle and will therefore become fixed in direction. In this way, equal numbers of domains will be magnetized in the positive and negative directions oriented along the axis of demagnetization, resulting in a net zero remanent field on the sample.

AF demagnetization is often effective in removing secondary NRM and isolating characteristic NRM (ChRM) in rocks with titanomagnetite as the dominant ferromagnetic mineral. In such rocks, secondary NRM is dominantly carried by multidomain (MD) grains, whereas ChRM is retained by single-domain (SD) grains. MD grains have coercivity (h_c) dominantly <20 mT (200 Oe), whereas SD grains have higher h_c. AF demagnetization thus can remove a secondary NRM carried by the low-h_c grains and leave the ChRM unaffected. AF demagnetization is a convenient technique because of speed and ease of operation and is thus preferred over other techniques when it can be shown to be effective.

Thermal Demagnetization

Relaxation Time and Blocking Temperature

In order to discuss the theory behind thermal demagnetization of a specimen, it is necessary to understand the principles of *relaxation time* and *blocking temperature* for a SD grain. Relaxation time, the time over which remanent magnetization of an assemblage of SD grains decays, may vary over many orders of magnitude. Relaxation time for SD grains of a given material at a constant temperature depends on grain volume (v) and microscopic coercive force (h_c). Grains with low product ($v \cdot h_c$)

have short relaxation time, whereas grains with high product ($v \cdot h_c$) have long relaxation time. Ultimately, these properties help to define the range over which an SD grain will remain stable.

Relaxation time, however, has strong temperature dependence. For instance, relaxation time for an elongate SD magnetite grain with a length of 0.1 µm and a width of 0.02 µm is <1 µs at 575°C but exceeds the age of Earth at 510°C. With decreasing temperature, this grain changes behavior from *superparamagnetic* (unstable; it will decay to zero very soon after removal of the magnetizing field) to stable SD at 550°C. The temperature at which this transition occurs is the *blocking temperature*. Between the *Curie temperature* (T_C; temperature at which saturation magnetization becomes zero; 580°C for magnetite) and the blocking temperature (T_B), the grain is superparamagnetic. Below T_B, relaxation time increases rapidly during continued cooling. SD grains with short relaxation time also have low T_B.

Rocks have distributions of ferromagnetic grain sizes and shapes yielding distributions of T_B between T_C and surface temperatures. The strong dependence of relaxation time on temperature and the transition in behavior from superparamagnetic above T_B to stable below T_B are critical to understanding acquisition of thermoremanent magnetism.

Theory of Thermal Demagnetization

The procedure for thermal demagnetization involves heating a specimen to an elevated temperature (T_{demag}) below the Curie temperature of the constituent ferromagnetic minerals and then cooling to room temperature in zero magnetic field. This causes all grains with blocking temperature (T_B) < T_{demag} to acquire a "thermoremanent magnetization" in H = 0, thereby erasing the NRM carried by these grains. In other words, the magnetization of all grains for which $T_B < T_{demag}$ is randomized, as with low h_c grains during AF demagnetization.

SD grains with short relaxation time also have low T_B and can more easily acquire secondary NRM, whereas SD grains with long relaxation time are stable against acquisition of secondary NRM. Thus, thermal demagnetizers are effective in selectively erasing secondary NRM when $T_{demag} > T_B$ of grains carrying secondary NRM, leaving unaffected the ChRM carried by grains with longer relaxation time (= higher T_B).

Schonstedt TSD-1 Thermal Demagnetizer

The TSD-1 (Fig. **F20**) is used to provide progressive thermal demagnetization of rock specimens by heating them to any specified temperature up to 800°C and then cooling them in a low magnetic field environment (<10 nT). External fields are attenuated by the shield assembly so that the instrument can be operated in a laboratory environment. Figure **F21** shows the magnetic field profile of the TSD-1 and the position in the cooling chamber between 70 and 105 cm in which the magnetic field is the lowest.

The instrument consists of two separate chambers: one for heating and one for cooling. They are arranged coaxially so that as soon as specimens in the furnace chamber reach thermal equilibrium, the specimen holder can be pushed directly into the cooling chamber. Complete chamber isolation and individual controls allow one specimen batch to be blower cooled while another batch is being heated. An outstanding feature of the instrument is its processing speed. The low thermal mass of both the furnace and sample holder promotes rapid heating and

F20. Schonstedt TSD-1 thermal demagnetizer, p. 80.

F21. Magnetic field vs. position, p. 81.

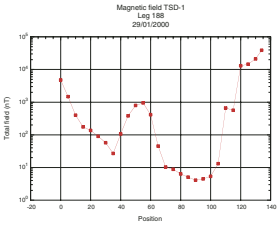

cooling of specimens. The short cycle time helps to minimize the amount of chemical change in specimens by limiting their exposure to high temperature.

The basic sample holder is an open assembly with two inconel tubes on which lies a quartz tray for placing specimens. The quartz tray can hold up to 10 specimens, each 2.5 cm in diameter × 2.5 cm in length. Scientists on board the *JOIDES Resolution* often find it convenient to heat/cool a batch of specimens in the TSD-1 while measuring a second batch on the cryogenic magnetometer and vice versa, thereby speeding up the processing of data on thermally demagnetized samples.

TSD-1 Operation Procedures

1. Place samples on the quartz tray aligned in the same orientation and place the tray on the inconel specimen holder. Open the door to the oven on the forward (left) end and gently insert the holder into the oven just far enough so that the door can be closed. Close the door.
2. Depress the white "POWER" button on the control panel and set the desired temperature with the thumbwheel. Depress the red "HEAT" button to begin heating the samples. The "HEAT" button will initially glow and then will cycle when the oven approaches the final temperature. The average rock specimen reaches equilibrium (heated to its center) between 5 and 10 min after the oven reaches its final temperature.
3. Once the specimens have reached thermal equilibrium, open the door and push the boat into the cooling chamber with a fire resistant, nonconductive rod (we use the wooden rod placed in front of the oven on the shelf, but DO NOT leave the rod in the oven). The boat should be pushed in ~1 in beyond the mouth of the cooling chamber. At this point, another boat of specimens may be inserted into the heating chamber if desired. Close the door and activate the cooling blower by pushing the blue "COOL" button. Cooling time is about half of heating time. *Note:* It is recommended that specimens be moved into the cooling chamber as quickly as possible so as to avoid freezing in undesired remanents.
4. Remove samples after they have been sufficiently cooled.
5. Measure the samples on the SRM and then repeat the process.

Caution: NEVER place plastic sample cubes in oven when heating above 200°C. Instead, remove sediment from the cube carefully and wrap in aluminum foil.

Sedimentary rocks may explode at high temperatures if they contain water. It is best to dry these samples at a moderate temperature before exposing them to higher temperatures.

Do not turn the power off while the samples are still in the oven or cooling chamber, as this may impart spurious magnetizations to the samples.

When handling samples, avoid placing hands on the quartz boat if possible. Fingerprints or smudges may cause permanent marks on the quartz when heated.

Be sure to engrave orientation arrows into the specimen before heating. Indelible ink will not remain visible at higher temperatures.

DTECH Model D-2000 Demagnetizer

A DTECH alternating field demagnetizer, model D-2000, is available for demagnetization of discrete samples of rock or sediment. The D-2000 unit consists of a an AF demagnetizer coil and sample access tube and is enclosed within a mu-metal shield (Fig. F22). The demagnetizer unit is connected to a D-2000 electronics controller and a Crest CA-9 power amplifier. The D-2000 hardware is entirely controlled via a user-friendly, windows-based software application located on a Compaq PC laptop computer.

The unit can demagnetize five to six samples simultaneously at peak AFs of up to 200 mT. The user may also choose a decay rate of the applied demagnetization field intensity within a range of 0.1–0.001 mT/half-cycle. An extremely thorough and useful online help manual is provided with the software.

F22. DTECH model D-2000 demagnetizer, p. 82.

DTech Operation Procedures

Startup Procedure

1. The DTech 2000 demagnetizer is controlled via an RS232 cable that connects the controller to the small Compaq laptop located at the forward end of the laboratory. Make certain this cable is plugged into the rear of the computer.
2. Click on the "D2000v30" icon on the desktop to start the program.
3. Turn on power to the D-2000 controller (switch in back).
4. Turn on power to the Crest power amplifier.
5. Turn both Crest power amplifier channels fully clockwise to "0dB."

Sample Loading and Demagnetization

1. Extract the green sample holder from the demagnetizing unit and place samples in the cutout in the sample holder insert. Be consistent and orient the samples similarly. The D-2000 coils will demagnetize specimens **along the Z-axis** of the unit (fore to aft).
2. Choose Demag Info "Settings" and enter in values for peak demagnetization field and decay rate. Choose "Add" and then "Accept."
3. Choose "Run Demag" and wait for the run to complete.
4. Remove samples and measure on the cryomagnetometer. If desired, repeat the process and enter in a higher peak field demagnetization value.
5. Consult the on-line Help menu for more detailed information concerning the operation of the DTech 2000.

Shutdown Procedure

1. Choose "Halt" if demagnetization is in progress.
2. **Important:** Turn both Crest power amplifier channels to "–80dB."
3. Power off the Crest power amplifier. **Important:** The coil fans are powered from the D-2000 controller power supply. In order to avoid overheating the demagnetizing coil, the fans should be

left running for several minutes after extensive demagnetizing at high field levels.
4. Power off the D-2000 controller.
5. Exit from the D-2000 control program.

LABORATORY-INDUCED MAGNETIZATION

Isothermal Remanent Magnetization and Coercivity of Remanence

Remanent magnetism resulting from short-term exposure to strong magnetizing fields at constant temperature is referred to as *isothermal remanent magnetism* (IRM). In the laboratory, IRM is imparted by exposure (usually at room temperature) to a magnetizing field generated by an electromagnet. IRM is the form of remanence produced in hysteresis experiments and is acquired by ferromagnetic grains with coercive force less than the applied field. The maximum remanence that can be produced is called the saturation isothermal remanent magnetization (SIRM). The field at which saturation is reached depends on the composition and microstructure of the specimen.

Coercivity of remanence is a very useful hysteresis parameter that can be used in determining magnetic mineralogy and grain size and in helping to characterize magnetic mixtures. It is the field that reduces the saturation isothermal remanence to zero.

Impulse Magnetizer

Principle

An impulse magnetizer is designed to produce a short-duration high field pulse for the purpose of magnetizing geological samples. The field is produced by the discharge of energy from a capacitator bank through a coil surrounding the sample cavity. The capacitator bank is first charged to the desired voltage (corresponding to the desired field). It is then discharged through the coil very quickly to magnetize the sample.

The impulse magnetizer is ideally suited for the study of acquisition of IRM and the coercivity of remanence of discrete samples. Both are characteristic rock magnetic properties that are used for a preliminary magnetic carrier identification.

ASC Model IM-10 Impulse Magnetizer

The ASC IM-10 impulse magnetizer (Fig. F23) is capable of imparting a magnetization of up to 1.5 T. The desired charging voltage can be approximately adjusted with the voltage adjustment knob and is precisely displayed on the charging voltmeter. The charging voltages corresponding to specific field levels for the unit on board are given in "Appendix D," p. 59. *Caution:* The magnetizer produces a strong magnetic field capable of remagnetizing material within 1 m of solenoid.

F23. ASC IM-10 impulse magnetizer, p. 83.

Operation of the ASC Model IM-10

1. Turn the "Power" switch on. No warm-up period is necessary.
2. Place the sample in the holder in the desired position. Insert the holder into the sample cavity until it hits the back of the cavity.

Make certain the bottom of the holder sits in the groove in the bottom of the cavity.
3. Set the voltage adjustment knob so that the ascending voltage displayed on the meter approaches the desired charging voltage slowly. There is a lag time between adjusting the voltage knob and charging of the capacitors to a given voltage. The set voltage is approached asymptotically over a 30- to 60-s time period. The voltage buildup can be monitored via the digital meter. The most accurate and reproducible results will be obtained if the adjusting knob is set to a point slightly above the desired voltage, so that the desired voltage is approached at a rate of 0.5 V/s.
4. If you overshoot the desired voltage, push the trim button until the displayed voltage drops below the desired value. Allow the charging voltage to ascend to the desired value and trigger.
5. Measure the induced magnetization in the cryogenic magnetometer or with the spinner magnetometer.
6. At the end of each work session, turn the voltage adjustment knob fully counterclockwise and trigger the circuit before turning off the power.

Note: after being magnetized, samples with a high concentration of magnetic minerals may become too strong to be measured in the SRM. In this case a small rock chip can be used for IRM acquisition experiments or SIRM determinations.

Anhysteretic Remanent Magnetization and Partial ARM

Anhysteretic remanent magnetization is imparted to a sample by applying a direct magnetic field in the presence of a decaying AF. This direct magnetic field will increase the applied field intensity in one direction along the axis of demagnetization, orienting mobile domains in the direction of the applied direct field. The result is a remanent magnetization of the sample over the range of coercivities below the peak applied demagnetizing field. By applying ARM, then demagnetizing with a series of increasing intensities and measuring the difference in remanent magnetization (differentiating AF demagnetization of ARM), a profile of the magnetic domains in the sample can be obtained.

PARM is imparted to a sample by magnetizing, via a direct magnetic field, over a specified range of coercivities. The sample is exposed to a large, decreasing, alternating magnetic field, and when the demagnetization level reaches a specified value, a small, direct magnetic field is applied until the AF decays to a preset lower value. If this "window" of coercivities is passed over the entire range of demagnetization and the remanent magnetization is measured at each interval, the pARM can be used for determining the distribution of remanence coercivities.

PARM, like ARM, can be used to map the grain size and preferred orientation of grain boundaries within a sample. The strength of pARM imparted at different coercivities is related to grain size distribution (Jackson et al., 1988; diagram in Tarling and Hrouda, 1993). PARM is applicable to many samples whose grain size falls above the stable SD threshold. Because only a small number of domains are magnetized at any time, pARM may reduce errors caused by grain interactions.

DTECH ARM/pARM Equipment

As previously described ("DTECH Model D-2000 Demagnetizer," p. 30, in "Alternating Field and Thermal Demagnetization"), a DTech 2000 AF demagnetizer (Fig. F22) is available in the shipboard laboratory for demagnetization of specimens up to 200 mT. The D-2000 can also be used to impart an ARM, in which a DC magnetic field is produced continuously across the AF demagnetizer coil, or a pARM, in which the user selects the demagnetization interval over which the field is applied. Direct fields within the range of 0.001 to 0.2 mT may be applied to samples. Both ARM and pARM experiments are useful for conducting rock magnetic studies.

CORE ORIENTATION

Principle

Paleomagnetism and many studies would be greatly enhanced if the azimuthal orientation of the core was known. While the principle of placing the core into proper geographic coordinates is simple, in practice such orientation is difficult and, when accomplished, is fairly crude. Currently, the only ODP drilling tool that can provide core orientation is the Tensor tool (Fig. F24; note that "Tensor" is a brand name of Tensor Inc., Austin, TX), which can only be used for APC coring. The Tensor tool has replaced the Eastman-Whipstock multishot tool (frequently referred to simply as the "multishot" tool). Scribing core catches have been attempted with rotary core barrel (RCB) coring as discussed in *Technical Note* 10 (Fisher and Becker, 1993), but these systems were never developed fully. Currently, ODP does not maintain any form of orientation tool for extended core barrel (XCB) or RCB cores. In addition to coring tools, other indirect methods can be used to estimate orientation on APC, XCB, and RCB cores as discussed below.

F24. Tensor tools, p. 84.

Tensor Tool

Equipment and Operation

The Tensor tool (see Storms et al., 2006) consists of a three-component fluxgate magnetometer and a three-component accelerometer rigidly attached to the core barrel to record the azimuth and dip (drift) of the hole and magnetic tool-face (MTF) angle, which is the angle between magnetic north and the double-line orientation mark on the core liner (Fig. F25). The instrument is divided into four modules: (1) the magnetometer triad including accelerometers, (2) the data acquisition module, (3) the control-power regulator-memory module, and (4) the battery pack. The battery pack is detachable for easy replacement.

The ODP downhole tools Marine Specialist and the paleomagnetism technician are responsible for all phases of operating the Tensor tool, including tool preparation, data download, and data interpretation. This tool requires a special nonmagnetic drill collar (the Monel collar) as part of the bottom-hole assembly, as well as batteries and additional setup time (10–15 min per core) on the part of the Marine Specialists. The decision to orient cores at a given site should therefore be made well in advance of the cruise. It is also important to provide the techni-

F25. Orientation terminology for the Tensor tool, p. 85.

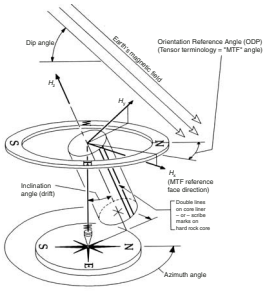

cal/logistics staff with an estimate of the number of cores to be oriented.

Before deployment with the APC core barrel, the probe is programmed via computer interface to determine the holdoff time and the interval between "shots" (sets of sensor readings). The instrument is designed to store a maximum of 1023 sensor readings. The tool stores data, which are uploaded to a computer and analyzed once the tool is back on deck. Orientation is not usually attempted for the top two or three cores (~20–30 mbsf) until the BHA is sufficiently stabilized in the sediment.

The output from the Tensor tool, which contains a variety of angles, including the inclination angle of the hole and the MTF angle, is archived in the Janus database (Figs. **F7, F8**). The dip or inclination of the hole is a measure of the deviation of the hole from vertical, which is typically <5° for ODP holes. The MTF angle is the angle between magnetic north and the double-line orientation mark on the core liner. The core liner is always cut so that the double lines are at the bottom of the working half. Using the ODP coordinate system for the archive and working halves or for samples taken from them (Fig. **F2**), the measured remanent declination can then be corrected to magnetic north by adding the MTF angle, and it can be further corrected to true north by adding the deviation of magnetic north from true north, the latter of which can be estimated from the International Geomagnetic Reference Field (IGRF) coefficients. The equation is

$$D_{True} = D_{Observed} + MTF + MIGRF,$$

where

D_{True} = the Tensor tool corrected or true declination,
$D_{Observed}$ = the observed declination output from the cryogenic magnetometer,
MTF = the MTF angle, and
MIGRF = the deviation of magnetic north from true north.

Standard Queries

Standard queries through the Web (Fig. **F8; www-odp.tamu.edu/database**) allow downloads of core orientation data that can be used to reorient APC cores into the geographical reference frame.

Other Orientation Methods

Currently, there is no hard rock or XCB and RCB orientation system in place. However, there are three methods that have been successfully applied to orient the azimuths of APC, XCB, and RCB cores:

1. Use the declination of intervals with known polarity (e.g., McLeod et al., 1996). This technique works well for relatively young sediments or rocks (<5 Ma) that have not been affected by tectonic rotations. The time-averaged direction for normal or reversed polarity intervals in such a case would be 0° or 180°, respectively. The method could also be used for older rocks, but the effect of past plate motion would need to be removed.
2. Compare borehole images obtained during the logging program with the FormationMicroScanner (FMS), which have known az-

imuthal orientation, with the core or images of the exterior of the core (e.g., Haggas et al., 2001).

3. Use the orientation of the recent (Brunhes) geomagnetic field, which may partially overprint the ChRM magnetization of the core (e.g., Shibuya et al. 1991). This technique is typically not applicable because present-day overprints often do not exist or are too small to be accurately estimated. Moreover, Brunhes overprints typically would be acquired by magnetic minerals with the low coercivity (short relaxation times), which are likely to be masked by drilling overprints.

MEASUREMENT GUIDELINES AND STRATEGIES

Core Flow

When measuring sections of core in the MST or the cryogenic magnetometer, paleomagnetists must find a balance between having measurement intervals as closely spaced as they would like and the potential that making large numbers of such measurements slows the flow of cores in the core laboratory, thereby preventing shipboard sedimentologists and other scientists from performing their duties. When APC coring is conducted in shallow water, cores can arrive on deck 15–30 min apart. There is finite space for storing the cores on the catwalk and in the core laboratory and for writing site reports. Thus, strategies must be devised that provide the necessary data within the available time. This usually means that a reduction in the number of demagnetization steps or an increase in the distance between measurements must be made. On high-recovery legs (>3 km of core), it is likely that all measurements to be conducted on a core section will have to be completed in <30 min and sometimes in <15 min. The measurement strategy (i.e., the number of demagnetization steps and measurement spacing) needs to be discussed with the Co-Chief Scientists and the shipboard party to determine a strategy that permits cores to be described and measured optimally.

Practical Measurement Guidelines

MST susceptibility measurements are generally made at 2- to 5-cm intervals along whole-core sections. The spacing between susceptibility measurements and the other MST instruments can be selected for the most efficient use of time while collecting the highest quality and quantity of data possible. Trial runs can be conducted to determine the time it will take to finish measuring a section for variable MST measurement settings. Additional susceptibility measurements can be made with the point susceptibility probe on the AMST track should higher resolution data be needed for some intervals.

For the SRM, measurements are also generally made at 2- to 5-cm intervals. Often the paleomagnetists will ensure that similar intervals are measured for the SRM as were for the MST susceptibility. The NRM (prior to demagnetization) should be measured on all archive-half sections that are sufficiently long and contain relatively undeformed core material. Given the length of the response functions of the sensors, it is unlikely that much useful information will be gained from sections that are shorter than ~20 cm or from sections that contain only scattered pieces of core (e.g., pebbles, cobbles, or small chunks of sediment sepa-

rated by large voids). Similarly, completely deformed core sections (e.g., cores that are dominated by "suck-in") will unlikely contribute useful information. Collecting marginal quality or meaningless data results in wasted effort on the part of the paleomagnetist, particularly because additional time will be required to explain or cull these data for site reports. Additionally, future users may inadvertently incorporate these bogus data in their studies.

Partial Demagnetization of Archive Sections

For the SRM, the most frequently asked question concerns the rules for demagnetization of the archive-half sections. In September 1992 the Information Handling Panel (IHP) recommended that shipboard paleomagnetists be allowed to partially demagnetize the archive half of any core to as high a level as is necessary to isolate the characteristic remanence. The in-line AF demagnetizer that is part of the SRM can demagnetize cores up to 80 mT, so this is ultimately the upper limit. The IHP also recommended that the maximum demagnetization step size be limited to 15 mT to prevent the destruction of core magnetization without a record of intermediate data. In practice, many high-recovery legs have time for only the NRM step and one demagnetization step. Because the drilling overprint is sometimes only partially removed at 15 mT, the demagnetization step chosen is often 20 or 25 mT. Although this violates the IHP recommendation for step size, it may be the only means for the shipboard paleomagnetist to obtain an unbiased and timely paleomagnetic record that can be used for magnetostratigraphy, devising sampling strategies, or other purposes. If time is available, every effort should be made to obtain data at an intermediate demagnetization step, again with the maximum step size being 15 mT.

Experiments with discrete samples can be used to devise demagnetization strategies for the split cores. Shipboard paleomagnetists are encouraged to take discrete shipboard samples that can then be demagnetized either thermally or with AFs up to 80 mT with the in-line AF unit or up to 200 mT with the D-Tech unit. These results can then be compared to the results of demagnetization of archive halves to determine whether or not secondary magnetizations were adequately removed from the archive halves. Drilling overprints may, however, be more resistant to demagnetization for the split cores because core material near the periphery is often more strongly magnetized by than that near the center of the core and discrete samples are typically taken from the interior of the core (Fig. F26)

Occasionally, requests are made to conduct demagnetization experiments on whole-round core sections. Because the entire cored interval is affected by whatever demagnetization is conducted, great care should be taken in selecting demagnetization steps. Such measurements are not part of standard shipboard procedures and so requests for demagnetizing whole-round sections need to be approved by the Sample Allocation Committee, as is the case for other nonstandard measurement or sampling strategies.

F26. Orthogonal vector demagnetization plots, p. 86.

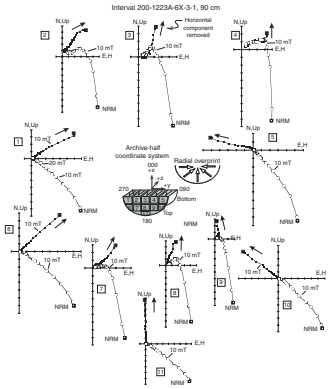

PROBLEMS WITH MAGNETIC MEASUREMENTS IN THE SHIPBOARD ENVIRONMENT

The purpose of this section is to discuss problems encountered by paleomagnetists on the *JOIDES Resolution*. Some of these can be avoided,

but many are part of drilling operations or are limitations of laboratory equipment.

By far the most significant problem for paleomagnetists is drilling overprints, which have and will continue to occur on all ODP cruises even though attempts have been made to reduce their size. Herein, we use the term "drilling overprint" in reference to any magnetic overprint acquired by the core during shipboard operations conducted up to the time the core is measured in the shipboard magnetometer. This includes piston or rotary coring, core recovery, and splitting or sawing the core for curation. Ultimately, cores acquire drilling overprints in a variety of ways, the most common of which are exposure of the cores for variable amounts of time to large magnetic fields, coring deformation or other forms of mechanical disturbance, and exposure of cores that have been in reducing conditions to oxygen.

In addition to drilling overprints, this section addresses problems related to magnetometer noise, weak sediments, reduction diagenesis, contamination by rust or other magnetic materials used in shipboard operations, magnetic edge effects that affect measurements made at the ends of sections and near voids, and contamination by sediments or rock falling downhole.

Observations and insights from previous legs have helped characterize the nature of the drilling overprints and other common problems. Besides our own experience on the ship, we have extracted information about shipboard paleomagnetic problems from "Explanatory Notes" chapters and site chapters of the *Initial Reports* volumes, papers by paleomagnetists in the *Scientific Results* volumes, the reports of the paleomagnetism technicians, and publications in other journals. Two recent papers that examine the overprint problem and contain lists of relevant references are those by Fuller (2002) and Acton et al. (2002). In **"Viscous Isothermal Remanent Magnetization (VIRM) Drilling Overprints,"** p. 37, and **"Drilling Deformation Overprints,"** p. 42, excerpts from Acton et al. (2002) are used liberally with modification where appropriate.

Viscous Isothermal Remanent Magnetization Drilling Overprints

Numerous ODP and Deep Sea Drilling Project (DSDP) paleomagnetic studies have found that the most prominent part of the overprinting is associated with exposure of the core to large magnetic fields (a few milliteslas to tens of milliteslas) during drilling, while the core is being pulled through the drill pipe to the rig floor, or, less likely, during subsequent cutting or splitting of the core as it is curated (e.g., Barton and Bloemendal, 1986; Bleil, 1989; Tauxe et al., 1989; Hall and Sager, 1990; Hounslow et al., 1990; Kroenke, Berger, Janecek, et al., 1991; Curry, Shackleton, Richter, et al., 1995; Sacks, Suyehiro, Acton, et al., 2000; Acton et al., 2002; Shipboard Scientific Party, 2003). The overprints are not surprising, given that the core is collected with a metal cutting shoe or drill bit in the vicinity of a highly magnetic BHA and must pass through a long metal drill string. Moreover, the core resides in a metal core barrel, separated from the core by only a thin plastic core liner, and passes near rig floor equipment that produces large magnetic fields. Magnetic field measurements around the BHA, core barrel, and other drilling equipment have indicated that fields may locally exceed 1T, although generally the fields generated near these are greater than ~20

mT (Keating, 1984; Sager and Hutton, 1986; Stocking et al., 1993; Fuller et al., 1998).

Past studies have suggested the overprint is an IRM or a VRM. We use the term "VIRM drilling overprint" to describe this component because unlike a standard laboratory IRM, where a magnetization is imparted to a sample virtually instantaneously, the core is instead exposed to a large magnetic fields over minutes or tens of minutes. Thus, the magnetization also has a viscous aspect, with VIRM being the acronym for viscous isothermal remanent magnetization. The relationship between longer coring times and larger overprints was observed during Leg 202, where Joe Stoner and Steve Lund noted the VIRM was larger in those APC cores that were collected when temperature estimates were being made with the Adara tool. In such cases, the piston corer is shot and left at the bottom of the hole for usually >10 min. During this time, the core would be sitting within the core barrel just below the bottom of the BHA. Temperature likely also plays a role in some of the deeper holes (e.g., temperatures exceeded 100°C below 1000 mbsf in Hole 504B, reaching a maximum of 180°C at the bottom of the hole). Vibration that occurs during coring and core retrieval may also contribute to this overprint. The VIRM component, although very large, can generally be removed by low AF demagnetization (<25 mT), although for some magnetic mineralogies, particularly those with low coercivities, the VIRM may completely overprint any remanent magnetic signal.

The VIRM drilling overprint is characterized by its near-vertical orientation, which can be either downward or upward directed (Figs. **F26, F27, F28**). In a rare but important example, Schneider and Van Damme (pp. 474–478 in Backman, Duncan, et al., 1988) noted intervals with steep negative inclinations and intervals with moderate-to-steep positive inclinations associated with overprinting within a single core. The pattern of overprinting was shown to be similar in other cores when the same core barrel was used, implicating the core barrel as a source of at least part of the VIRM. From our experience, the VIRM drilling overprint is nearly constant within a core barrel and between core barrels, with the NRM inclinations prior to AF demagnetization being steep and positive (60°–90°). Possibly the core barrels are completely remagnetized, preferentially with a vertical orientation, over time by some common mechanism, such as traveling up and down the drill string. Subsequently, cores collected within them have near-vertical overprint owing to the core barrel magnetization and to the trip through the drill string.

Besides the near-vertical component, a smaller radial-horizontal component also appears to be present in oceanic drill cores (Figs. **F26, F27, F28**) and has been documented in continental drill cores as well (Audunsson and Levi, 1989). Following Fuller et al. (1998), we use the term radial-horizontal rather than just radial because, as they note, even when the radial-horizontal component is present, "the inclination can actually be steep and remain so throughout demagnetization." The radial-horizontal overprint mainly biases the horizontal component, which, given the ODP orientation system used in measuring the remanence of archive-half sections (Fig. **F2**), results in declinations biased toward 0° or 180°, depending on whether the overprint is directed toward or away from the center of the core, respectively. Inwardly directed radial-horizontal overprints appear to be the most common, but both forms exist. As Audunsson and Levi (1989) suggested, such a drilling-related VIRM may be acquired near the drill bit or cutting shoe where the ambient magnetic field lines might be expected to have a significant inward component on the interior and an outward component on

F27. Orthogonal vector demagnetization diagrams, p. 87.

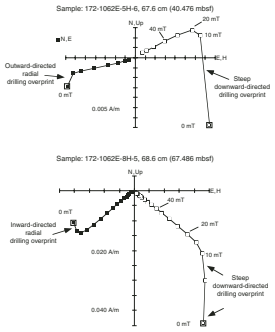

F28. Inclinations and declinations after demagnetization, p. 88.

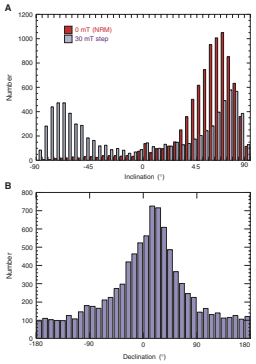

the exterior as they radiate from the end of the drill string. Indeed, Fuller et al. (1998) observed radial, as well as vertical, magnetic fields up to 5 mT from measurements made inside and around a core barrel fitted with an APC cutting shoe.

VIRM overprints are not homogeneous across the core, and the vertical and radial-horizontal components are not always equally easy to remove with low AF demagnetization (Fig. **F26**). Closer examination illustrates that the direction and size of the VIRM drilling overprint varies across a core. The overprint is more extensive near the periphery than in the center of the core and is steeper in the center of the core than near the periphery (Fig. **F27;** see also Schneider and Van Damme's fig. 12 [note, the inclination-axis on this plot appears to have been inadvertently inverted] on p. 478 of Backman, Duncan, et al. [1988]; Roperch, Stokking, and Zhao, on pp. 77–78 of Collot, Greene, Stokking, et al. [1992]; and Richter, Schneider, and Valet on pp. 167–168 of Curry, Shackleton, Richter, et al. [1995]). The vector sum across the core is very steep because of the radial nature of the overprint, which results in cancellation or near cancellation of the horizontal component for whole-round samples and a 0° or 180° declination bias for split cores.

The relative importance of each of the elements of the coring system—drill string, BHA, core barrel, and so on—as a source for the drilling-induced remanence has been debated. Obviously, the core barrel plays a significant role as noted above and as indicated by the alternating pattern of large and small drilling-induced components in successive cores (Fig. **F29,** which appeared as fig. 6.12 in *Technical Note* 18). These patterns result from the use of the same core barrel every other core because typically two core barrels are used during coring operations. After a core has been collected, the standard practice is to pull the full core barrel to the rig floor and then drop the other empty core barrel down the pipe for collecting the next core. While this new core barrel is going down the hole, the core is removed from the full core barrel, and the process is repeated. Even though the core barrel is a known source for overprinting, this does not mean the BHA and drill string do not also play a significant role. Because large magnetic fields have been measured around them, surely they have some role but determining exactly the relative contribution to the total drilling overprint difficult.

The principal cause of magnetization of the core barrel, BHA, and drill string is probably the routine jars, vibrations, and rotation stresses experienced during racking, tripping, deployment, drilling, and recovery. It is unlikely that any significant change could be made to reduce acquisition of remanence during these processes. Magnetic inspection of the BHA (see below) may add to the magnetization of this part of the drill string. Although nonmagnetic drill collars are deployed in the BHA when magnetic orientation of cores is carried out, it would be impractical to replace all of the BHAs and/or drill strings with nonmagnetic materials because of both the far higher cost of these materials and their reduced tensile strength. Degaussing of the drill string by the use of an AF coil mounted beneath the drill floor was attempted by DSDP. This resulted in the rapid physical destruction of the coil, however, and it is questionable whether the degaussing the pipe received as it was tripped had any lasting effect once the pipe was again exposed to the shocks and vibrations related to coring. Degaussing of the core barrel (see discussion below) has also been attempted, and previous reports (sometimes anecdotal) have provided equivocal evidence of whether this was helpful in reducing the overprint.

F29. Intensity after demagnetization, p. 89.

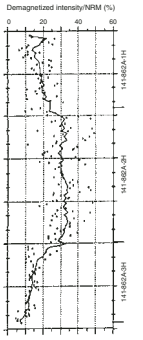

Magnetic Inspection of the BHA

On Leg 144 intense overprinting of APC cores was attributed to magnetic inspection of the BHA conducted before drilling. Magnetic inspection (Betz, 1967), also referred to as Magnaflux inspection (after the Magnaflux Corporation), is conducted on the ends of BHA joints as well as on pipe joints used near the top drive, which include the drill collars, transition pipe, and knobby joints.

Magnetic inspection of pipe joints typically involves the use of a magnetizing coil that is passed over the end of a pipe, with the focus on the threads where joints are screwed together. A DC magnetic field is applied that magnetizes the pipe; the coil is also capable of producing an AC magnetic field for demagnetizing the joint, but the actual inspection process uses a DC field created by an electromagnet. The electromagnet is produced by Drilco (model serial number 0112). The coil, with 2000 turns and a current of 5.25 A DC, produces a full-wave DC magnetic field.

A solution with suspended ferromagnetic particles (currently Fe_2O_3 with mean size 6 µm, although the composition of the particles may vary) with a florescent coating is then painted onto the area being inspected. The particles tend to concentrate along microfractures, if microfractures are present. Those regions with high concentrations can be observed under black light owing to their greater florescence. As a result of magnetic inspection, which typically occurs at the end of each cruise, the BHA can be expected to have a large permanent magnetization and to have a high concentration of magnetic particles attached to it. The BHA threads are cleaned and redoped with grease following the inspection. It is likely that some particles remain. Given that rust also forms on the BHA joints between legs, it seems likely that the first few cores of a leg will more likely be more contaminated with magnetic particles than subsequent cores. To reduce this contamination, the interior of the BHA joints are cleaned, although somewhat rarely, with a pipe rattler, which is an abrading tool. Other inspections of pipe connections, and of the pipe itself, may involve the use of half-wave rectified fields, which would induce a remanence in the pipe; these tests are conducted less frequently, however.

The BHA is highly magnetic as a result of normal use as well as the inspection. Wrenches and other metal objects have been observed to cling to the BHA (G. Pollard, pers. comm., 2004). Thus, the BHA is likely a source for part of the VIRM drilling overprint.

Core Barrel Demagnetization

A quantitative test of the magnitude of the magnetization of the core barrel and the effect on this of AF demagnetization was carried out on Leg 146. The internal axial field in two core barrels was measured with a Hall-effect probe, centered along the axis of the barrel and linked to the meter by a shielded cable. The field was measured at 0.5-m intervals along each barrel. Each barrel was then demagnetized using the Smith Drilco Magnafluxer set to full-wave, and the barrel lowered down the pipe to take an APC core. After recovery of the core, the magnetization was measured again at the same intervals.

The results are given in Figure **F30.** The quantitative reliability of the measurements is questionable: very high fields experienced on the rig floor made zero calibration of the Hall-effect meter difficult and unstable. However, it is clear that a very strong axial field can exist in the

F30. Axial field, p. 90.

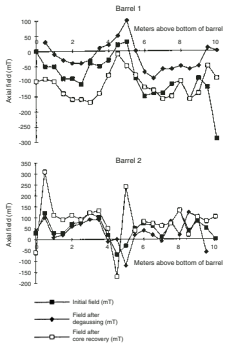

core barrel, sufficiently intense to induce a substantial IRM (average = ~90 mT, with local values ranging from 20 mT to as high as 160 mT—compare with the maximum coercivity of SD magnetite at ~200 mT). Even higher transient core barrel fields may be present when the magnetic brake is in action (perhaps as high as 400 mT?). Degaussing did reduce the core barrel magnetization, but this remained at an average value of ~40–50 mT, still sufficiently strong to induce an IRM. Following the taking of a core and the recovery of the barrels on deck, the axial magnetization returned to similar values to those measured before demagnetization. Although it was not possible to measure the core barrel magnetization while the barrel was in the drill pipe, it is likely that remagnetization of the core barrel occurred through shock and vibration while the barrel was in the strongly magnetized drill pipe and that a substantial part of the remagnetization had already occurred on the downward trip of the barrel, before the core was taken.

Two further noteworthy observations were made during this study. Although the axial magnetization of the first core barrel was directed upward (negative sign), corresponding to the common observation that the drilling-induced remanence is steeply upward, the magnetization of the second barrel was dominantly directed downward (positive sign). These directions of magnetization were repeated when the barrels were remagnetized during their coring deployment, even though the conditions to which the two barrels were exposed were presumably similar. The explanation for the different magnetization of the two barrels is not clear, but this effect may contribute to the observation of differences in the drilling-induced overprint with alternation of corebarrels. The other surprise was the intensity of the field measured near the joint at the top of a stand of drill pipe as this was sitting in the elevator: a field of 1700 mT was apparently measured. Although it is probable that the Hall Effect meter had gone out of calibration at this point, it is clear that a very strong field was present, and this is consistent with anecdotal stories of iron wrenches being stuck hard to the pipe.

What is clear from this study is that core barrel demagnetization is of little value as an isolated measure. Remagnetization of the barrel occurs during a single deployment, and high field sources remain in the drill pipe and on the rig floor. Some advantage might be gained by the use of nonmagnetic monel core barrels, but this would have to be weighed against the cost and limited tensile strength of these barrels (which would lower the overpull limit on APC coring, for instance). However, such nonmagnetic core barrels may be justified in cases where minimization of drilling-induced remanence is of paramount importance.

Nonmagnetic Core Barrels

Largely through the efforts of Mike Fuller, a complete nonmagnetic core barrel with nonmagnetic seal subs, core catcher sub, and inner barrel sub was purchased for use on Leg 174B. Initial tests conducted on that leg and on several subsequently legs were somewhat ambiguous because the sediments being cored were weakly magnetized and because the coring operations were not ideal for the tests. Ideally, coring multiple holes at a sites with a variety of lithologies would be best, as then the results of the nonmagnetic core barrel could be compared with the magnetic core barrel both downhole and laterally and the role of lithology/magnetic mineralogy could be considered. Results from Leg 202 (J. Stoner and S. Lund, pers. comm., 2004) illustrate that the nonmagnetic core barrel is successful at reducing the VIRM drilling over-

print, particularly in the coarser grained lithologies. As a result, a second nonmagnetic core barrel and associated parts was ordered and was available to paleomagnetists for Leg 205 and beyond. Shipboard paleomagnetists should request the use of the nonmagnetic core barrel to ensure that they are used. Given the extra costs for the nonmagnetic parts, operations personnel may opt to use the magnetic core barrels in coring intervals where damage to the core barrel seems more probable.

Drilling Deformation Overprints

A variety of forms of deformation or drilling disturbance affect the cores. Some of these include drilling biscuit in XCB cores, gas expansion, suck-in or flowing deformation, shear near the periphery of the core, mud worms (which result from extursion of sediment through small holes drilled in the core liner of gassy cores), soupy sediments, drilling-induced fractures, faults, breccia, and many others (e.g., see the "Lithostratigraphy" section of the "Explanatory Notes" of Shipboard Scientific Party, 1995). Information about core disturbance is recorded on the visual core descriptions and barrel sheets by the sedimentologists; it is recommended that as part of their shore-based studies paleomagnetists compare their personal sample inventory with the barrel sheets for evidence of disturbance.

The *Handbook for Shipboard Sedimentologists* (Mazzullo and Graham, 1988) lists three common types of drilling disturbance in sediments and sedimentary rocks recovered by ODP:

1. Bed flexures: The weight of the drill string can flex or bow downward beds of soft sediment. Soft material can also be bowed or flexed upward while the core barrel is pulled out of the hole. Beds that are flexed only along their edges are considered slightly deformed, if the beds are bowed across the core are termed moderately deformed, and beds that display diapirlike structures are completely disturbed.
2. Soupy beds: Sediment that is water-saturated can flow up into a core barrel under the weight of the drill string; the original bedding and the orientation of magnetic particles in these sediments are destroyed. This can occur in sand, calcareous grainstones, and ooze and is common in the mudline core in poorly consolidated sediments.
3. Fractures: Beds of hard sedimentary rock can be fractured by excess drill pressures. The rock can be considered slightly fractured when it is broken into a few large pieces by a small number of well-defined fractures, moderately fractured when core pieces are in place or partly displaced but original orientation is maintained, or highly fractured when pieces are probably in correct stratigraphic sequence (although they may not represent the entire sequence) but original orientation is lost. Drilling breccia is rock crushed and broken into many small and angular pieces, with original orientation and stratigraphic position lost; often drilling breccia is completely mixed with drilling slurry. Beds of semilithified sediment can also be split along their bedding planes by the rotation of the core barrel during rotary coring. In this case, the fracturing produces disc-shaped drilling biscuits that commonly float within a matrix of soupy sediment. Drilling biscuits can be very common in rotary-cored sections, and can be difficult if not impossible to identify.

Intervals with extreme deformation are typically easy to note and avoid when sampling. When measuring split core sections on the ship, the software for the SRM allows the user to select intervals to skip if they wish to skip such intervals.

More commonly, the shipboard paleomagnetist will make measurements along split-core sections that have very minor amounts of deformation. The most common deformation in soft sediment is that related to the shoe of the piston corer cutting through the sediment and ensuing drag of the sediment on the inside walls of the corer as the sediment slides up into the plastic core liner. The result is that sediment near the core liner is typically bent or sheared downward, and within <1 mm of the core liner, a zone of vertically smeared sediment often exists. The downward bending can be seen to rapidly decrease toward the center of the core in cores with horizontal layers or laminae (Fig. **F31**).

F31. Core deformation, p. 91.

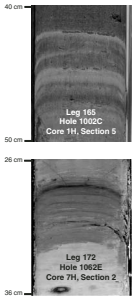

During Leg 172, Okada (in Keigwin, Rio, Acton, et al., 1998) noted that if the radial thickness of the region with deformed sediment is >1 cm, which is commonly the case, then the deformed sediment volume exceeds the undeformed sediment volume for a standard split-core section. Therefore, the deformed sediment may contribute significantly to the mean remanent magnetization measured on split-core sections. He then proposed a simple shear model to describe this observed deformation and to explain how shear could deflect the remanence vector. Acton et al. (2002) further developed the model, and they present graphics that illustrate how the remanence vector is deflected by shear deformation. Differences in the remanence vector (after AF demagnetization) measured on split-core sections from APC cores, which typically have visible shear deformation, relative to remanence vectors measured on U-channel samples, which presumably have little or no shear deformation as they are collected from the center of the APC cores, were shown to be consistent in size with that expected for a shear deformation model. In the model, shear along the periphery of the core caused rotation of sediment grains and associated magnetic particles, with the size of rotation decaying toward the center of the core. The difference in remanence observed between sediment from the periphery and center of the core may also be compatible with some degree of VIRM that is resistant to demagnetization. Separating the two causes is difficult because they can produce very similar deflections of the original (predrilling) remanence.

Voids

The susceptibility meter on the MST and the cryogenic magnetometer are both designed and intended to measure completely filled APC cores. Tests conducted during Leg 131 indicate that in places where the core is not uniformly magnetized, either through natural processes or artifacts (such as voids in the core or differential rotation of segments in the core liner), the values of declination, inclination, and intensity should be treated with caution.

Sections containing substantial voids should not be measured. The Long Core software permits data records to include comments about the presence and location of voids so that the data can be interpreted correctly.

Section Boundaries

The upper and lower boundaries of each section introduce an edge effect in continuous cryogenic magnetometer measurements. This is reflected both in a decrease in the intensity measured near section breaks and in localized anomalies in declination and inclination. When section records are concatenated, the origin of these anomalous intensities and directions as edge effects can be overlooked and there is a risk that they may be interpreted as having real paleomagnetic significance. The Web queries allow to cull data at section and core breaks at the desired distance from the break (e.g., half the response curve of the sensor).

Rust Contamination

Steel drill pipe exposed to seawater will inevitably rust. Usually rust contamination is not a serious problem. ODP drill pipe is coated to minimize rusting, both to extend the life of the pipe and to minimize contamination of the magnetic record. Cycling of the drill pipe for recoating occurs on a roughly 2- to 3-year rotation, which should be frequent enough to minimize rust development. Nevertheless, rust contamination of the cores does occur and may sometimes seriously degrade, or even completely obscure, both the magnetization and susceptibility records. Usually, rust will be seen as a high-susceptibility/magnetization "spike" at the top of cores, resulting from offscraping of internal rust during the up and down passage of the core barrel between intervals of coring. Occasionally this problem can be more severe, and the effects of rust may extend throughout the core. Severe rust contamination is most likely when a deepwater hole follows an extended period of drilling in shallower water, so that pipe which has not been used for some time (and in which rust has had the opportunity to accumulate) is reintroduced to the drill string. The problem may also occur after pipe is rotated around in the racker, or after new pipe has been brought on to the ship during a port call.

Rust contamination will be present on the upper surface of the core and may be present in the drilling slurry annulus around the core inside the core liner. It is only likely to be present deeper inside the core when the core has been fluidized, in which case magnetic measurements may be of no value. Rust in the annulus of drilling slurry will affect susceptibility measured using the MST and intensity and direction measured in archive-half sections using the cryogenic magnetometer. However, it should still be possible to select uncontaminated discrete samples for remanence and susceptibility measurements.

Avoiding Drilling Overprints and Contamination

Paleomagnetists should be aware of some possible sources of contamination and how to minimize the effects. The outer surface of the core (in contact with the core liner) may be contaminated by younger material displaced downhole by the core liner during the coring process. These regions (each roughly a few millimeters thick) should be trimmed away before processing the sample. For APC cores, shear deformation is greatest nearer the periphery of the core, so sampling near the center of the core will minimize shear deformation. Similarly, the VIRM drilling overprint is larger near the periphery for all types of cores. Other regions of the core with high contamination potential are the top 10–20 cm (or more) of each core, zones of flow-in at the base of some APC

cores, the drilling slurry between "biscuits" in some XCB or RCB cores, and any other interval displaying high drilling disturbance. As the drilling program evolves, hopefully drilling overprints and contamination can be minimized with new drilling tools and improved coring and sampling strategies.

Existence of the Characteristic Remanence after Removal of Overprints

Despite the various difficulties discussed in this section, the majority of ODP paleomagnetic studies have been successful. Frequently little or no significant drilling overprints remain after 25 mT of AF demagnetization of split-core sections. In such cases, shipboard measurements are useful for a number of paleomagnetic studies. More often than not, shipboard results at least allow recognition of the magnetic polarity, which aids in constructing the magnetostratigraphy at a site. AF and/or thermal demagnetization of discrete samples is usually able to totally remove drilling overprints, allowing characteristic remanences to be isolated. Only rarely have drilling overprints totally obscured the characteristic remanence. Of more concern is the replacement of the present-day or Brunhes VRM by drilling overprints, which precludes the use of this VRM as a reference orientation for the core. Even though drilling overprints are a complication for paleomagnetic studies of drill cores, a vast array of information resides in the characteristic remanences that can typically be resolved through careful laboratory measurements and data analysis.

REFERENCES

Acton, G.D., Okada, M., Clement, B.M., Lund, S.P., and Williams, T., 2002. Paleomagnetic overprints in ocean sediment cores and their relationship to shear deformation caused by piston coring, *J. Geophys. Res., 107,* (EPM 3, p. 1–15). **doi:10.1029/2001JB000518**

Acton, G.D., Borton, C.J., and the Leg 178 Shipboard Scientific Party, 2001. Palmer Deep composite depth scales for Leg 178 Sites 1098 and 1099. *In* Barker, P.F., Camerlenghi, A., Acton, G.D., and Ramsay, A.T.S. (Eds.), *Proc. ODP, Sci. Results,* 178: College Station, TX (Ocean Drilling Program), 1–35. **doi:10.2973/odp.proc.sr.178.202.2001**

Alexandrovich, J.M., and Hays, J.D., 1989. High-resolution stratigraphic correlation of ODP Leg 111 Holes 677A and 677B and DSDP Leg 69 Hole 504. *In* Becker, K., Sakai, H., et al., *Proc. ODP, Sci. Results,* 111: College Station, TX (Ocean Drilling Program), 263–276. **doi:10.2973/odp.proc.sr.111.146.1989**

Audunsson, H., and Levi, S., 1989. Drilling-induced remanent magnetization in basalt drill cores. *Geophys. J.,* 98:613–622.

Backman, J., Duncan, R.A., et al., 1988. *Proc. ODP, Init. Repts.,* 115: College Station, TX (Ocean Drilling Program). **doi:10.2973/odp.proc.ir.115.1988**

Barker, P.F., 2001. Data report: composite depths and spliced sections for Leg 178 Sites 1095 and 1096, Antarctic Peninsula continental rise. In Barker, P.F., Camerlenghi, A., Acton, G.D., and Ramsay, A.T.S. (Eds.), *Proc. ODP, Sci. Results,* 178: College Station, TX (Ocean Drilling Program), 1–15. **doi:10.2973/odp.proc.sr.178.219.2001**

Barton, C.E., and Bloemendal, J., 1986. Paleomagnetism of sediments collected during Leg 90, southwest Pacific. *In* Kennett, J.P., von der Borch, C.C., et al., *Init. Repts. DSDP,* 90: Washington (U.S Govt. Printing Office), 1273–1316.

Behrmann, J.H., Lewis, S.D., Musgrave, R.J., et al., 1992. *Proc. ODP, Init. Repts.,* 141: College Station, TX (Ocean Drilling Program). **doi:10.2973/odp.proc.ir.141.1992**

Betz, C.E. 1967. *Principles of Magnetic Particle Testing:* Chicago (Magnflux Corporation).

Bleil, U., 1989. Magnetostratigraphy of Neogene and Quaternary sediment series from the Norwegian Sea: Ocean Drilling Program, Leg 104. *In* Eldholm, O., Thiede, J., Taylor, E., et al., *Proc. ODP, Sci. Results,* 104: College Station, TX (Ocean Drilling Program), 829–901. **doi:10.2973/odp.proc.sr.104.181.1989**

Blum, P., 1997. Physical Properties handbook: a guide to the shipboard measurement of physical properties of deep-sea cores. *ODP Tech. Note,* 26 [Online]. Available from World Wide Web: <**http://www-odp.tamu.edu/publications/tnotes/tn26/INDEX.HTM**>.

Blum, P., Allan, J., Coyne, J., Hagelberg, T., MacLeod, C., Mato, C., deMenocal, P., Merrill, R., Mithal, R., Rhinehart, B., Weaver, P., Wilkens, R., and Coarser, G., 1995. Depth data acquisition, processing, and archiving in the Ocean Drilling Program. Results and recommendations from the ODP/TAMU Depth Workshop.

Butler, R.F., 1992. *Paleomagnetism: Magnetic Domains to Geologic Terranes:* Boston (Blackwell).

Collot, J.-Y., Greene, H.G., Stokking, L.B., et al., 1992. *Proc. ODP, Init. Repts.,* 134: College Station, TX (Ocean Drilling Program). **doi:10.2973/odp.proc.ir.134.1992**

Curry, W.B., Shackleton, N.J., Richter, C., et al., 1995. *Proc. ODP, Init. Repts.,* 154: College Station, TX (Ocean Drilling Program). **doi:10.2973/odp.proc.ir.154.1995**

Farrell, J.W., and Janecek, T.R., 1991. Late Neogene paleoceanography and paleoclimatology of the northeast Indian Ocean (Site 758). *In* Weissel, J., Peirce, J., Taylor, E., Alt, J., et al., *Proc. ODP, Sci. Results,* 121: College Station, TX (Ocean Drilling Program), 297–355. **doi:10.2973/odp.proc.sr.121.124.1991**

Fisher, A.T., and Becker, K., 1993. A guide to ODP tools for downhole measurements. *ODP Tech. Note,* 10 [Online]. Available from World Wide Web: <**http://www-odp.tamu.edu/publications/tnotes/tn10/10toc.html**>.

Fuller, M., Hastedt, M., and Herr, B., 1998. Coring-induced magnetization of recovered sediment. *In* Weaver, P.P.E., Schmincke, H.-U., Firth, J.V, and Duffield, W. (Eds.), *Proc. ODP, Sci. Results,* 157: College Station, TX (Ocean Drilling Program), 47–56. **doi:10.2973/odp.proc.sr.157.103.1998**

Fuller, M., 2002. Magnetic artifacts in APC cores. *JOI/USSAC Newsl.,* 14(1):14–16.

Goree and Fuller, 1976. Magnetometers using RF-driven SQUIDS and their applications in rock magnetism and paleomagnetism. *Rev. Geophysics,* 14: 591–608.

Hagelberg, T., Shackleton, N., Pisias, N., and Shipboard Scientific Party, 1992. Development of composite depth sections for Sites 844 through 854. *In* Mayer, L., Pisias, N., Janecek, T., et al., *Proc. ODP, Init. Repts.,* 138: College Station, TX (Ocean Drilling Program), 79–85. **doi:10.2973/odp.proc.ir.138.105.1992**

Hagelberg, T.K., Pisias, N.G., Shackleton, N.J., Mix, A.C., and Harris, S., 1995. Refinement of a high-resolution, continuous sedimentary section for studying equatorial Pacific Ocean paleoceanography, Leg 138. *In* Pisias, N.G., Mayer, L.A., Janecek, T.R., Palmer-Julson, A., and van Andel, T.H. (Eds.), *Proc. ODP, Sci Results,* 138: College Station, TX (Ocean Drilling Program), 31–46. **doi:10.2973/odp.proc.sr.138.103.1995**

Haggas, S., Brewer, T.S., Harvey, P.K., and Iturrino, G., 2001. Relocating and orienting cores by the integration of electrical and optical images: a case study from Ocean Drilling Program Hole 735B. *J. Geol. Soc. (London, U. K.),* 158:615–623.

Hall, S.A., and Sager, W.W., 1990. Paleomagnetic and rock magnetic properties of sediment samples from Ocean Drilling Program Leg 116, central Indian Ocean. In Cochran, J.R., Stow, D.A.V., et al., *Proc. ODP, Sci. Results,* 116: College Station, TX (Ocean Drilling Program), 337–344. **doi:10.2973/odp.proc.sr.116.140.1990**

Hext, G.R., 1963. The estimation of second order tensors with related tests and design. *Biometrika,* 60:353–373.

Hounslow, M.W., Bootes, P.A., and Whyman, G., 1990. Remanent magnetization of sediments undergoing deformation in the Barbados accretionary prism: ODP Leg 110. *In* Moore, J.C., Mascle, A., et al., *Proc. ODP, Sci. Results,* 110: College Station, TX (Ocean Drilling Program), 379–391. **doi:10.2973/odp.proc.sr.110.155.1990**

Hvorslev, M.J., 1949. Subsurface exploration and sampling of soil for civil engineering purposes: report on a research project of the Committee on Sampling and Testing Soil Mechanics and Foundations Division. *Am. Soc. Civ. Eng., Waterways Experiment Station.*

Jackson, M., Gruber, W., Marvin, J., and Banerjee, S.K., 1988. Partial anhysteretic remanence and its anisotropy: applications and grainsize-dependence. *Geophys. Res. Lett.,* 15:440–443.

Jelinek, V., 1978. Statistical processing anisotropy of magnetic susceptibility measured on groups of specimens. *Studio Geophys. Geod.,* 22:50–62.

Keating, B.H., 1984. Magnetometer measurements on the drilling floor of the *Glomar Challenger*: possible causes of rock remagnetization. *In* Hay, W.W., Sibuet, J.-C., et al., *Init. Repts. DSDP,* 75: Washington (U.S. Government Printing Office), 1219–1226.

Keigwin, L.D., Rio, D., Acton, G.D., et al., 1998. *Proc. ODP, Init. Repts.,* 172: College Station, TX (Ocean Drilling Program). **doi:10.2973/odp.proc.ir.172.1998**

Kroenke, L.W., Berger, W.H., Janecek, T.R., et al., 1991. *Proc. ODP, Init. Repts.,* 130: College Station, TX (Ocean Drilling Program). **doi:10.2973/odp.proc.ir.130.1991**

MacKillop, A.K., Moran, K., Jarrett, K., Farrell, J., and Murray, D., 1995. Consolidation properties of equatorial Pacific Ocean sediment and their relationship to stress history and offsets in the Leg 138 composite depth sections. *In* Pisias, N.G., Mayer, L.A., Janecek, T.R., Palmer-Julson, A., and van Andel, T.H. (Eds.), *Proc. ODP, Sci. Results,* 138: College Station, TX (Ocean Drilling Program), 357–369. **doi:10.2973/odp.proc.sr.138.118.1995**

Mazzullo, J., and Graham, A.G., 1988. Handbook for Shipboard Sedimentologists. *Tech. Note,* 8: College Station, TX (Ocean Drilling Program).

McElhinny, M.W., and McFadden, P.L., 2000. *Paleomagnetism: Continents and Oceans:* New York (Academic Press).

MacLeod, C.J., Boudier, F., Yaouancq, G., and Richter, C., 1996. Gabbro fabrics from Site 894, Hess Deep: implications for magma chamber processes at the East Pacific Rise. *In* Mével, C, Gillis, K.M., Allan, J.F., and Meyer, P.S. (Eds.), *Proc. ODP, Sci. Results,* 147: College Station, TX (Ocean Drilling Program), 317–328. **doi:10.2973/odp.proc.sr.147.018.1996**

Moran, K., 1997. Elastic property corrections applied to Leg 154 sediment, Ceara Rise. *In* Shackleton, N.J., Curry, W.B., Richter, C., and Bralower, T.J. (Eds.), *Proc. ODP, Sci. Results,* 154: College Station, TX (Ocean Drilling Program), 151–155. **doi:10.2973/odp.proc.sr.154.132.1997**

Nagy, E.A., and Valet, J.-P., 1993. New advances for paleomagnetic studies of sediment cores using U-channels. *Geophys. Res. Lett.,* 20:671–674.

ODP Information Technology and Data Services, 2007. ODP prime scientific data: collection, archive, and quality. *ODP Tech. Note,* 37 [Online]. Available from World Wide Web: <**http://www-odp.tamu.edu/publications/tnotes/tn37/INDEX.HTM**>.

Opdyke, N.D., and Channell, J.E.T., 1996. *Magnetic Stratigraphy:* New York (Academic Press).

Piper, J.D.A, 1987. *Palaeomagnetism and the Continental Crust:* Milton Keynes (Open University Press).

Prell, W.L., Gardner, J.V., et al., 1982. *Init. Repts. DSDP,* 68: Washington (U.S. Govt. Printing Office).

Richter, C., Hayashida, A., Guyodo, Y., Valet, J.-P., and Verosub, K.L., 1999. Magnetic intensity loss and core diagenesis in long-core samples from the East Cortez Basin and the San Nicolas Basin (California Borderland). *Earth, Planets Space,* 51:329–336.

Robinson, S.G., 1990. Applications for whole-core magnetic susceptibility measurements of deep-sea sediments: Leg 115 results. *In* Duncan, R.A., Backman, J., Peterson, L.C., et al., *Proc. ODP, Sci. Results,* 115: College Station, TX (Ocean Drilling Program), 737–771. **doi:10.2973/odp.proc.sr.115.198.1990**

Ruddiman, W.F., Kidd, R.B., Thomas, E., et al., 1987. *Init. Repts. DSDP,* 94 (Pts. 1 and 2): Washington (U.S. Govt. Printing Office).

Ruddiman, W.F., Cameron, D., and Clement, B.M., 1987. Sediment disturbance and correlation of offset holes drilled with the hydraulic piston corer: Leg 94. *In* Ruddiman, W.F., Kidd, R.B., Thomas, E., et al., *Init. Repts. DSDP,* 94 (Pt. 2): Washington (U.S. Govt. Printing Office), 615–634.

Ruddiman, W., Sarnthein, M., Baldauf, J., et al., 1988. *Proc. ODP, Init. Repts.,* 108: College Station, TX (Ocean Drilling Program). **doi:10.2973/odp.proc.ir.108.1988**

Sacks, I.S., Suyehiro, K., Acton, G.D., et al., 2000. *Proc. ODP, Init. Repts.,* 186: College Station, TX (Ocean Drilling Program). **doi:10.2973/odp.proc.ir.186.2000**

Sager, W.W., and Hutton, H.H., 1986. Magnetic-field measurements aboard the *JOIDES Resolution* and implications for shipboard paleomagnetic studies. *In* Austin, J.A., Jr., Schlager, W., Palmer, A.A., et al., *Proc ODP, Init. Repts.,* 101: College Station, TX (Ocean Drilling Program), 33–37. **doi:10.2973/odp.proc.ir.101.103.1986**

Shibuya, H., Merrill, D.L., Hsu, V., and Leg 124 Shipboard Scientific Party, 1991. Paleogene counterclockwise rotation of the Celebes Sea—orientation of ODP cores utilizing the secondary magnetization. *In* Silver, E.A., Rangin, C., von Breymann, M.T., et al., *Proc. ODP, Sci. Results,* 124: College Station, TX (Ocean Drilling Program), 519–523. **doi:10.2973/odp.proc.sr.124.169.1991**

Shipboard Scientific Party, 1995. Explanatory notes. *In* Curry, W.B., Shackleton, N.J., Richter, C., et al., *Proc. ODP, Init. Repts.,* 154: College Station, TX (Ocean Drilling Program), 11–38. **doi:10.2973/odp.proc.ir.154.102.1995**

Shipboard Scientific Party, 2000. Explanatory notes. *In* Plank, T., Ludden, J.N., Escutia, C., et al., *Proc. ODP, Init. Repts.,* 185: College Station, TX (Ocean Drilling Program), 1–76. **doi:10.2973/odp.proc.ir.185.102.2000**

Shipboard Scientific Party, 2003. Explanatory notes. *In* Stephen, R.A., Kasahara, J., Acton, G.D., et al., *Proc. ODP, Init. Repts.,* 200: College Station, TX (Ocean Drilling Program), 1–66. **doi:10.2973/odp.proc.ir.200.102.2003**

Stacey, F.D., and Banerjee, S.K., 1974. *The Physical Principles of Rock Magnetism:* Dev. Solid Earth Geophys., 5: New York (Elsevier).

Stokking, L.B., Musgrave R.J., Bontempo, D., and Autio, W., 1993. Handbook for Shipboard Paleomagnetists. *ODP Tech. Note,* 18 [Online]. Available from World Wide Web: <**http://www-odp.tamu.edu/publications/tnotes/tn18/f_pal.htm**>.

Storms, M.A., Robinson, M., Pollard, E.C., Schulte, E.J., and Graber, K.K. (Eds.), 2006. *Advanced Piston Corer operations manual*. Available from Word Wide Web:

Tarling, D.H., and Hrouda, F., 1993. *The Magnetic Anisotropy of Rocks:* London (Chapman and Hall).

Tauxe, L., 1993. Sedimentary records of relative paleointensity of the geomagnetic field: theory and practice. *Rev. Geophys.,* 31:319–354.

Tauxe, L., LaBrecque, J.L., Dodson, R., and Fuller, M., 1983. "U" channels—a new technique for paleomagnetic analysis of hydraulic piston cores. *Eos, Trans. Am. Geophys. Union,* 64:219.

Tauxe, L., Valet, J.-P., and Bloemendal, J., 1989. Magnetostratigraphy of Leg 108 advanced hydraulic piston cores. *In* Ruddiman, W., Sarnthein, M., et al., *Proc. ODP, Sci. Results,* 108: College Station, TX (Ocean Drilling Program), 429–439. **doi:10.2973/odp.proc.sr.108.154.1989**

Verosub, K.L., Steiner, M., and Opdyke, N., Conveners, 1986. Paleomagnetic Objectives for the Ocean Drilling Program, JOI/USSAC Workshop Report: Washington, D.C. (Joint Oceanographic Institutions, Inc.).

Weeks, R.J., Laj, C., Endignoux, L., Fuller, M.D., Roberts, A.P., Manganne, R., Blanchard, E., and Goree, W., 1993. Improvements in long-core measurement techniques: applications in palaeomagnetism and palaeoceanography. *Geophys. J. Int.,* 114:651–662.

Yamazaki, T., Solheid, P.A., and Frost, G.M., 2000. Rock magnetism of sediments in the Angola-Namibia upwelling system with special reference to loss of magnetization after core recovery. *Earth, Planets Space,* 52:329–336.

APPENDIX A: MAGNETIC UNITS

Quantity	Symbol (SI)	Unit (SI)	Symbol (cgs)	Unit (cgs)	Relationship
Energy	E	Joule (J)	—	erg	1 J = 10^7 erg
Force	F	1N = kg·m/s^2	—	dyne = g·m/s^2	1 N = 10^5 dyne
Current	I	Ampere(A) = Cs	—	abampere = 10 C/s	1 A = 0.1 abampere
Induction in free space (field)	B_0	Tesla (T)	B	Gauss (G)	1 T = 10^4 G
Magnetic force (field)	H	A/m	H	Oersted (Oe)	1 A/m = $4\pi 10^{-3}$ Oe; 1 Oe = 10^{-4} T = 0.1 mT
Permeability of a vacuum	$\mu_0 = 4\pi 10^{-7}$ Hm^{-1}	—	$\mu_0 = 1$	—	1 Hm^{-1} = $10^7/4\pi$ G/Oe
Induction:					
Induction in free space (field)	$B_0 = \mu_0 H$	—	H	—	1T = 10^4 G
Induction in medium	$B = B_0 + \mu_0 M$	—	$B = H + 4\pi$	—	1T = 10^4 G
Magnetization:					
Per unit volume	M	A/m	I	G	1 A/m = 10^{-3} G
Per unit mass	$\sigma = M/\rho$	Am^2/kg	$\sigma = I/\rho$	G·cm^3/g	1 Am^2/kg = 1 G·cm^3/g
Susceptibility:					
Per unit volume	$\kappa = M/H$	Dimensionless	$\kappa = I/H$	Dimensionless	1 (SI unit) = 4π G/Oe = 1 (cgs unit)/4π
Per unit mass	$\chi = \kappa/\rho$	m^3/kg	$\chi = \kappa/\rho$	cm^3/g	1 m^3/kg = $4\pi 10^{-3}$ G/Oe·cm^3/g

APPENDIX B: FILE FORMATS

Revisions

Leg Initials Date

Indented revision notes. If this file undergoes revisions, copy the original to a new file named for the leg on which the revisions first applied (e.g., PMAG FILE FORMATS.030.html). Only information for that leg is documented.

194 dmaf 1/31/2001

Alternate Treatment comment field is a line by itself (line 6) rather than an appendage of line 5 as previously documented. Actual Long Core program output has been this way for many legs previous. Line 5 may contain the lone text *NONE;* indicating that no treatment was applied on that sample run. In this case the second and third fields are NOT output, nor are the intervening tabs. Corrected documented file naming standard. File naming convention changed, circa Leg 181, to allow for six-digit run numbers.

File Naming Conventions

CMnnnnnn.DATCMnnnnnn.TRY

- Where *nnnnnn* is a zero-padded run number.
- DAT files contain calibration data in the file header and sample data in the file body. At present only files of this type have their content loaded into the central database. The sample data may be for either discrete samples (archive or working half) or for continuous sections of core. The LONG CORE program allows the distinct data sets to be separated automatically into two different storage locations. The same file format definitions apply to both sets of files.
- TRY files contain additional calibration data. These are NOT currently loaded into the central database.

CMnnnnnn.DAT Files

- File format implemented in software system **Long Core** (v191) by source modules named *Long Core Header Writer.vi* and *Long Core Data Writer.vi.*
- Data upload supported by **Generic Uploader** (v192) by modules first deployed for production use on leg 194: pmag.cfg, pmag\dat.cfg, pmag\dat.sql.
- Data edits for routine or procedural errors supported by **CryoEdit** (v194). Upload capabilities removed from this program; superseded by Generic Uploader.
- Data reporting supported by **JanusWeb** modules *Cryomagnetometer* and *Z-Plot:* http://janusaxp.tamu.edu/predef_queries/links/links_all.shtml
- Standard shipboard storage paths for raw files (DATA1): *r:\janus_q\cryo_mag\continuous*, *r:\janus_q\cryo_mag\discrete*. These subdirectories are further subdivided by hole, e.g. 1192a\.
- Standard shore archival storage paths for raw files (PRIME DATA): *p:\Prime Data\14a Paleomag*\leg*cryo_mag*\...

Table AT1. Long Core data matrix for DAT files (from *Technical Note* 37 [ODP Information Technology and Data Services, 2007]).

File line	Field name	Field format	Content (Long Core notes)	Database and upload notes
1	run_number	6	zero-padded 6-digit whole number	Uploads to pmag_run_num of pmag_run, pmag_run_data, and pmag_section_data.
	run_date_time	13	mm/dd/yy hhmi	In SQL use to_date format mm/dd/**rr** hh24mi. **rr** accomodates appropriate handling of 4-digit years. pmag_calib.pmag_calib_date_time
2	system_id	20	CRYO | SPINNER	Value ignored by uploader, hard-coded as pmag_run.system_id=1
3	run_type	20	SAMPLE	Ignored by uploader
	measurement_type	20	CONTINUOUS | DISCRETE	pmag_run.pmag_meas_type
	core_status	20	WHOLE | ARCHIVE | WORKING	pmag_run.pmag_core_status
4	X_response	7.4		pmag_calib.pmag_response_x
	Y_response	7.4		pmag_calib.pmag_response_y
	Z_response	7.4		pmag_calib.pmag_response_z
	X_calibration	11.4E3	SQUID calibration constant (emu/flux_quanta)	pmag_calib.pmag_calib_x
	Y_calibration	11.4E3	SQUID calibration constant (emu/flux_quanta)	pmag_calib.pmag_calib_y
	Z_calibration	11.4E3	SQUID calibration constant (emu/flux_quanta)	pmag_calib.pmag_calib_z
5	Demag_axis	4	For alternating frequency (AF) demagnetization yields any combination of the characters XYZ. Will be NONE if a non-AF treatment is applied.	XYZ when present populates pmag_run.pmag_demag_x|y|z_flag. Presence of XYZ causes pmag_section_data.pmag_demag_type to be set to "AF."
	Applied demagnetization level	7.2	milliTesla (mT). When demag axis = NONE this and the following field are omitted. Intervening tabs also omitted.	pmag_section_data.pmag_demag_level
	Unit		For demag treatments this is always mT (milliTesla). Long Core acquisition doesn't currently define anything else.	Mapped to pmag_run.pmag_alternate_treatment when XYZ combination is present.
6	alternate_treatment	40	Comment field	pmag_run.pmag_alternate_treatment. Presently not used by Long Core.
7	core_length	5.1	Empty if measurement type = DISCRETE (cm)	pmag_run.pmag_core_length
	requested_daq_interval	5.1	Empty if measurement type = DISCRETE (cm)	pmag_run.pmag_req_daqs_interval
	number_daqs_samples	3	# of measurements taken at a point and averaged	pmag_run.pmag_num_daqs_sample
8	tray_corrected	3	YES | NO	YES = 1, NO = 0; pmag_run.pmag_tray_corr_flag
	tray_date_time	13	empty if tray corrected = NO. Intervening tab is preserved.	pmag_run.pmag_tray_date_time
9	drift-corrected	3	YES | NO	pmag_run.pmag_drift_corr_flag
	bkgnd_1_X	11.4E3	when drift-corrected = NO, this and subsequent fields on the line are blank. Intervening tabs are preserved.	pmag_run.pmag_drift_bkgd_1_x
	bkgnd_2_X	11.4E3		pmag_run.pmag_drift_bkgd_2_x
	bkgnd_1_Y	11.4E3		pmag_run.pmag_drift_bkgd_1_y
	bkgnd_2_Y	11.4E3		pmag_run.pmag_drift_bkgd_2_y
	bkgnd_1_Z	11.4E3		pmag_run.pmag_drift_bkgd_1_z
	bkgnd_2_Z	11.4E3		pmag_run.pmag_drift_bkgd_2_z
	bkgnd_1_time	10		pmag_run.pmag_drift_bkgd_1_time
	bkgnd_2_time	10		pmag_run.pmag_drift_bkgd_2_time
10	section_id	7	0	pmag_section_data.section_id looked up based on L/S/H/C/T/S keys provided in sample data. Upload fails if no match.
11	number of data points	4		Ignored by uploader.
12	START OF DATA		"N" rows of data follow.	Used by uploader to flag start of repeated body records.
13	<extra space>	1	SampleID is formatted according to the **old** ODP standard.	These keys are used to look up the database section IDs in the core log.
	Leg	3	For continuous runs, L/S/H/C/T/S are the same for each sample record. In discrete runs, these values are different, but each run goes in its own separate file (i.e., only one sample point per discrete run-file vs many points in a single continuous run-file).	pmag_run.leg, pmag_section_data.leg, pmag_run_data.leg
	sub leg	1		Ignored by uploader.
	site	4		
	Hole	1		
	Core	4		
	Type	1		
	Section	2	Section number or CC	pmag_section_data.section_id

Table AT1 (continued).

File line	Field name	Field format	Content (Long Core notes)	Database and upload notes
	top_interval	5.1		pmag_run_data.pmag_top_interval. For discretes uploader looks up PMAG sample table IDs based on this information. Plugged into pmag_section_data.pmag_sample_id and pmag_section_data.pmag_sam_location
	bottom_interval	5.1		pmag_run_data.pmag_bottom_interval
	corrected_inclination	6.2		pmag_section_data.pmag_inclination
	corrected_declination	7.2		pmag_section_data.pmag_declination
	corrected_intensity	11.4E3		pmag_section_data.pmag_intensity
	corrected_X_intensity	11.4E3		pmag_run_data.pmag_corr_intensity_x
	corrected_Y_intensity	11.4E3		pmag_run_data.pmag_corr_intensity_y
	corrected_Z_intensity	11.4E3		pmag_run_data.pmag_corr_intensity_z
	corrected_X_moment	11.4E3		pmag_run_data.pmag_corr_moment_x
	corrected_Y_moment	11.4E3		pmag_run_data.pmag_corr_moment_y
	corrected_Z_moment	11.4E3		pmag_run_data.pmag_corr_moment_z
	uncorrected_X_moment_mean	11.4E3		pmag_run_data.pmag_uncorr_moment_x_mean
	uncorrected_X_moment_sd	11.4E3		pmag_run_data.pmag_uncorr_moment_x_sd
	uncorrected_Y_moment_mean	11.4E3		pmag_run_data.pmag_uncorr_moment_y_mean
	uncorrected_Y_moment_sd	11.4E3		pmag_run_data.pmag_uncorr_moment_y_sd
	uncorrected_Z_moment_mean	11.4E3		pmag_run_data.pmag_uncorr_moment_z_mean
	uncorrected_Z_moment_sd	11.4E3		pmag_run_data.pmag_uncorr_moment_z_sd
	sample_time	10	Zero-padded relative time from a high-frequency counter	pmag_run_data.pmag_sample_time
	core_diameter	5.2	Present when measurement type = CONTINUOUS. Otherwise blank. Intervening tabs are preserved.	pmag_run_data.pmag_core_diam
	sample_volume	5.2	Present when measurement type = DISCRETE. Otherwise blank. Intervening tabs are preserved the core_diameter is blank and sample_volume is present.	Not uploaded. Already logged in sample.volume
	data_type	20	LEADER | TRAILER | SAMPLE	pmag_run_data.pmag_data_type
13+N	END OF DATA		Marks the beginning of data points	

Example Discrete File Output

0558 01/12/01 1634
CRYO
SAMPLE DISCRETE WORKING
6.0710 6.2080 9.9230 8.2100E-5 -8.3400E-5 4.3200E-5
NONE
1
YES 01/08/01 2112
YES 0.0000E+0 2.1510E-10 0.0000E+0 3.1692E-11 0.0000E+0 -3.5856E-11 0000000000 0000037374 0000000
0001
START OF DATA
194 1192 A 2 H 2 50.0 50.0 50.24 271.18 6.1530E-4 8.1327E-6 -3.9346E-4 4.7299E-4 4.8796E-11 -2.3608E-9 2.8379E-9 1.0919E-10 0.0000E+0 -2.3519E-9 0.0000E+0 2.8279E-9 0.0000E+0 0000010494 6.00 SAMPLE
END OF DATA
Example Continuous File Output with Demag Level Applied
0001 01/10/01 0408
CRYO
SAMPLE CONTINUOUS ARCHIVE
6.0710 6.2080 9.9230 8.2100E-5 -8.3400E-5 4.3200E-5
XYZ 5 mT
147.0 5.0 1
YES 01/08/01 2112
YES 0.0000E+0 1.4548E-9 0.0000E+0 4.5536E-10 0.0000E+0 -3.9744E-11 0000000000 0000138746 0000000

0032
START OF DATA
194 1192 A 1 H 1 -5.0 -5.0 12.25 206.31 4.7994E-3 -4.2042E-3 -2.0789E-3 1.0184E-3 -4.2348E-7 -2.1413E-7 1.6767E-7 -4.2343E-7 0.0000E+0 -2.1411E-7 0.0000E+0 1.6766E-7 0.0000E+0 0000005248 16.59 LEADER
194 1192 A 1 H 1 0.0 0.0 21.43 14.97 1.4044E-2 1.2630E-2 3.3762E-3 5.1304E-3 1.2722E-6 3.4775E-7 8.4466E-7 1.2723E-6 0.0000E+0 3.4778E-7 0.0000E+0 8.4466E-7 0.0000E+0 0000009473 16.59 SAMPLE
...
194 1192 A 1 H 1 145.0 145.0 -2.55 1.08 4.6061E-3 4.6007E-3 8.6665E-5 -2.0489E-4 4.6342E-7 8.9265E-9 -3.3732E-8 4.6477E-7 0.0000E+0 9.3491E-9 0.0000E+0 -3.3769E-8 0.0000E+0 0000128764 16.59 SAMPLE
194 1192 A 1 H 1 150.0 150.0 -3.62 300.91 7.9815E-4 4.0922E-4 -6.8340E-4 -5.0366E-5 4.1220E-8 -7.0390E-8 -8.2922E-9 4.2613E-8 0.0000E+0 -6.9954E-8 0.0000E+0 -8.3303E-9 0.0000E+0 0000132860 16.59 TRAILER
END OF DATA

CMnnnnnn.TRY Files

- File format implemented in software system **Long Core** (version 191) by source modules named *Long Core Header Writer.vi* and *Long Core Data Writer.vi*.
- Data upload is currently not supported for the content of these files.

Table AT2. Long Core data matrix for TRY files.

File line	Field name	Field format	Content (Long Core notes)
1	run_number	6	zero-padded 6-digit whole number
	run_date_time	13	mm/dd/yy hhmi
2	system_id	20	CRYO | SPINNER
3	run_type	20	TRAY
	measurement_type	20	CONTINUOUS
	core_status	20	Field is blank. Preceding tab is preserved.
4	X_response	7.4	Calibration data recorded just as in the DAT format.
	Y_response	7.4	
	Z_response	7.4	
	X_calibration	11.4E3	SQUID calibration constant (emu/flux_quanta)
	Y_calibration	11.4E3	SQUID calibration constant (emu/flux_quanta)
	Z_calibration	11.4E3	SQUID calibration constant (emu/flux_quanta)
5	core_length	5.1	Empty if measurement type = DISCRETE (cm)
	requested_daq_interval	5.1	Empty if measurement type = DISCRETE (cm). Interval at which consecutive measurements are taken.
	number_daqs_samples	3	# of measurements taken at a point and averaged.
6	Blank line	40	Comment field?
7	drift-corrected	3	YES | NO
	bkgnd_1_X	11.4E3	When drift-corrected = NO, this and subsequent fields on the line are blank. Intervening tabs are preserved.
	bkgnd_2_X	11.4E3	
	bkgnd_1_Y	11.4E3	
	bkgnd_2_Y	11.4E3	
	bkgnd_1_Z	11.4E3	
	bkgnd_2_Z	11.4E3	
	bkgnd_1_time	10	
	bkgnd_2_time	10	
8	number of data points	4	
9	START OF DATA		"N" rows of data follow. Data acquired at fixed down the length of the 'core boat' or tray.
10	run_date_time		mm/dd/yy hhmi
	top_interval	5.1	cm
	bottom_interval	5.1	cm
	corrected_inclination	6.2	
	corrected_declination	7.2	
	corrected_intensity	11.4E3	
	corrected_X_intensity	11.4E3	
	corrected_Y_intensity	11.4E3	
	corrected_Z_intensity	11.4E3	
	corrected_X_moment	11.4E3	
	corrected_Y_moment	11.4E3	
	corrected_Z_moment	11.4E3	
	uncorrected_X_moment_mean	11.4E3	
	uncorrected_X_moment_sd	11.4E3	
	uncorrected_Y_moment_mean	11.4E3	
	uncorrected_Y_moment_sd	11.4E3	
	uncorrected_Z_moment_mean	11.4E3	
	uncorrected_Z_moment_sd	11.4E3	
	sample_time+SAMPLE	10	Zero-padded relative time from a high-frequency counter. No intervening tab between the number and the text SAMPLE.
10+N	END OF DATA		

Example Tray (TRY) File

```
1061 01/13/01 0500
CRYO
TRAY CONTINUOUS
6.0710 6.2080 9.9230 8.2100E-5 -8.3400E-5 4.3200E-5
160.3 5.0 1
YES 0.0000E+0 6.6501E-11 0.0000E+0 5.0874E-11 0.0000E+0 -1.0800E-10 0000000000 0000149118
0035
START OF DATA
```

```
01/13/01 0500 -5.0 -5.0 1.3488E-10 1.9012E-10 -2.0461E-10 1.3711E-10 0.0000E+0 1.9182E-10
    0.0000E+0 -2.0822E-10 0.0000E+0 0000004993LEADER
01/13/01 0500 0.0 0.0 7.0775E-10 5.7403E-10 -1.0185E-10 7.1181E-10 0.0000E+0 5.7713E-10 0.0000E+0
    -1.0843E-10 0.0000E+0 0000009088SAMPLE
...
01/13/01 0500 160.0 160.0 -2.8734E-10 7.6537E-11 4.3005E-11 -2.2495E-10 0.0000E+0 1.2427E-10
    0.0000E+0 -5.8320E-11 0.0000E+0 0000139901SAMPLE
01/13/01 0500 165.0 165.0 -3.7945E-11 -4.9245E-12 -3.8270E-11 2.6272E-11 0.0000E+0 4.4202E-11
    0.0000E+0 -1.4256E-10 0.0000E+0 0000143996TRAILER
END OF DATA
```

APPENDIX C: KAPPABRIDGE OPERATION PROCEDURES

Zeroing and Calibration

1. Turn on the KLY-2 power switch.
2. Set "range selector" to 5. Needles in zero setting windows move according to position of the sensor
3. Zero setting: Adjust the **Im** (Imaginary component) knob until the needle points to zero. Adjust the **Re** (Real component) knob located on the sensor until the needle points to zero. When adjusting **Re**, you may need to first select a higher range and then work your way down to Range 5.
4. Standard calibration: It's recommended that the bridge be calibrated every day before use. For calibration we use the standard found in the black briefcase. Zero the bridge. Set the range **R** corresponding to the range indicated on the standard. Measure the standard (see below). If the value indicated on the display data is higher than the standard value, turn the potentiometer CALIBRATION counterclockwise. If lower, turn potentiometer clockwise. Repeat until both values coincide.
5. Phase calibration: As documented on Leg 152, there is a procedure for calibrating the phase between the imaginary component (**Im**) and the real component (**Re**). The imaginary component should not influence the real component unless the samples are electric conductive. This should not need to be done frequently.
6. Move the **Im** to zero.
7. Move the **Re** to zero.
8. Move the **Im** to one side of zero.
9. Find zero for **Re** by adjusting the phase pot.
10. Continue adjusting the components and pot until **Im** has only a small or no influence on the **Re.** It may take several turns. This procedure will prevent overadjusting the coil on the sensor and breaking it.

Measuring Samples

1. Set range selector to 5 (if specific range not previously known).
2. Be sure both the **Im** and **Re** are zeroed.
3. If the bridge is in the status **WAIT**, wait until it converts to the status **READY** by automatic zeroing.
4. Press the button **START/RESET**, the bridge enters the status **MEASURE.** Insert the specimen into the pick-up coil as quickly as possible.
5. After the beep sounds, remove the specimen from the pick-up coil.
6. After a few seconds the bridge enters the status **HALT.** If blinking 1999 appears in the display **DATA**, the bridge is overloaded and the measurement must be repeated in a higher range. If the display does not blink, decide whether the correct measuring range has been selected (range correction factors taped to the bridge) and adjust accordingly.
7. To take another measurement, press the **START/RESET** button, wait for **READY.**

Data Input

A computer interface program for the Kappabridge is currently installed on both the small PC and the Compaq laptop in the laboratory. Unfortunately, automatic data input is not available due to a communication problem between the instrument and the computer. A new interface box may need to be installed. For the meantime, data must be input manually. Before starting the program, make sure the Panasonic printer (sitting on top of DTech) is connected and set as the default printer.

1. To start the program, click on the MS-DOS Kly-2 shortcut icon on the desktop (C:\KP\KLY2.EXE)
2. Manual input only?…choose **Y**.
3. Operator Name, enter whatever name you want
4. Change the current set of orientation factors, etc.?…choose **N**.

5. Output on disk?…choose **Y**.
6. Specify if new [**1**] or existing file [**2**].
7. Type the output file path, for example "a:" for drive A, or "c:\data", or whatever you want.
8. Type the output file name, one file for each core is fine. For example, "999B-1H."
9. Specimen name. Enter the specimen name as follows: "core, section, top interval." For example, "1H,3,123" for a sample from Core 1H, Section 3, 123–125 cm. The commas are important because another program is used to make a comma-delimited ASCII text file of the data.
10. For locality name, enter the Hole, "999B."
11. New data or <CR>, hit **Return.**
12. Sampling angles theta and psi (more commonly known as declination and inclination). Caution: When entering this data, be aware of how the samples were taken. Simply pressing Return will enter in theta and psi values of 180,90 since samples are collected from the working half of the split core. However, if you have already accounted for this by drawing on the cube the three reference arrows for the AMS rotation scheme (see diagram taped to wall and/or sensor), then enter **0,90.** If the sample is oriented with the tensor tool, you can enter in the correct declination of the sample instead of **0.**
13. Tectonic systems T1 and T2 are asking for a bedding correction, and a lineation correction. Hit **Return** for both T1 and T2.
14. Kill the data?…**N** (unless you made a mistake in the above, then choose **Y**).
15. Select the measuring range (any range lower than 5 will not likely work due to the noisy surroundings). After selecting range, hit **Return.**
16. Begin measuring using the 15 sample positions.
17. After entering data for Position 15, hit **Return.** The program will automatically make the calculations and display the data. If everything looks good, choose [**1**] Print and then either quit the program or continue making measurements. The files are saved as "filename.KL2" ("999B-1H") in the directory you specified earlier.

Processing Data

The following directions will describe how to properly format the .KL2 files into .CAL files, and then finally into .TXT format, which can be imported into a spreadsheet.

First, open "Amskly.exe" found in the "Kly2" folder on the small PC hard drive (c:\Kly2\Amskly.exe). The program is menu driven, moving from choice to choice with the arrow keys, then hitting return. Choose **Import** and then **Set Directory** to where your files are. Then, choose to **Read File** and a list of all your .KL2 files will pop up. Select one by moving the arrow key to highlight it and hit return. Next, **Convert File.** This will make a "filename.CAL" file. After you have converted all of your .KL2 files to .CAL files, hit **ESC** to get back to the main screen.

Now you can analyze and plot the AMS data and make an ASCII text file. First choose **Read File** and select the .CAL file you want and hit return. Next, choose **Define Job** (this will allow only certain subgroups of specimens in a file to be read). You are asked how to define the job. Enter **1** for sites. Then type the Hole from which your samples came (that you entered during the measurement program) and press **Return.** For example, "**999B**". Press **Return.** Now you can look at the data, plot the principal axes, flinn plots, and so on. Ask one of the marine computer specialists for help if you have trouble printing plots.

The last step is to export the ASCII file. Select **ASCII Output** and hit Return. You are asked to type the name of the file. Type the filename and ".txt" extension (i.e., "999B-1H.txt"). The text file is set up as follows:

Core, section, top interval, kmax declination, kmax inclination, kint dec, kint incl, kmin dec, kmin incl, kmax (1×10^{-6} SI), kint, kmin

For example: 1H,3,123,300,0,210,0,120,90,435.9,420.1,418.7

The files are easily imported into Excel or another spreadsheet.

APPENDIX D: CONVERTING VOLTAGE TO MAGNETIC FIELDS FOR THE IM-10 IMPULSE MAGNETIZER

Voltage	Field (mT)	Voltage	Field (mT)	Voltage	Field (mT)	Voltage	Field (mT)	Voltage	Field (mT)	Voltage	Field (mT)
1	1	68	229	135	459	202	689	269	918	336	1144
2	2	69	233	136	462	203	692	270	921	337	1147
3	3	70	236	137	466	204	696	271	924	338	1151
4	5	71	240	138	469	205	699	272	928	339	1154
5	7	72	243	139	473	206	702	273	931	340	1158
6	9	73	246	140	476	207	706	274	935	341	1161
7	12	74	250	141	480	208	709	275	938	342	1164
8	15	75	253	142	483	209	713	276	941	343	1168
9	18	76	257	143	486	210	716	277	945	344	1171
10	22	77	260	144	490	211	720	278	948	345	1174
11	26	78	264	145	493	212	723	279	952	346	1178
12	30	79	267	146	497	213	726	280	955	347	1181
13	34	80	270	147	500	214	730	281	958	348	1184
14	38	81	274	148	504	215	733	282	962	349	1188
15	42	82	277	149	507	216	737	283	965	350	1191
16	46	83	281	150	510	217	740	284	969	351	1194
17	51	84	284	151	514	218	744	285	972	352	1198
18	55	85	288	152	517	219	747	286	975	353	1201
19	59	86	291	153	521	220	750	287	979	354	1204
20	63	87	294	154	524	221	754	288	982	355	1208
21	68	88	298	155	528	222	757	289	985	356	1211
22	72	89	301	156	531	223	761	290	989	357	1215
23	75	90	305	157	535	224	764	291	992	358	1218
24	79	91	308	158	538	225	767	292	996	359	1221
25	83	92	312	159	541	226	771	293	999	360	1225
26	86	93	315	160	545	227	774	294	1002	361	1228
27	89	94	318	161	548	228	778	295	1006	362	1231
28	93	95	322	162	552	229	781	296	1009	363	1235
29	96	96	325	163	555	230	785	297	1013	364	1238
30	100	97	329	164	559	231	788	298	1016	365	1241
31	103	98	332	165	562	232	791	299	1019	366	1245
32	106	99	336	166	565	233	795	300	1023	367	1248
33	110	100	339	167	569	234	798	301	1026	368	1251
34	113	101	342	168	572	235	802	302	1029	369	1255
35	117	102	346	169	576	236	805	303	1033	370	1258
36	120	103	349	170	579	237	808	304	1036	371	1261
37	124	104	353	171	583	238	812	305	1040	372	1265
38	127	105	356	172	586	239	815	306	1043	373	1268
39	130	106	360	173	589	240	819	307	1046	374	1271
40	134	107	363	174	593	241	822	308	1050	375	1275
41	137	108	366	175	596	242	826	309	1053	376	1278
42	141	109	370	176	600	243	829	310	1057	377	1281
43	144	110	373	177	603	244	832	311	1060	378	1285
44	147	111	377	178	607	245	836	312	1063	379	1288
45	151	112	380	179	610	246	839	313	1067	380	1291
46	154	113	384	180	613	247	843	314	1070	381	1294
47	158	114	387	181	617	248	846	315	1073	382	1298
48	161	115	390	182	620	249	849	316	1077	383	1301
49	164	116	394	183	624	250	853	317	1080	384	1304
50	168	117	397	184	627	251	856	318	1084	385	1308
51	171	118	401	185	631	252	860	319	1087	386	1311
52	175	119	404	186	634	253	863	320	1090	387	1314
53	178	120	408	187	637	254	866	321	1094	388	1318
54	182	121	411	188	641	255	870	322	1097	389	1321
55	185	122	414	189	644	256	873	323	1100	390	1324
56	188	123	418	190	648	257	877	324	1104	391	1328
57	192	124	421	191	651	258	880	325	1107	392	1331
58	195	125	425	192	655	259	884	326	1110	393	1334
59	199	126	428	193	658	260	887	327	1114	394	1338
60	202	127	432	194	661	261	890	328	1117	395	1341
61	205	128	435	195	665	262	894	329	1121	396	1344
62	209	129	438	196	668	263	897	330	1124	397	1348
63	212	130	442	197	672	264	901	331	1127	398	1351
64	216	131	445	198	675	265	904	332	1131	399	1354
65	219	132	449	199	679	266	907	333	1134	400	1357
66	223	133	452	200	682	267	911	334	1137		
67	226	134	456	201	685	268	914	335	1141		

PUBLISHER'S NOTES

Richter, C., Acton, G., Endris, C., and Radsted, M., 2007. Handbook for shipboard paleomagnetists. *ODP Tech. Note,* 34 [Online]. Available from World Wide Web: <http://www-odp.tamu.edu/publications/tnotes/tn34/INDEX.HTM>. [Cited YYYY-MM-DD]

Distribution: Electronic copies of this publication may be obtained from the ODP Publications homepage on the World Wide Web at **http://www-odp.tamu.edu/publications**.

This publication was prepared by the Ocean Drilling Program, Texas A&M University, as an account of work performed under the international Ocean Drilling Program, which is managed by Joint Oceanographic Institutions, Inc., under contract with the National Science Foundation. Funding for the program is provided by the following agencies:

Australia/Canada/Chinese Taipei/Korea Consortium for Ocean Drilling: Department of Primary Industries and Energy (Australia), Natural Resources Canada, National Taiwan University in Taipei, and Korean Institute for Geology, Mining, and Minerals
European Science Foundation Consortium for Ocean Drilling (Belgium, Denmark, Finland, Iceland, Ireland, Italy, The Netherlands, Norway, Portugal, Spain, Sweden, and Switzerland)
Federal Republic of Germany, Bundesanstalt fur Geowissenschaften und Rohstoffe
France, Institut National des Sciences de l'Univers–Centre National de la Recherche Scientifique (INSU-CNRS)
Japan, University of Tokyo, Ocean Research Institute
People's Republic of China, Marine High-Technology Bureau of the State Science and Technology Commission of the People's Republic of China
United Kingdom, Natural Environment Research Council
United States, National Science Foundation

DISCLAIMER

Figure F1. Schematic of ship (modified from graphic completed by Robert West) and layout of shipboard paleomagnetism laboratory with a photograph of the laboratory.

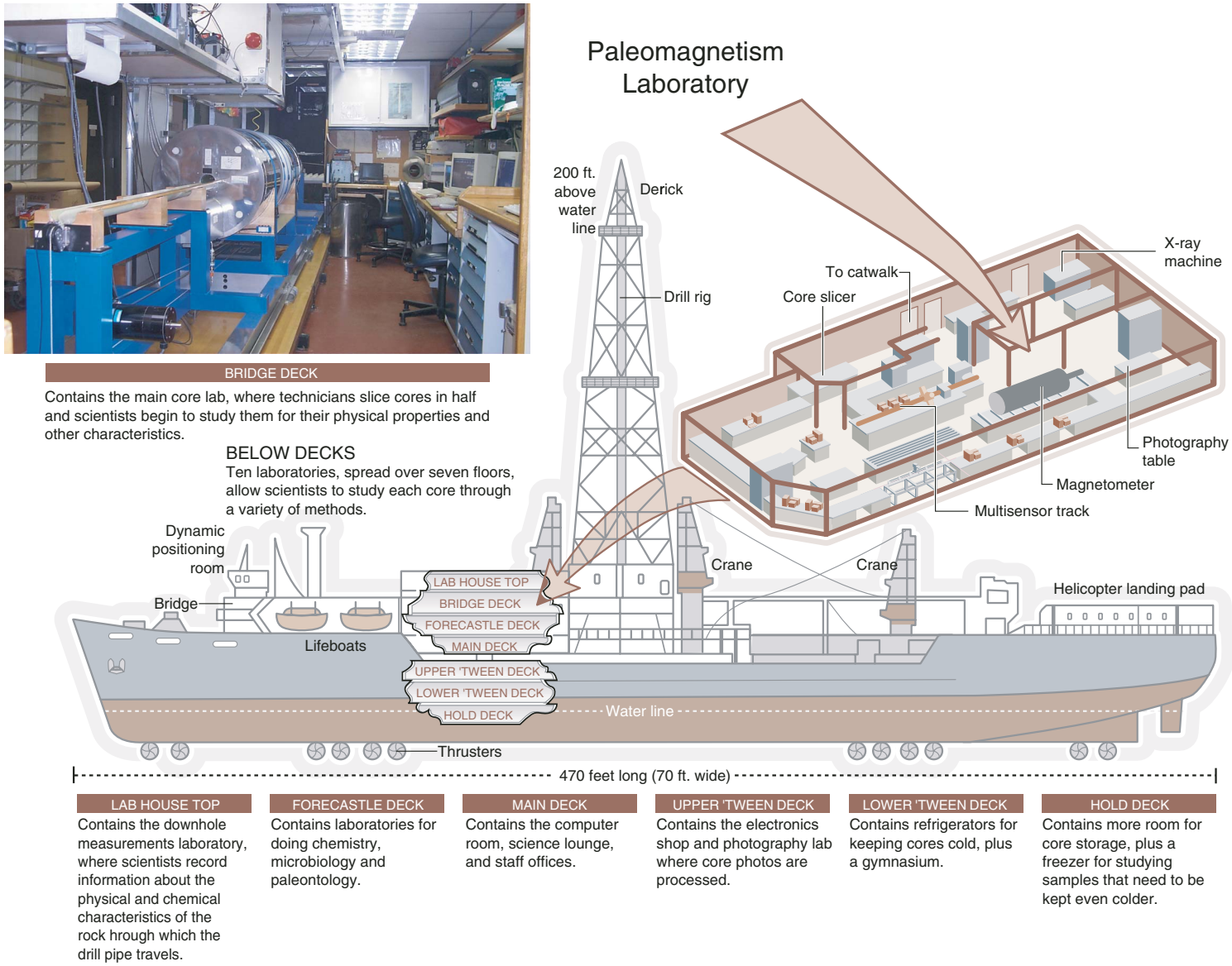

Figure F2. Orientation system used by ODP.

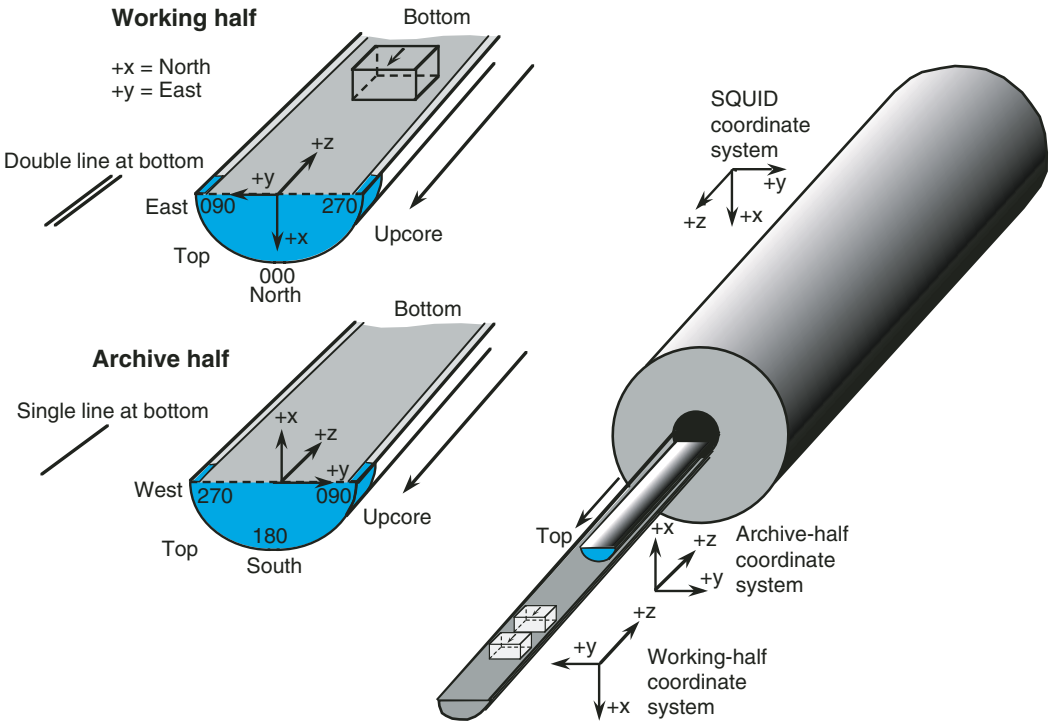

Figure F3. Standard plastic sampling U-channel and boxes used by ODP.

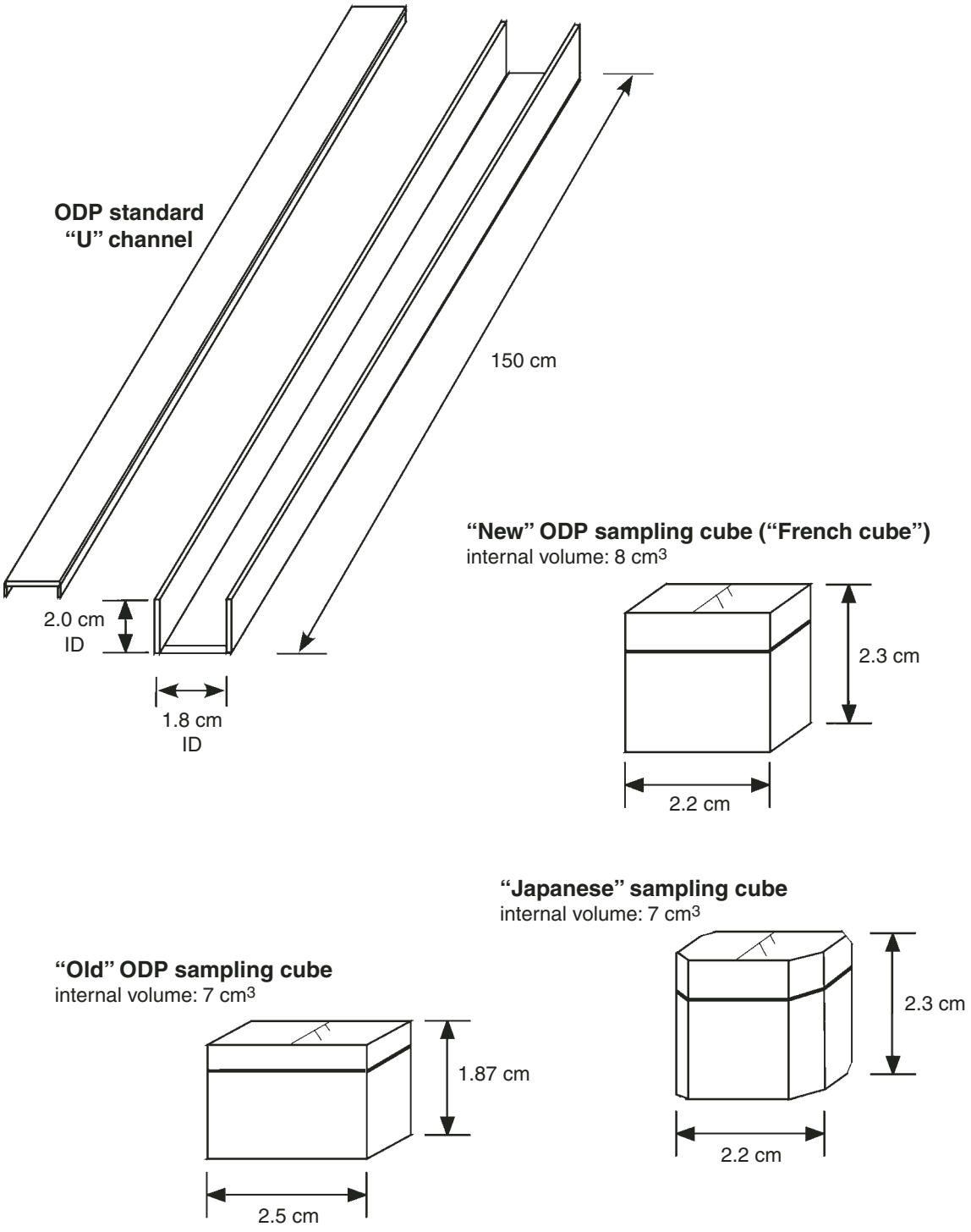

Figure F4. Sampling techniques used for collecting sediments in plastic sampling boxes.

Sampling method 1: Push the sample box into the soft sediment and then remove it with a U-shaped wire mounted on a wooden handle.

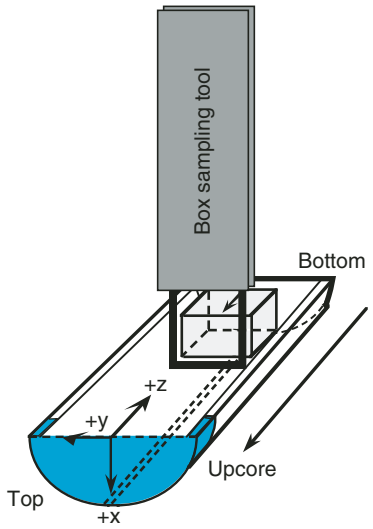

Sampling method 2: Push the extruder (two types are available) into the soft sediment, remove extruder with sediment inside, trim excess sediment from the base of the extruder with a spatula, and then extrude the sediment into the sample box.

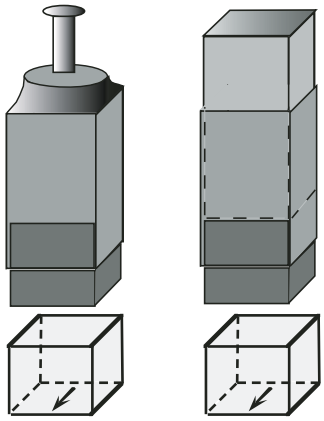

The three main plastic boxes used for paleomagnetic samples

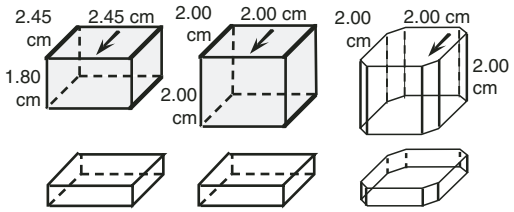

Figure F5. U-channel sample being collected in soft sediment.

Figure F6. Database data model for paleomagnetism data collected by the cryogenic magnetometer.

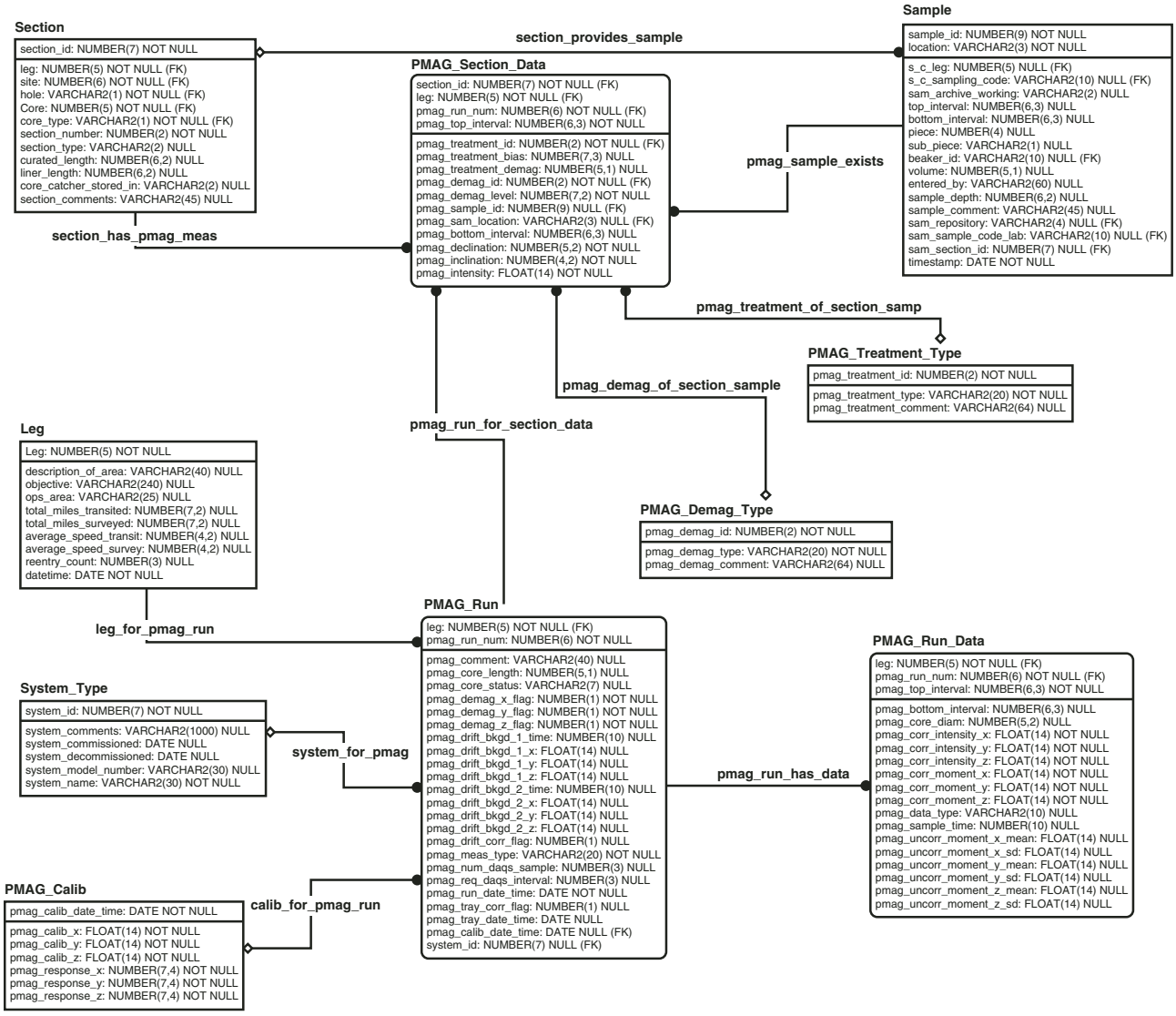

Figure F7. Database data model for core orientation data collected by the Tensor tool.

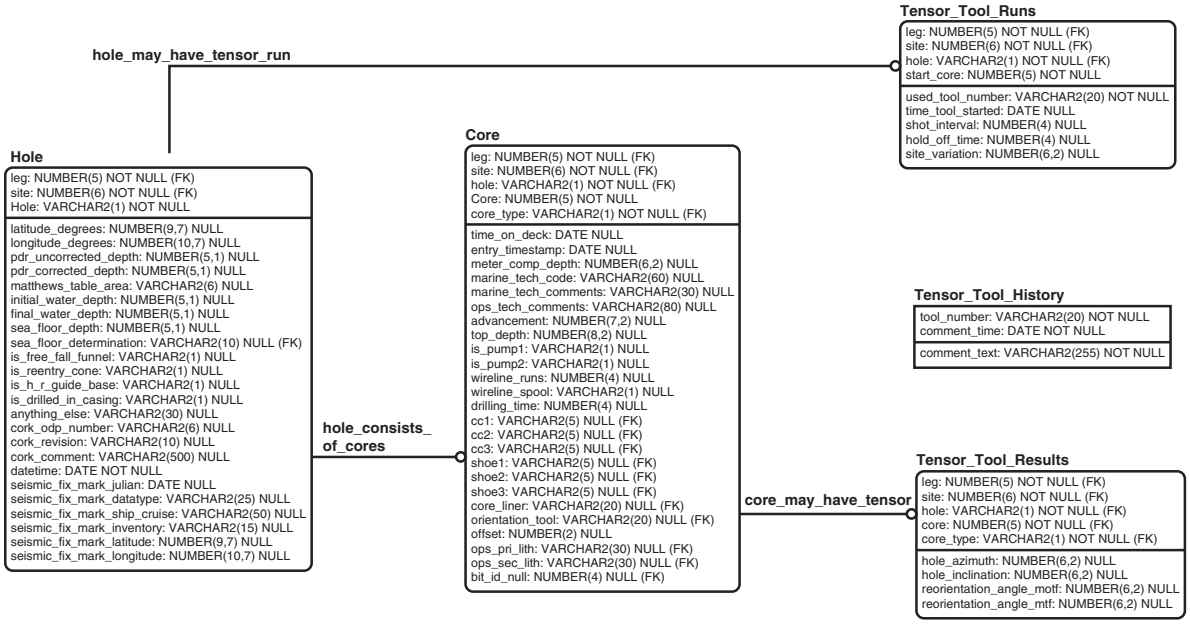

Figure F8. Web page for database queries.

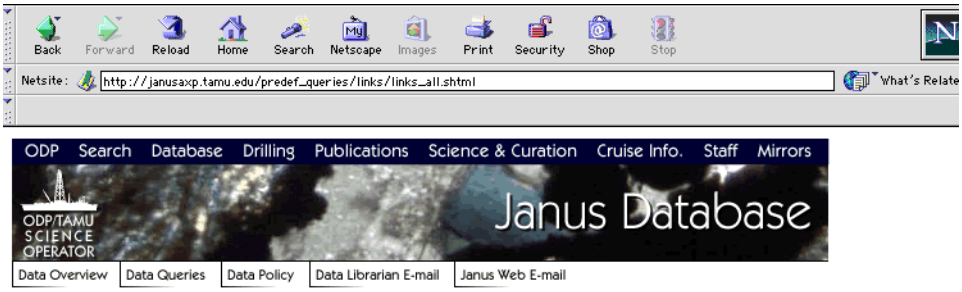

Figure F9. Database data model for core log information.

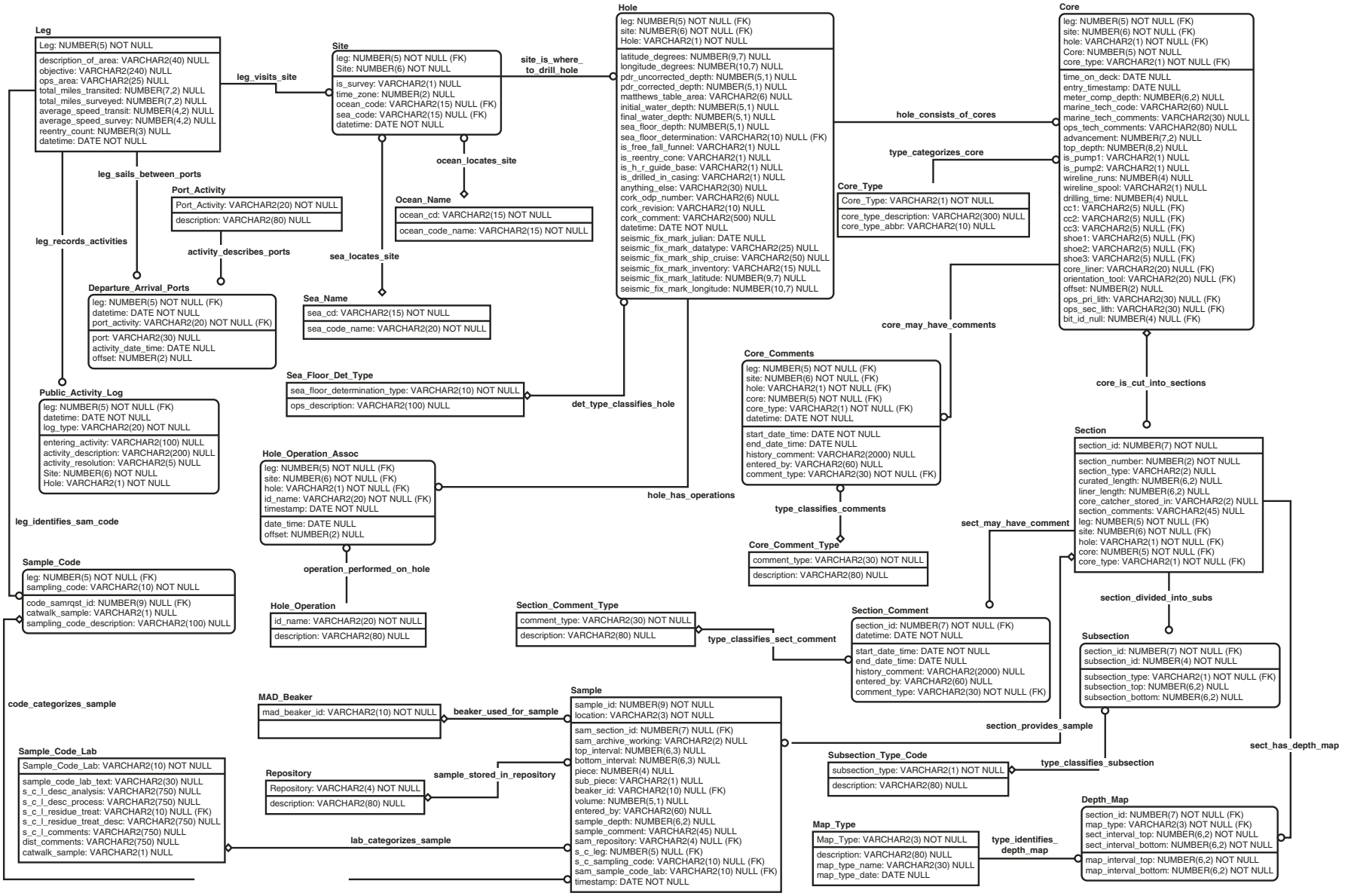

Figure F10. Shipboard cryogenic magnetometer.

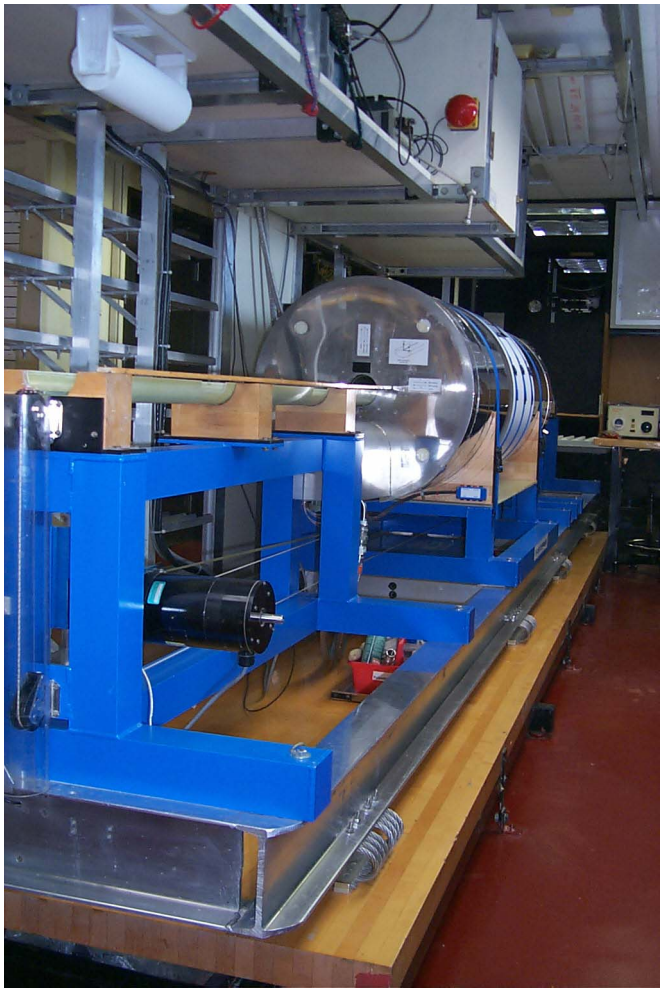

Figure F11. Various electronic boxes for the cryogenic magnetometer.

Figure F12. Magnetic field profile from within the shield for the cryogenic magnetometer.

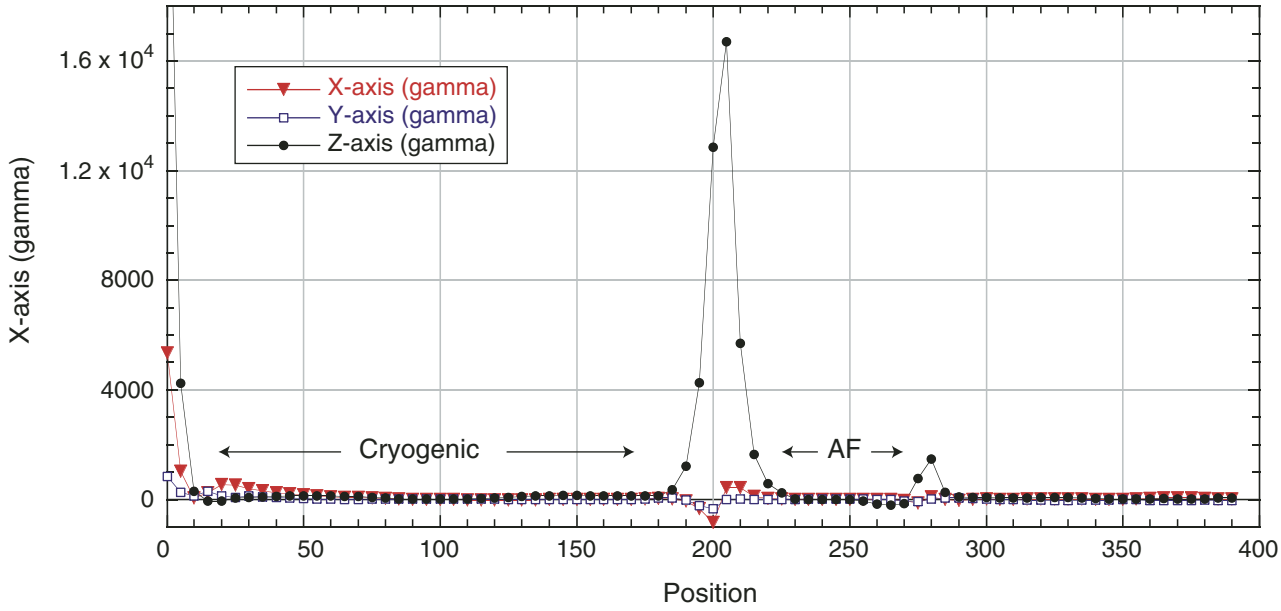

Figure F13. Long Core application screen.

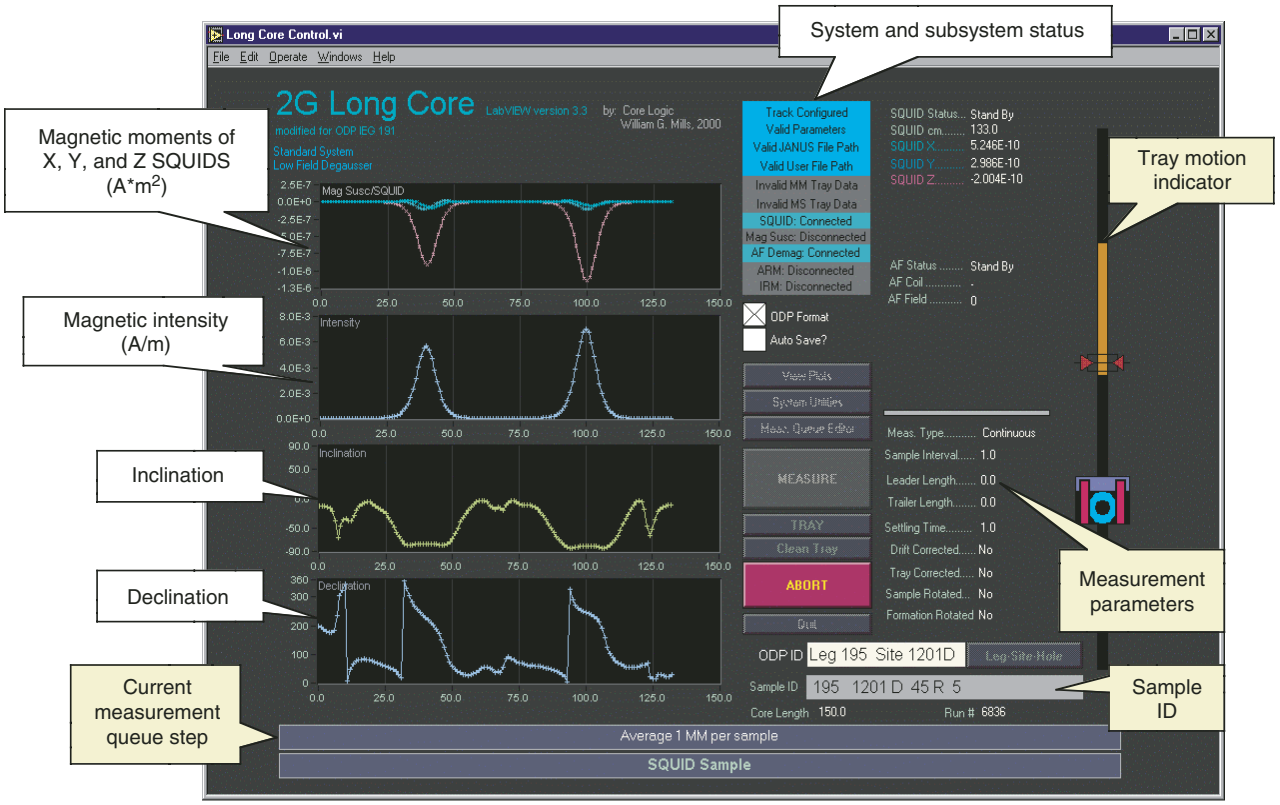

Figure F14. Profile of SQUID voltage as a function of distance from the sensor for a small dipole sample.

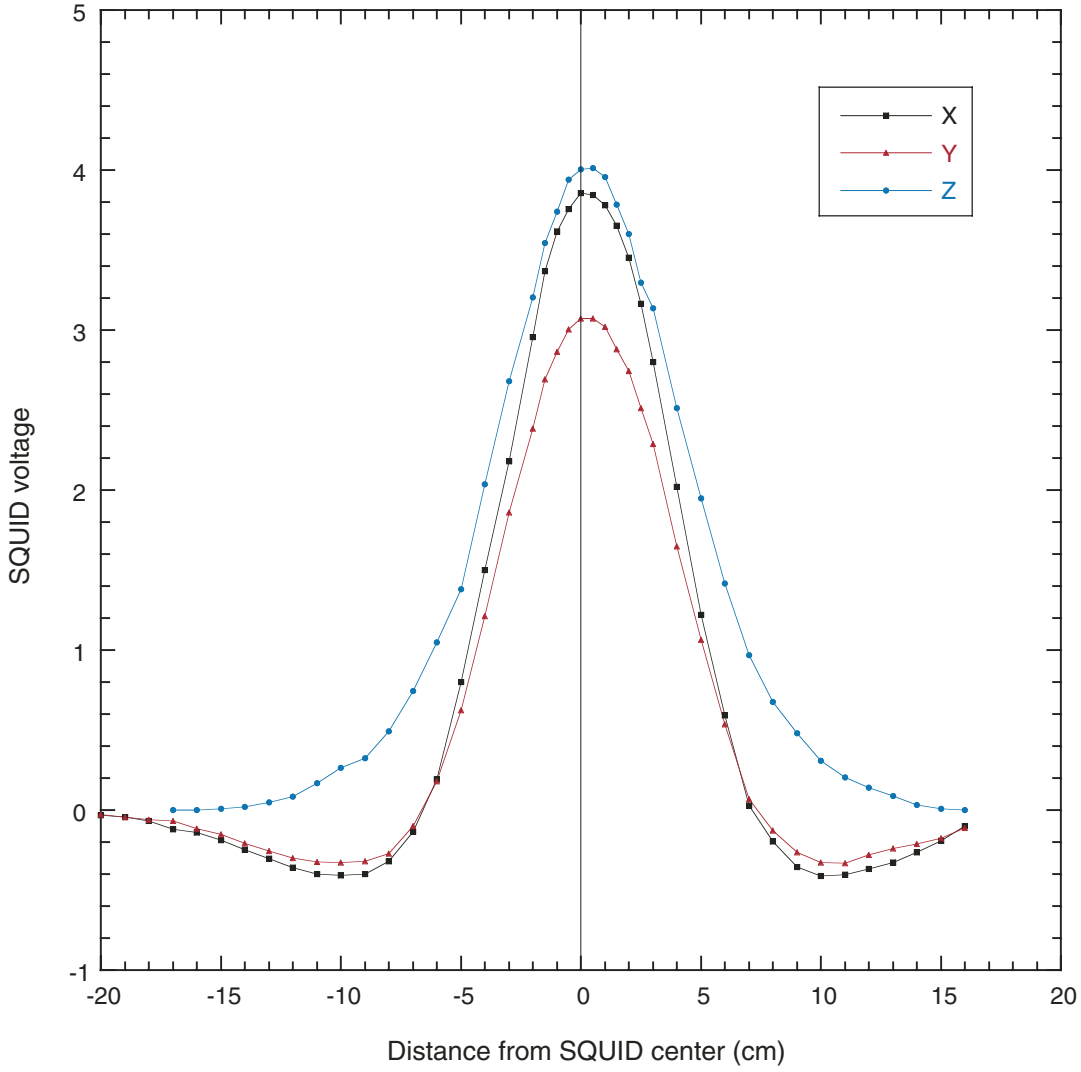

Figure F15. Web browser interface for downloading paleomagnetic data from the ODP database.

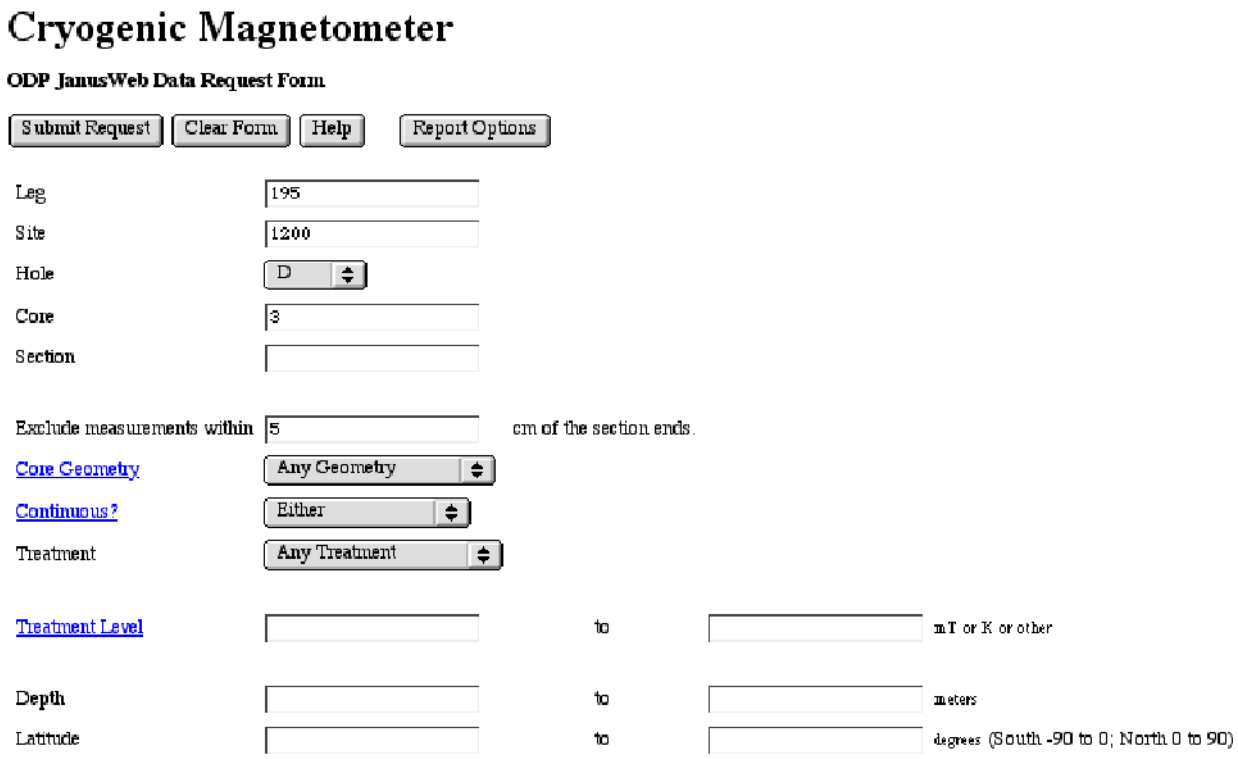

Figure F16. Molspin Minispin spinner magnetometer.

Figure F17. Bartington Instruments magnetic susceptibility meter (model MS2).

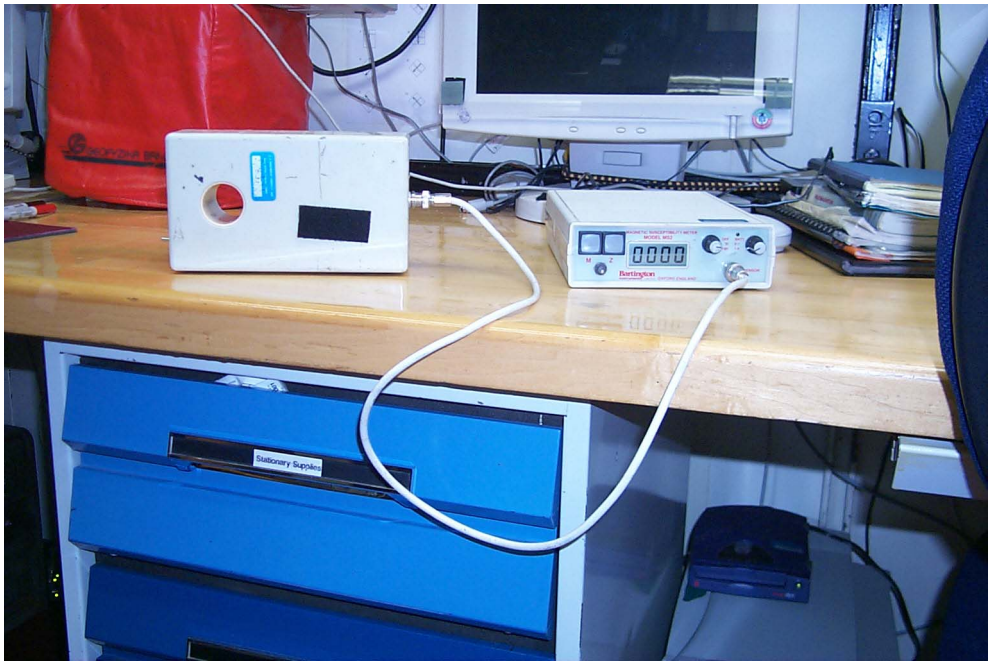

Figure F18. Kappabridge KLY-2 magnetic susceptibility system.

Figure F19. Orientations used to determine the magnetic anisotropy for a cube sample measured in the Kappabridge.

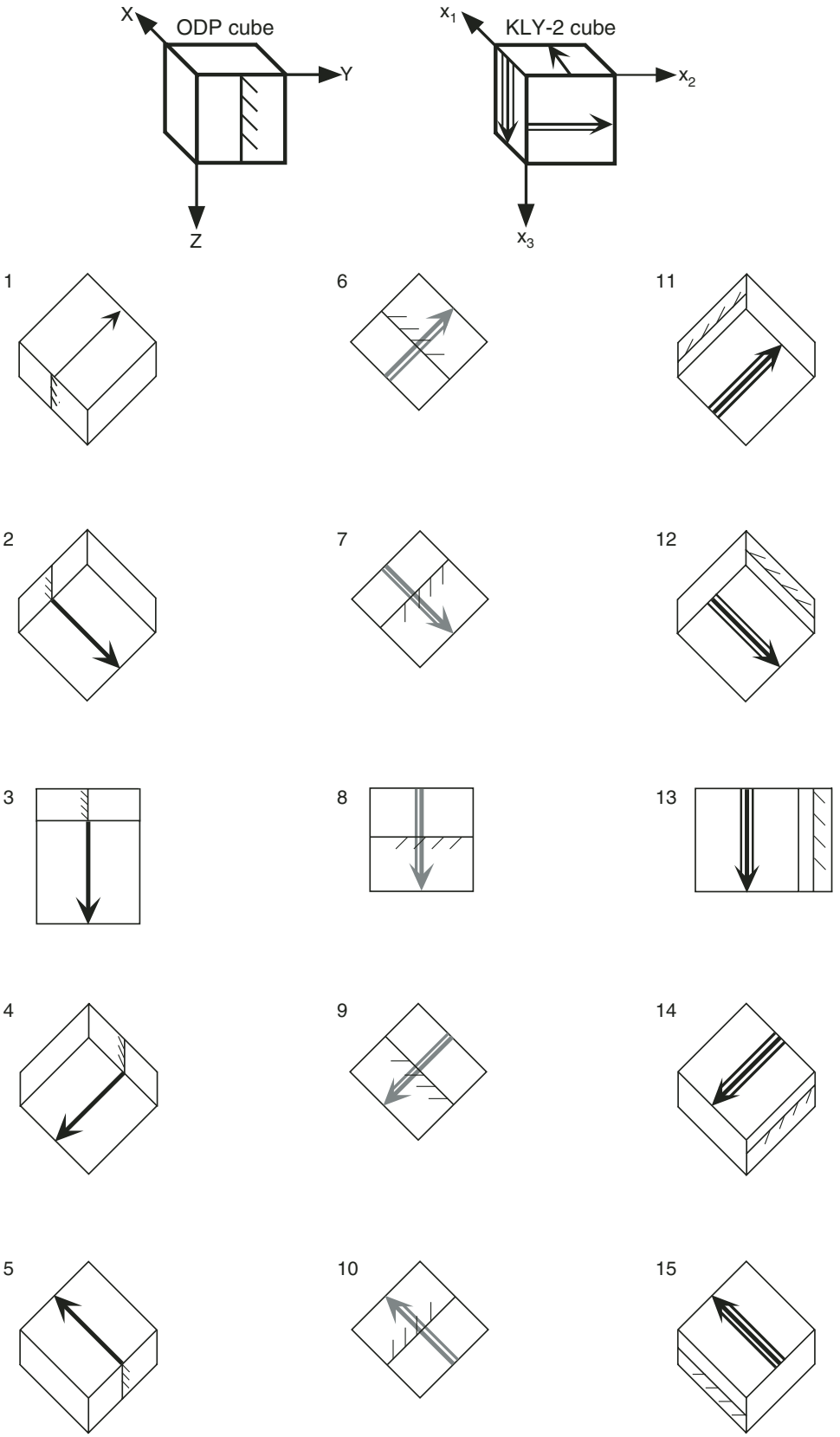

Figure F20. Schonstedt TSD-1 thermal demagnetizer.

Figure F21. Profile of magnetic field versus position along the chamber of the Schonstedt TSD-1 thermal demagnetizer.

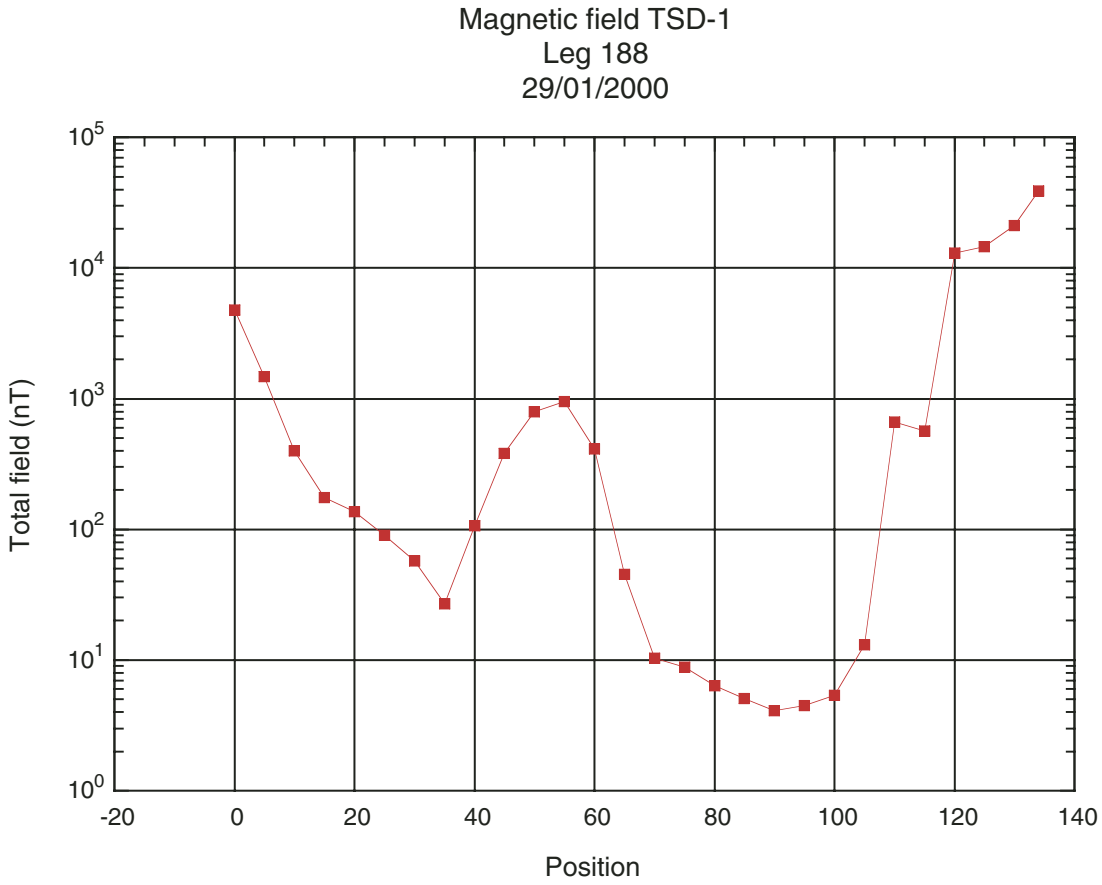

Figure F22. DTECH model D-2000 demagnetizer.

Figure F23. ASC IM-10 impulse magnetizer.

Figure F24. Two of the Tensor tools used for core orientation.

Figure F25. Orientation terminology for the Tensor tool. MTF = magnetic toolface.

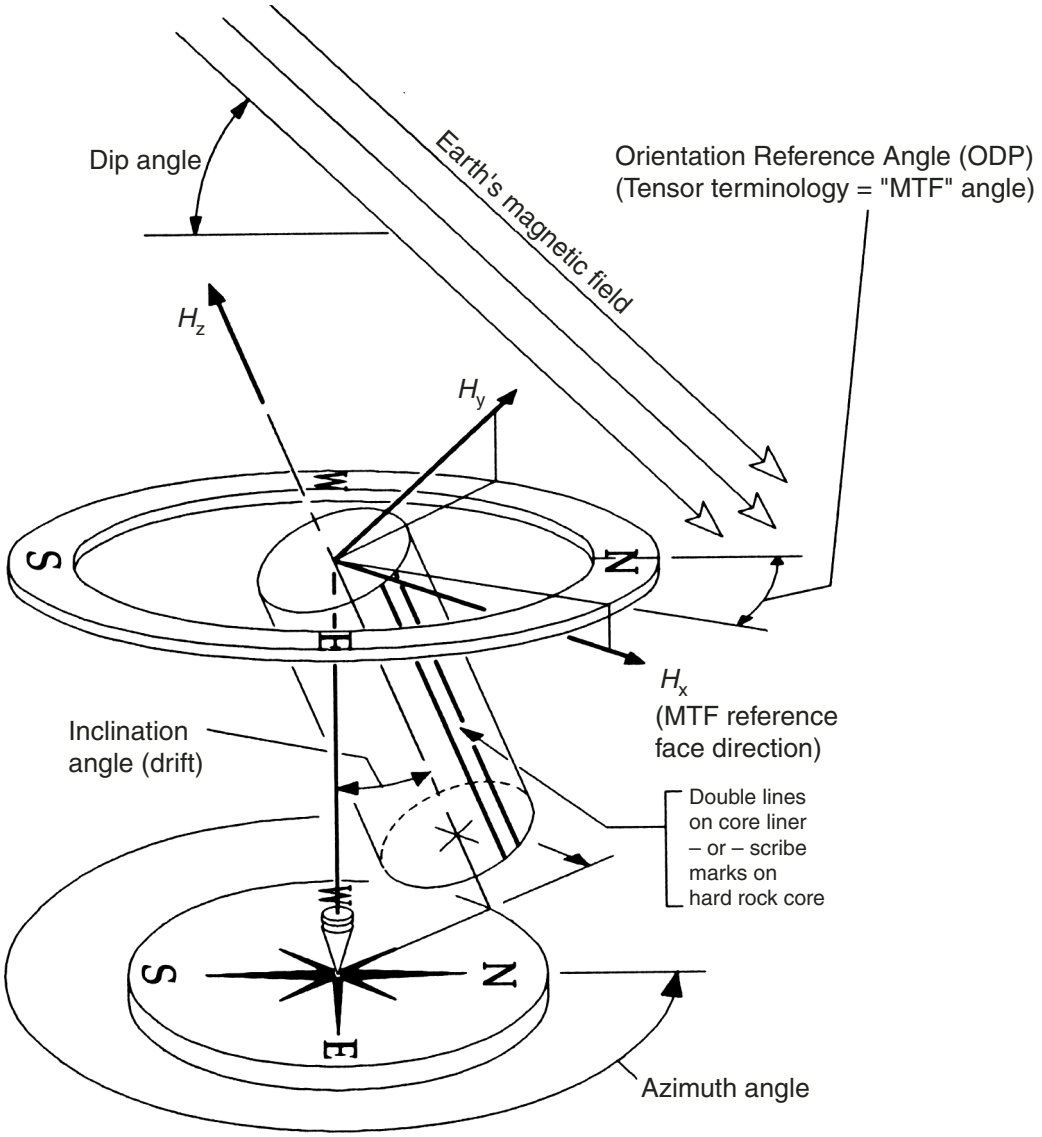

Figure F26. Orthogonal vector demagnetization plots for 11 samples taken from a 1-cm-thick slice of vitric tuff. The <1-cm³ pieces from near the periphery differ from those near the center in the degree of drilling overprint. For example, Pieces 3 and 4 are the least overprinted, and they are nearest the center of the core. They also have a steeper overprint than those samples near the periphery. The drilling overprint deflects the declination of all samples toward the center of the core as shown by the arrows on each diagram (from Leg 200 Shipboard Scientific Party, 2003).

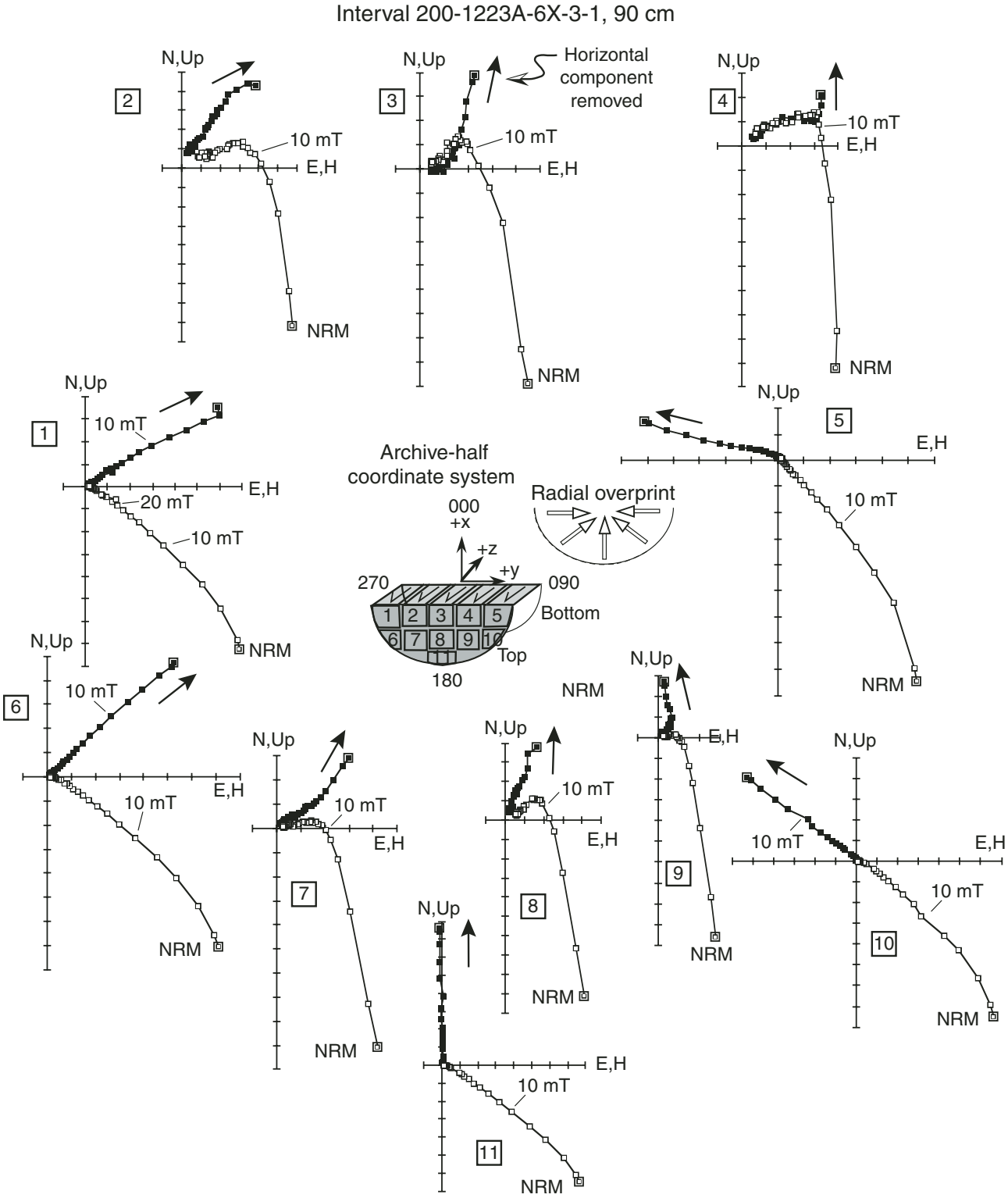

Figure F27. Orthogonal vector demagnetization diagrams for two samples from Hole 172-1062E illustrating the existence of a steep downward-directed drilling overprint and a smaller radial overprint. The steep overprint, which produces a strong deflection of the inclination (hollow squares), and the radial component, which produces a small deflection of the declination, are removed following about 10 to 20 mT AF demagnetization. In this example, the radial component appears to be outward directed (declination deflected toward 180°) for the reverse polarity sample (top) and to be inward directed (declination deflected toward 0°) for the normal polarity samples (bottom) (from Acton et al., 2002).

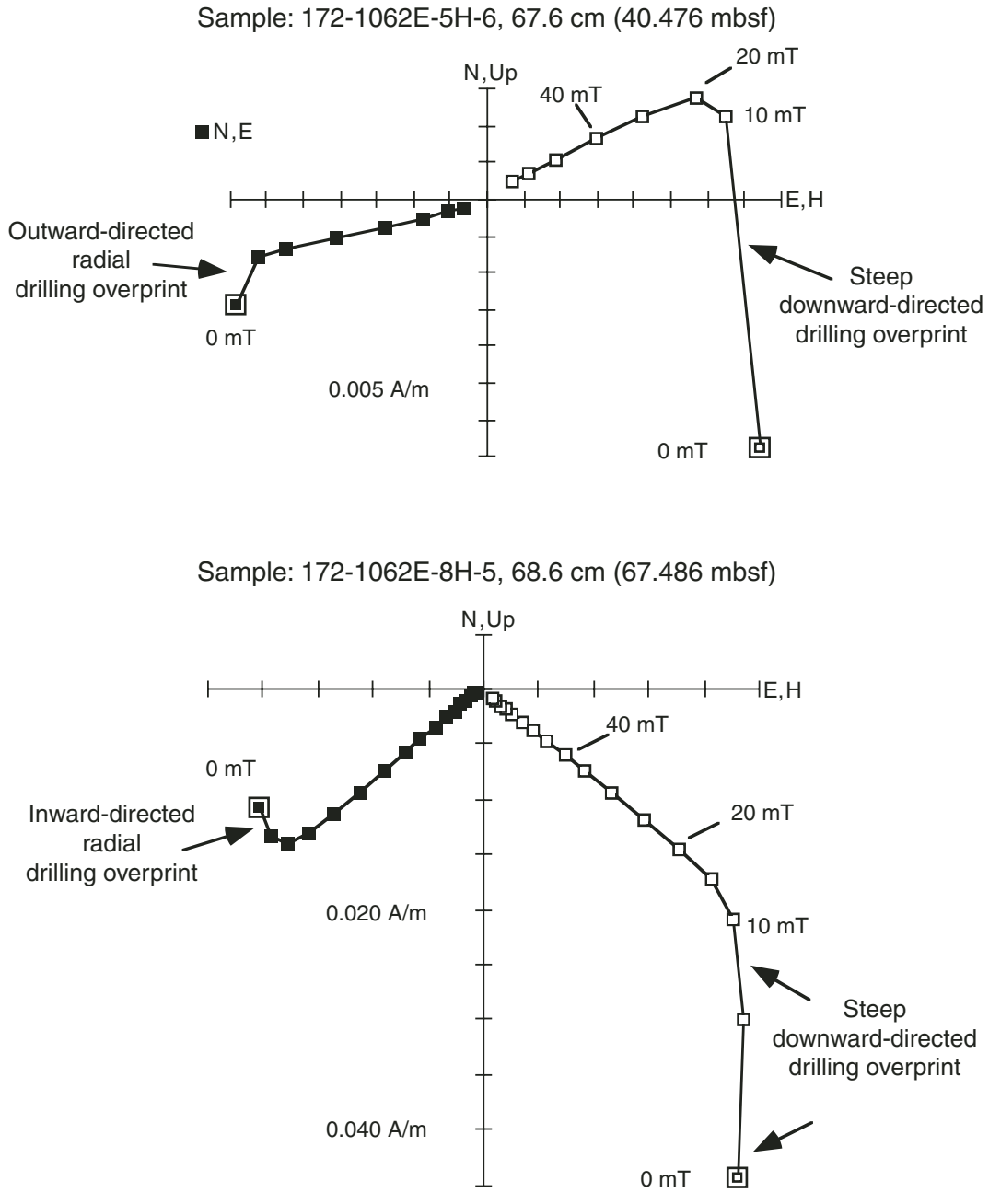

Figure F28. Inclinations from Holes 1095A and 1095B, cored in a sediment drift deposit off the West Antarctic margin, at the 0-mT (NRM) and 30-mT demagnetization step. The overprint is steeply inclined downward, mimicking a reversed polarity in the NRM for the high southern latitude site. B. Declinations from Holes 1095A and 1095B after 30-mT demagnetization. Although these cores are not oriented, there is a strong bias toward zero declination, which suggests a radial component to the remaining overprint.

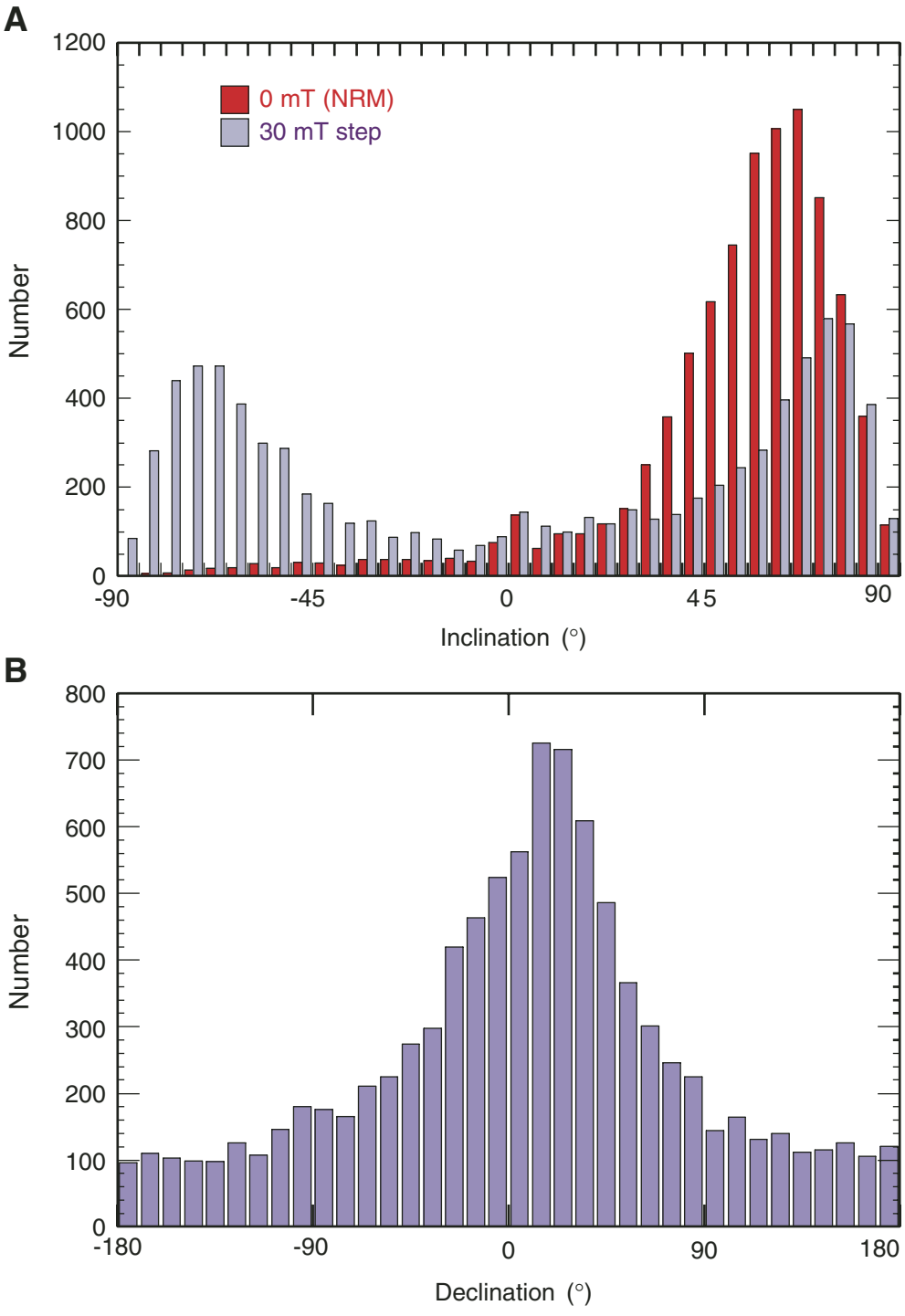

Figure F29. Intensity after 15-mT demagnetization as a proportion of NRM for three consecutive APC cores from Site 862, Leg 141. The pattern reflects a higher proportion of overprinting in Cores 141-862A-1H and 3H than in 2H; this probably results from the use of two alternating core barrel, one less magnetized (used for collecting Core 141-862A-2H) and one more magnetized (used for collecting Cores 141-862A-1H and 3H) (from Behrmann, Lewis, Musgrave, et al., 1992).

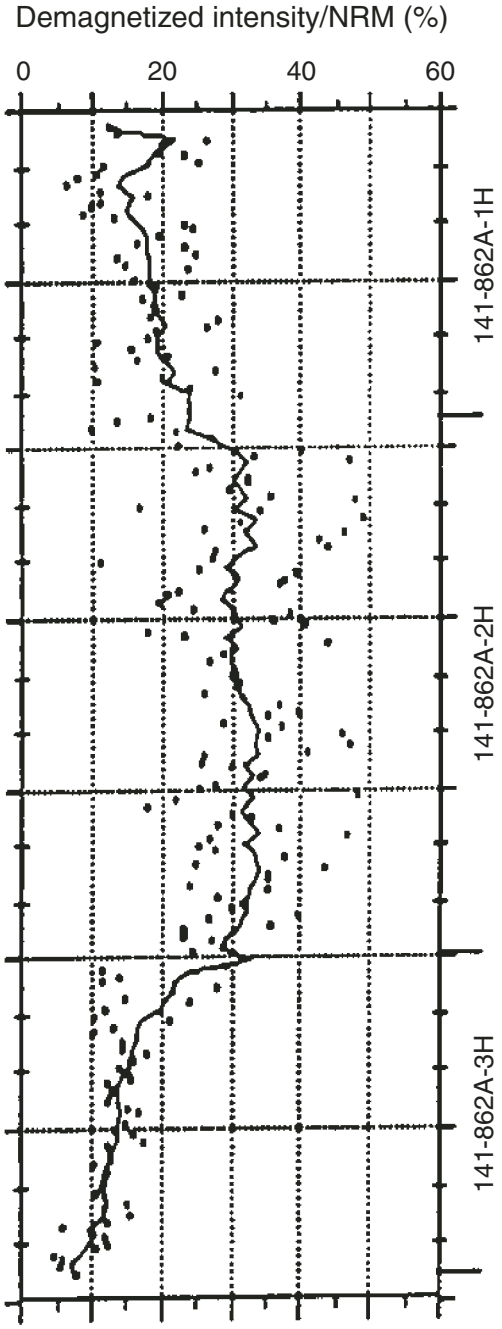

Figure F30. Axial field in two APC core barrels before demagnetization (filled squares), after demagnetization (diamonds), and after the demagnetized barrel completed a "round trip" to recover a core (open squares). Positive fields are downward relative to an upright core barrel and negative fields are upward (from Stokking et al., 1993).

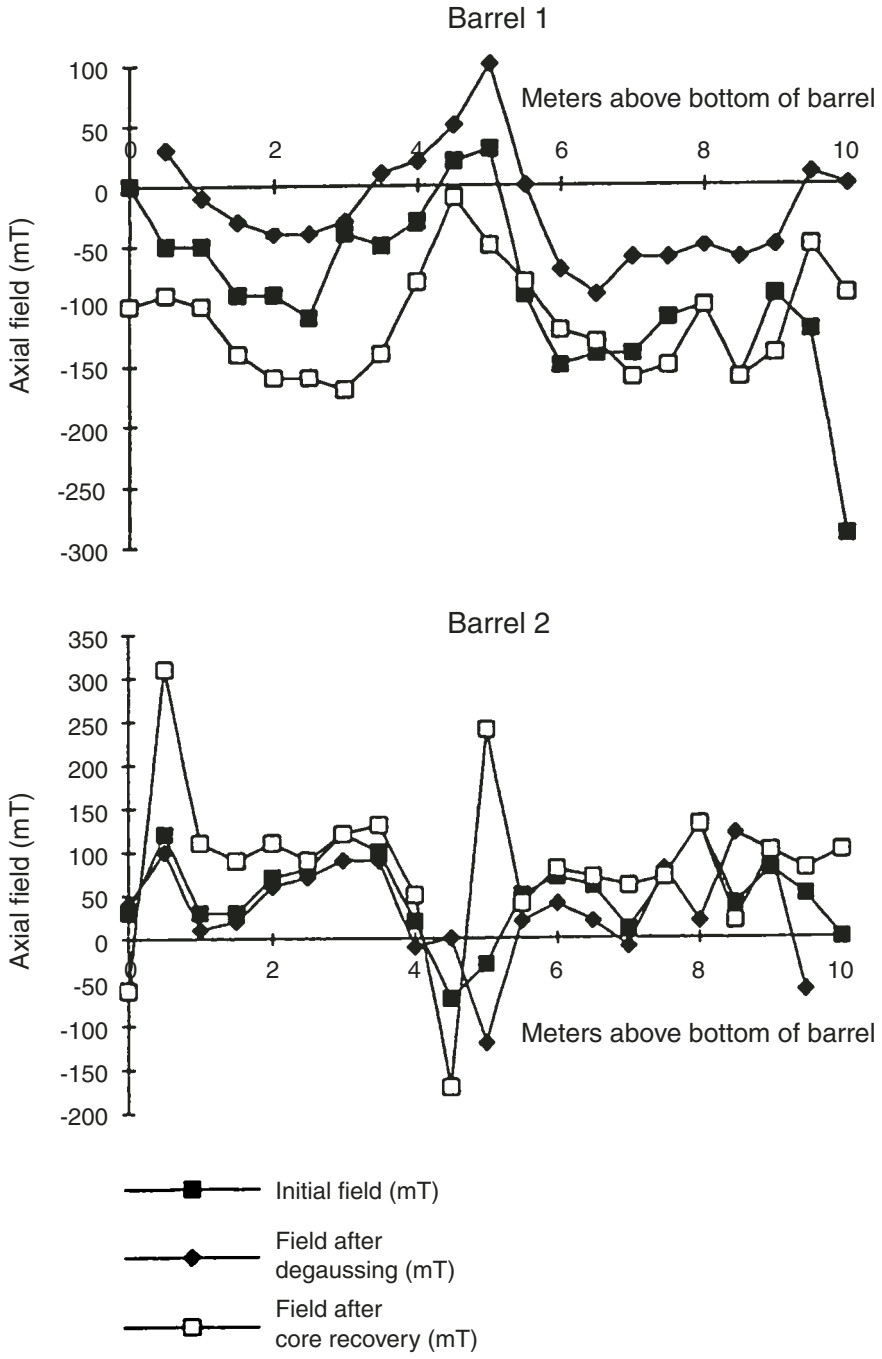

Figure F31. Images showing core deformation in soft sediment cores resulting from piston coring with the APC. The downward bent layers illustrate that the amount of shear rapidly decays away from the core liner (modified from Acton et al., 2002).